THERMODYNAMICS OF AQUEOUS METHYLDIETHANOLAMINE AND METHYLDIETHANOLAMMONIUM CHLORIDE OVER A WIDE RANGE OF TEMPERATURE AND PRESSURE: APPARENT MOLAR VOLUMES, HEAT CAPACITIES, COMPRESSIBILITIES, AND EXCESS MOLAR HEAT CAPACITIES

BRENT HAWRYLAK

THERMODYNAMICS OF AQUEOUS METHYLDIETHANOLAMINE AND METHYLDIETHANOLAMMONIUM CHLORIDE OVER A WIDE RANGE OF TEMPERATURE AND PRESSURE:

APPARENT MOLAR VOLUMES, HEAT CAPACITIES, COMPRESSIBILITIES, AND EXCESS MOLAR HEAT CAPACITIES

by

Brent Hawrylak

A thesis submitted to the
School of Graduate Studies
in partial fulfilment of
the requirements for the
degree of Master of Science

Department of Chemistry
Memorial University of Newfoundland

Fall 1999

St. John's Newfoundland

Abstract

Alkanolamines are an industrially important class of compounds that are used in a wide variety of applications because of their thermal stability, volatility, and basicity. Since they are ideal for probing solvation behavior in high temperature water, they are of considerable interest in the development of theoretical models for ionic solvation. Standard partial molar volumes $V°$, heat capacities C_p°, and compressibilities $\kappa°$ are important in this context because they define the temperature and pressure dependence of important parameters such as the ionization constant. This comprehensive study presents thermodynamic data leading to standard partial molar properties and excess properties of the tertiary alkanolamine, methyldiethanolamine (MDEA) and its chloride salt over a wide temperature range at various pressures.

Apparent molar volumes of aqueous methyldiethanolamine and its salt were determined with platinum vibrating tube densitometers over a range of temperatures from 283 to 573 K and at pressures from 0.1 MPa to 20 MPa. Apparent molar heat capacities were obtained using a Sodev Picker flow microcalorimeter at a pressure of 0.1 MPa and within the temperature range of 283 to 328 K. The experimental results for the neutral amine were well represented using linear expressions with corrections for partial ionization and then extrapolated to infinite dilution to obtain values for $V°$ and C_p°. The experimental results for the salt were determined as a function of ionic strength and analyzed by means of the Guggenheim form of the extended Debye-Hückel equation to

obtain values for V° and C_p°. Apparent molar isothermal compressibilities κ_T° at a pressure of 0.1 MPa were obtained at temperatures from 283 to 313 K with speed of sound measurements. Compressibilities were important in this study since they account for the small pressure dependence observed in the measured apparent molar volumes.

The standard partial molar volumes V° for the neutral amine and its ionized form show increasingly positive and negative values at high temperatures and pressures, as predicted by corresponding states and group additivity arguments. The standard partial molar volume data were used to successfully extrapolate low temperature C_p° data to elevated temperatures. The density model and the revised Helgeson-Kirkham-Flowers (HKF) model have been used to represent the temperature and pressure dependence of the standard partial molar properties to yield a full thermodynamic description of the systems. Further, using appropriate expressions, the density model was employed to obtain the concentration dependence of the apparent molar properties.

Excess heat capacities C_p^{EX} from 278 to 373 K were determined with a CSC 4100 differential scanning calorimeter over the entire mole fraction range for the water-methyldiethanolamine system and the results were analyzed using Redlich-Kister type equations. Calculations were made in accordance with appropriate water vapor corrections based on Raoult's law and the Clausius-Clapeyron equation. The excess heat capacities are positive in magnitude over the entire mole fraction range which is typical of completely miscible water + polar organic systems and indicates a large positive

deviation from ideality. In general, the C_p^{EX} become progressively more positive as the temperature increases with the maxima shifting to larger mole fractions in the water-rich region. Direct data reduction yields reduced excess heat capacities which appear to be consistent with solute-induced structural changes in the intermolecular structure of the water/MDEA system.

Acknowledgments

Thanks to my supervisor Dr. Peter Tremaine....for recruiting me; for discussions and conversation; for suggestions and input; and for his time and patience.

Thanks to Liliana...for her help and enthusiasm; for Spanish lessons; and for not killing me...it was never boring, no? Can you say sheet?

Thanks to Rodney...for enormous input, assistance, suggestions, ideas, and conversation; for groceries; for the densitometer diagram; Au revoir.

Thanks to Wei...for assistance with the Picker; for ping pong, and tennis matches; and for assistance with my seminar.

Thanks to Kai...for Chinese lessons and for food during long nights at the lab.

Thanks to Chris...for computer assistance and for help with solution preparation and calculations.

Thanks to Jenene...for being Jenene and for bringing sarcasm into the lab.

Thanks to Randy Thorne, Carl Mulchahy and Lou Feltham for machine, electronic, and welding assistance.

Thanks to BJ...for good times while at 24 Whiteway.

Thanks to Ben Harper, Bob Dylan, Hothouse Flowers, Blues Traveler, Jimariquai, and Philosopher Kings for inspiration and distractions

Thanks to R. Palepu, G. Marangoni, and St. F.X. University.

Thanks to NSERC and MUN for financial support.

Thanks to Jockey Club, Black Horse, India and Bacardi-Lemon for making it all seem worth it.

Table of Contents

List of Figures

List of Tables

Nomenclature

Abbreviations

aq	Aqueous
DHLL	Debye-Hückel limiting law
exp	Experimental
HKF	Helgeson-Kirkham-Flowers (equation)
MDEA	Methyldiethanolamine
$MDEAH^+Cl^-$	Methyldiethanolammonium chloride
rel	Chemical relaxation contribution
sp	Species

Symbols

A_C, A_V, A_K	DHLL slope for apparent molar heat capacity, volume, and compressibility
Å	Angstrom (length, $1Å = 10^{-10}$ m)
c_p	massic heat capacity
C_p°	Standard partial molar heat capacity
$C_{p,\phi}$	Apparent molar heat capacity
$C_{p,l}^*$	Heat capacity of water
C_p^{EX}	Excess heat capacity
E_ϕ	Apparent molar expansivity

G	Gibbs free energy
H	Enthalpy
I	Ionic strength
K	Densitometer constant; Equilibrium
f_m	Mass flow rate
ff	Heat leak correction factor
m	Molality
M	Molar mass
N_A	Avogadro's number
N	Born equation derivative in HKF equations
n_i	Number of moles of species i
p	Pressure
Q	Born equation derivative in HKF equations
r_i	radius of ion i
R	Gas constant, 8.314 $J \cdot K^{-1} \cdot mol^{-1}$
S	Entropy
T	Temperature
U	Sound velocity
[U]	Relative molar increment of sound velocity
V	Volume

V°	Standard partial molar volume
V_ϕ	Apparent molar volume
W	Electric power input to heater
X	Born equation derivative in HKF equations
X_1	Mole fraction of water
X_2	Mole fraction of MDEA
Y	Generic symbol for apparent molar properties
Z	Charge
α	Degree of dissociation
α_1^*	Thermal expansivity of water
β_1^*	Isothermal compressibility of water
δ	Excess mixing term in Young's rule
ε	Dielectric constant
η	A constant defined in Born equations
Θ	Solvent parameter in HKF equations (228 K)
$\kappa_{S,\phi}$	Apparent molar adiabatic compressibility
κ_T°	Standard partial molar isothermal compressibility
$\kappa_{T,\phi}$	Apparent molar isothermal compressibility
μ	Chemical potential
υ	Stoichiometry coefficient

ρ	Density
ρ_l^*	Density of water
τ	Resonance period of the vibrating tube densitometer
Ψ	Solvent parameter in HKF equations (260 MPa)
ω	Valence factor
ω_e	Effective Born coefficient

Chapter 1: Introduction

1.1 The Importance of Methyldiethanolamine

Alkanolamines are bifunctional molecules with one or more alcohol groups and an amine group on the same molecule. This allows them to react in a wide variety of ways, with similarities to primary, secondary, and tertiary amines, and primary and secondary alcohols. In general, it can be considered that the hydroxyl group serves to reduce the vapor pressure and increase the water solubility, while the amino group provides the necessary alkalinity in water solutions for industrial applications.

Alkanolamines are used as pH additives in the boiling water of thermal and nuclear steam generators. The corrosivity of the water used as a coolant in modern electric power plants depends in a complex manner on the additives and impurities in the water. One of the primary chemical factors in the corrosivity of the water is the pH, and it is important to control that property in the steam generator to prevent the transport of iron and copper corrosion products and sludge. Modern thermal power plants operate at temperatures as high as 643 K and 20 MPa. The high-temperature pH in these systems depends on the thermodynamic properties of the dissolved substances. Ammonia is the most widely used pH control agent but there has been considerable interest in other compounds, such as methyldiethanolamine (commonly abbreviated as MDEA), that have higher base strength and lower volatility to be used as replacements for ammonia.

Various (water + alkanolamine) systems are also used for the removal of acidic gases such as carbon dioxide and hydrogen sulfide from gas streams in the natural gas and petroleum industries. Alkanolamines in aqueous solution react with these acidic constituents to yield water-soluble salts. The dissociation of the salts upon heating (steam stripping) results in recovery of the original starting material. These reactions form the basis of an important industrial application: the "sweetening" of natural gas. Aqueous alkanolamine systems are also of increasing importance in treating acidic gas streams in several chemical production industries. A detailed knowledge of several physical-chemical properties is required for the engineering design and for subsequent operations, as summarized by Astarita *et al.* (1983). Information about phase equilibria, absorption enthalpy, solubility, density, heat capacity, and viscosity of both the pure components and their mixtures at different steps is important in process design and operation.

Credit for the development of alkanolamines as absorbents for acidic gases goes to R.R. Bottoms who in 1930 was granted a patent covering the application. Historically the two amines which have proved to be of principal commercial interest for gas purification are monoethanolamine (MEA) and diethanolamine (DEA) which have been previously investigated by our laboratory. Aqueous solutions of MEA and DEA have been widely used due to their high reactivity, low solvent cost, ease of reclamation, and low absorption of hydrocarbons. Due to the formation of rather stable carbamates by

primary and secondary amines with CO_2,

$$2R_1R_2NH(aq) + CO_2(aq) \rightleftharpoons R_1R_2N^+COO^-(aq) + R_1R_2N^+H_2(aq) \qquad (1.1.1)$$

the loading capacity of these amines cannot reach a value beyond 0.5 mole of CO_2 per mole of amine. A different behavior is exhibited by tertiary amines (such as MDEA) which are unable to form carbamates. Tertiary alkanolamines cannot react directly with CO_2 because they lack a hydrogen attached to the amino nitrogen. Thus, the aqueous tertiary amine reaction with CO_2 only leads to formation of the bicarbonate ion:

$$CO_2(aq) + R_1R_2R_3N(aq) + H_2O \rightleftharpoons HCO_3^-(aq) + R_1R_2R_3NH^+(aq) \qquad (1.1.2)$$

and stoichiometric absorption of CO_2 can now reach 1 mole CO_2 per mole of amine. While the high CO_2 pickup possible with tertiary amines is very attractive, the low reaction rates of CO_2 absorption in tertiary amine solutions limits their practical use.

As a result of this behavior, methyldiethanolamine (MDEA) solutions are used for selective removal of H_2S from gas streams which contain both CO_2 and H_2S. Examples of such streams include some natural gases, synthesis gases from the gasification of coal and heavy oils, and tail gases from sulfur plants. The use of MDEA solutions was first described by Frazier and Kohl (1950). At that time no economic advantage was seen in

the replacement of MEA or DEA in gas processing plants. In the 1970s, the use of MDEA was reconsidered for selective removal of H_2S. The main advantages of MDEA over primary and secondary amines, besides the selectivity for H_2S, is a lower enthalpy of reaction with the acid gases and a lower vapor pressure of the solution. The smaller enthalpy of reaction leads to lower energy requirements for regeneration, while the lower vapor pressure results in smaller losses of solvent by vaporization. Another advantage of MDEA is that it does not degrade readily; that is, it does not react irreversibly to form higher molecular weight compounds that accumulate in the solution.

Methyldiethanolamine is also of interest in basic research. Because it is a relatively small, ionizable, thermally-stable molecule it can be used as a useful probe to examine the behavior of the partial molar properties of aqueous organic systems at elevated temperatures and pressures. In addition to the well-established industrial need of experimental data for these completely miscible systems, there is interest in using volumetric and heat capacity data in combination with molecular models or theories of solutions to extend our understanding of molecular interactions.

1.2 Partial and Apparent Molar Properties and Ionic Strength Effects

Partial molar quantities of chemical components or species are defined at constant temperature T, pressure p, and composition n by:

$$Y_i = \left(\frac{\partial Y}{\partial n_i}\right)_{T,p,n_j} \tag{1.2.1}$$

where Y is an extensive property and Y_i is the corresponding partial molar quantity. They represent the change in an extensive property per mole of added component for an infinitesimal addition of solute at a given composition and are themselves intensive properties of a system. The chemical potential is defined to be the partial molar Gibbs free energy:

$$\mu_i = \left(\frac{\partial G}{\partial n_i}\right)_{T,p,n_j} = \overline{G}_i \qquad (1.2.2)$$

Partial molar properties can be derived by considering the total differential of the Gibbs free energy. For systems of variable composition, the Gibbs free energy must be a function of temperature T, pressure p, and the amount of each component (moles):

$$G = G(T, p, n_1, n_2, \ldots n_i) \qquad (1.2.3)$$

All of the thermodynamic equations that describe the relationship between the Gibbs free energy and derivatives of the Gibbs free energy with respect to temperature and pressure are valid for the corresponding relations with partial molar properties. In the description of the properties of dilute aqueous solutions, partial molar properties play an instrumental role. The temperature dependence of the partial molar heat capacities and volumes of aqueous solutions at constant pressure can be integrated to obtain the partial molar Gibbs

free energy as a function of temperature and pressure.

In studies of solution chemistry, the extensive properties of a solution are described in terms of the properties of the individual components (partial molar and apparent molar quantities). Apparent molar properties are calculated directly from experiment while partial molar properties are determined from manipulation of data. Apparent molar properties are defined by equations of the type:

$$Y_{\phi,2} = \frac{Y_{sol} - n_1 Y_1^*}{n_2} = \frac{Y_{sol} - (1000 Y_1^* / M_1)}{m} \qquad (1.2.4)$$

where Y_{sol} is the extensive property of a specified quantity of solution, n_1 is the amount of solvent, Y_1^* is the molar property of pure solvent (water), n_2 is the amount of solute in the specified quantity of solution. As mentioned, apparent molar properties are calculated from directly measured quantities such as specific heat capacities and densities. For example, the apparent molar volume V_ϕ and apparent molar heat capacity $C_{p,\phi}$ are given by:

$$V_\phi = \frac{1000(\rho_1^* - \rho)}{m\rho_1^*\rho} + \frac{M_2}{\rho} \qquad (1.2.5)$$

$$C_{p,\phi} = \frac{c_p(1 + mM_2) - c_{p,1}^*}{m} \qquad (1.2.6)$$

where m is the molality of the solution, M_2 is the molar mass of the solute, ρ_1^* and $c_{p,1}^*$ are the density and specific heat capacity of water, respectively; ρ and c_p are the density and specific heat capacity of the solution, respectively. An apparent molar property for a solute in water can be thought of as the "apparent" change that n_2 moles of a solute contributes to a volume of solution containing n_1 moles of solvent. For example, equation 1.2.4 can be rearranged into the form:

$$Y_{sol} = n_1 Y_1^* + n_2 Y_{\phi,2} \tag{1.2.7}$$

From the definition of apparent molar properties, equation 1.2.7 can be differentiated with respect to n (holding n_1 as constant) to obtain:

$$\overline{Y}_2 = Y_{\phi,2} + n_2 \left(\frac{\partial Y_{\phi,2}}{\partial n_2} \right)_{n_1,T,p} \tag{1.2.8}$$

and since the molality m is defined for constant n_1, this becomes

$$\overline{Y}_2 = Y_{\phi,2} + m \left(\frac{\partial Y_{\phi,2}}{\partial m} \right) \tag{1.2.9}$$

At infinite dilution ($n_2 = 0$), the standard partial molar property, $Y^\circ = \lim(m \to 0) Y_\phi$ is obtained, where Y° refers to the hypothetical one mol·kg^{-1} thermodynamic standard state. Standard partial molar properties of aqueous electrolytes give insight into the nature of

ion-solvent interactions and their determination requires the extrapolation of experimental data to infinite dilution.

A simple extended Debye-Hückel equation often satisfactorily represents the apparent molar properties of aqueous electrolytes to moderate ionic strengths and can be used for the extrapolation to infinite dilution:

$$Y_{\phi,2} = Y_2^{\circ} + A_Y \omega I^{1/2} + B_Y I \qquad (1.2.10)$$

In this equation, A_Y is the Debye-Hückel limiting slope for apparent molar properties (Bradley and Pitzer, 1979) and is obtained from the compilation of Archer and Wang (1990) and B_Y is an adjustable parameter that represents the ionic strength dependence of the apparent molar properties that deviate from the Debye-Hückel limiting law. The valence factor $\omega = (Z_-Z_+)$ and the ionic strength are defined by:

$$I = \omega m = \frac{1}{2}\sum m_i Z_i^2 \qquad (1.2.11)$$

The Debye-Hückel theory gives correct limiting behavior for electrolytes at infinite dilution and is also useful at finite but very low concentrations. It is very difficult to obtain accurate experimental values of V_ϕ, $C_{p,\phi}$, and κ_ϕ for aqueous electrolyte solutions with molalities less than 0.1 mol· kg^{-1}. The Debye-Hückel limiting laws are instrumental for extracting standard partial molar properties because they provide a means of

extrapolating experimental data to infinite dilution.

Debye-Hückel theory considers only long-range electrostatic interactions between ions and it cannot be expected to work in solutions above a certain limiting concentration. Because of this, many attempts have been made to extend the range of validity of the Debye-Hückel theory. The functional dependence of the apparent molar volumes and heat capacities are well represented by extended Debye-Hückel equations in Guggenheim's form (Millero, 1979):

$$Y_\phi = Y^\circ + 1.5\frac{\omega A_Y}{I}\left[I - 2I^{1/2} + 2\ln(1 + I^{1/2})\right] + B_Y I \qquad (1.2.12)$$

The ability of the above equations to represent the behavior at moderate concentrations and to extrapolate the standard-state values is quite satisfactory. Extended versions for high concentrations have been developed by Pitzer *et al.* (1984), Helgeson *et al.* (1981), and Holmes and Mesmer (1983).

1.3 Thermodynamic Relationships

A complete thermodynamic description of a chemical system requires knowledge of how its thermodynamic characteristics (i.e. volume, heat capacity, compressibility, and expansivity) vary with both temperature and pressure.

An equilibrium constant K at a given temperature and pressure can be calculated from the corresponding change in the Gibbs free energy associated with the reaction:

$$\ln K = \frac{-\Delta G^\circ}{RT} \tag{1.3.1}$$

Other relationships for changes of the Gibbs free energy with temperature and pressure are:

$$\left(\frac{\partial \Delta G^\circ}{\partial T}\right)_p = -\Delta S^\circ \tag{1.3.2}$$

$$\left(\frac{\partial \Delta G^\circ}{\partial p}\right)_T = \Delta V^\circ \tag{1.3.3}$$

$$\left(\frac{\partial \Delta H^\circ}{\partial T}\right)_p = \Delta C_p^\circ \tag{1.3.4}$$

$$\left(\frac{\partial V^\circ}{\partial p}\right)_T = \Delta \kappa_T^\circ \tag{1.3.5}$$

where ΔS°, ΔV°, ΔC_p°, $\Delta \kappa_T^\circ$ are the changes in the standard partial molar entropy, volume, heat capacity, and isothermal compressibility associated with the reaction at the temperature and pressure of interest.

Integration of the above equations yields the following expression for $\Delta G_{T,p}^\circ$.

$$\Delta G_{T,p}^\circ = \Delta G_{Tr,pr}^\circ - \Delta S_{Tr,pr}^\circ + \int_{T_r}^{T} \Delta C_p^\circ dT - T\int_{T_r}^{T} \frac{\Delta C_p^\circ}{T} dT + \int_{p_r}^{p} \Delta V_{Tr,pr}^\circ dp \tag{1.3.6}$$

where T is the temperature of interest, $T_r = 298.15$ K is the reference temperature, p is the

pressure of interest and p_r = 100 kPa is the reference pressure.

1.4 Hydration

Many authors describe the structure of water near a hydrated ion by defining three regions initially used in the structural treatment of ion-solvent interactions by Bernal and Fowler (1933). In the "primary" region immediately adjacent to the ion, the water molecules are oriented and immobilized by the ionic field. In the "secondary", or "structure-broken", region in which the normal bulk structure of water is broken to varying degrees. In the third region, at sufficient distance from the ion, the water structure is unaffected by the ion so that ion-solvent interactions can be described by dielectric continuum models.

Consider an isolated ion in the gas phase above the solvent. The total work done to transfer this ion from the ideal gas reference state to a cavity inside the solvent defines the free energy of solvation (i.e. the Gibbs free-energy change arising from ion-solvent interactions). The Gibbs free energy associated with transferring a species into a solvent can be determined from the expression:

$$\Delta G^{\circ}_{solv} = \Delta G^{\circ}_{pol} + \Delta G^{\circ}_{hydr} + \Delta G^{\circ}_{int} \qquad (1.4.1)$$

where ΔG°_{pol} is the term which arises from the long-range interactions between the hydrated ion and the solvent (Gibbs free energy of polarization), ΔG°_{hydr} is the

electrostatic energy of the short-range interaction (Gibbs free energy of hydration) and ΔG°_{int} represents changes in the internal vibrations and rotations of the species as it moves from the gaseous to aqueous phase (intrinsic Gibbs free energy). In transferring the species from the gas phase to solution there is a change in the reference state. For the gas phase the reference state is the ideal gas at $p_r = 100$ kPa whereas for solutions the reference state is the hypothetical 1 molal solution.

Semi-continuum models for the calculation of standard state changes in Gibbs free energy, enthalpy, and entropy treat the water in the primary hydration sphere as discrete molecules, and consider the secondary hydration sphere to be a dielectric continuum model with added empirical terms. Goldman and Bates (1972) developed a semi-continuum model for ionic solvation and Tremaine and Goldman (1978) have extended this model to high temperature.

As stated above ΔG°_{hydr} represents the short range interactions between the dissolved species and the surrounding solvent molecules which may include hydrogen bonding between the dissolved species and the solvent molecules and the deformation of the bulk structure in the proximity of the dissolved species.

1.5 The Born Equation

Born (1920) showed that the free energy change associated with removing an ion j of effective radius $r_{e,j}$ and charge $Z_j e$ from a vacuum and placing it in a solvent of

dielectric constant ε is:

$$\Delta G^{\circ}_{Born} = -\frac{N_A (Z_j e)^2}{2r_{e,j}}\left(1-\frac{1}{\varepsilon}\right) \tag{1.5.1}$$

where N_A is Avogadro's number. The Born theory for ion-solvent interactions provides a simple and important model for the role of long-range polarization in the hydration of ions by viewing the ion as a rigid conducting sphere bearing a charge and the solvent is taken to be a structureless dielectric continuum. The Born model is based on the assumption that only the ionic charge on the ion is responsible for ion-solvent interactions and they are solely electrostatic in origin. Therefore, the model views the free energy of ion-solvent interactions as equal to the work of transferring a charged sphere from a vacuum into a continuum of static dielectric constant ε.

It is desirable to recover from the theoretical expression for the free energy, the enthalpy, entropy, volume, heat capacity, and compressibility changes associated with ion-solvent interactions. Expressions for the above properties associated with a dissolved ionic species were obtained through the following relationships:

$$\Delta H^{\circ}_{Born} = \left(\frac{\partial\left(\Delta G^{\circ}_{Born}/T\right)}{\partial(1/T)}\right)_p \tag{1.5.2}$$

$$\Delta S^{\circ}_{Born} = -\left(\frac{\partial \Delta G^{\circ}_{Born}}{\partial T}\right)_p \tag{1.5.3}$$

$$\Delta V^{o}_{Born} = \left(\frac{\partial \Delta G^{o}_{Born}}{\partial p}\right)_{T} \tag{1.5.4}$$

$$\Delta C^{o}_{p,Born} = \left(\frac{\partial \Delta H^{o}_{Born}}{\partial T}\right)_{p} \tag{1.5.5}$$

$$\Delta \kappa^{o}_{T,Born} = -\left(\frac{\partial \Delta V^{o}_{Born}}{\partial p}\right)_{T} \tag{1.5.6}$$

Hence:

$$\Delta H^{o}_{Born} = -\frac{N_A (Z_j e)^2}{2 r_{e,j}}\left[1 - \frac{1}{\varepsilon} - \frac{T}{\varepsilon^2}\left(\frac{\partial \varepsilon}{\partial T}\right)_{p}\right] \tag{1.5.7}$$

$$\Delta S^{o}_{Born} = \frac{N_A (Z_j e)^2}{2 r_{e,j}}\left(\frac{1}{\varepsilon^2}\right)\left(\frac{\partial \varepsilon}{\partial T}\right)_{p} \tag{1.5.8}$$

$$\Delta V^{o}_{Born} = \frac{N_A (Z_j e)^2}{2 r_{e,j}}\left(\frac{-1}{\varepsilon}\right)\left(\frac{\partial \varepsilon}{\partial p}\right)_{T} \tag{1.5.9}$$

$$\Delta C^{o}_{p,Born} = -\frac{N_A (Z_j e)^2}{2 r_{e,j}}\left(\frac{2T}{\varepsilon^3}\right)\left(\frac{\partial^2 \varepsilon}{\partial T^2}\right)_{p} \tag{1.5.10}$$

$$\Delta \kappa^{o}_{T,Born} = \left(-\frac{N_A (Z_j e)^2}{2 r_{e,j}}\right)\left[\left(\frac{2}{\varepsilon^3}\right)\left(\frac{\partial \varepsilon}{\partial p}\right)^{2}_{T} - \left(\frac{1}{\varepsilon^2}\right)\left(\frac{\partial^2 \varepsilon}{\partial p^2}\right)_{T}\right] \tag{1.5.11}$$

1.6 The Helgeson-Kirkham-Flowers Model

A practical tool for extrapolating properties to elevated temperature and pressures

is provided by the equations of state that comprise the revised Helgeson-Kirkham-Flowers (HKF) model. This is a semi-empirical model which allows for the prediction of the standard partial molar thermodynamic parameters of aqueous ions and electrolytes, developed by Helgeson and co-workers between 1974 and 1981 with extensive modifications added by Tanger and Helgeson (1988) and Shock and Helgeson (1988).

The Born equation provides a satisfactory description of the effect of long-range interactions on the thermodynamic properties of aqueous ions and it serves as the basis of the HKF model. The model assumes that the standard partial molar properties consist of two contributions: an electrostatic term, derived from the Born equation, and a non-electrostatic term. The Born equation is used for the electrostatic term with $r \geq r_{cryst}$ to represent the primary solvation layer (where $\varepsilon_1 = 1$). The non-electrostatic term consists of an empirical portion for the secondary solvation layer (described in Section 1.4), an intrinsic property attributed to the ion itself, and the standard state term.

The non-solvation contribution ΔV_n° to the standard partial molar volume is represented by:

$$\Delta V_n^\circ = \sigma + \xi\left(\frac{1}{T - \Theta}\right) \tag{1.6.1}$$

where Θ is a solvent parameter equal to 228 K. The temperature independent coefficients σ and ξ are represented by:

$$\sigma = a_1 + a_2\left(\frac{1}{\Psi + p}\right) \tag{1.6.2}$$

$$\xi = a_3 + a_4\left(\frac{1}{\Psi + p}\right) \tag{1.6.3}$$

where Ψ is a solvent parameter equal to 260 MPa, and a_1, a_2, a_3, and a_4 are temperature and pressure independent parameters.

The solvation term ΔV°_{solv} comes directly from the relationship of the partial molar free energy to partial molar volumes represented by the Born model:

$$\Delta V^{\circ}_{Born} = \left(\frac{\partial \Delta G^{\circ}_{Born}}{\partial p}\right)_T = \omega_e\left(\frac{\partial \varepsilon^{-1}}{\partial p}\right)_T = -\omega_e \varepsilon^{-1}\left(\frac{\partial \ln \varepsilon}{\partial p}\right)_T = -\omega_e Q \tag{1.6.4}$$

where ω_e is the temperature and pressure independent effective Born coefficient, ε is the dielectric constant of the solvent, and Q is the term containing the pressure derivative of the dielectric constant that results from the Born equation.

Hence, the expression given by Shock and Helgeson (1990) to predict the standard partial molar volume of a neutral organic species is:

$$V^{\circ} = a_1 + a_2\left(\frac{1}{\Psi + p}\right) + \left[a_3 + a_4\left(\frac{1}{\Psi + p}\right)\right]\left(\frac{1}{T - \Theta}\right) - \omega_e Q \tag{1.6.5}$$

The effective Born coefficient is represented by:

$$\omega_e = \frac{(Z_e e)^2 N_A}{2r_e} = \frac{\eta Z_e}{r_e} \qquad (1.6.6)$$

where Z_e is the effective charge on the neutral aqueous organic species and $\eta = 6.9466\times10^{6}$nm·J·mol^{-1}. The effective radius r_e was used in the Born equation rather than the crystallographic radii. Helgeson and Kirkham (1976) found that the effective radii for anions could be taken to be equivalent to their cystallographic radii whereas the effective radii of cations could be related to their crystallographic counterpart by:

$$r_e = r_c + 0.94Z \qquad (1.6.7)$$

Similarily, the Helgeson-Kirkham-Flowers equation of state for standard partial molar heat capacities has the form:

$$C_p^o = c_1 + c_2\left(\frac{1}{T-\Theta}\right)^2 - 2T\left(\frac{1}{T-\Theta}\right)^3\left[a_3(p-p_r) + a_4\ln\left(\frac{\Psi+p}{\Psi+p_r}\right)\right] + \Delta C^o_{p,Born} \qquad (1.6.8)$$

where c_1 and c_2 are fitting coefficients, a_3 and a_4 are the coefficients determined from the partial molar volumes, p is the pressure and $p_r = 0.1$ MPa is the standard state pressure. The expression for the partial molar heat capacity of polarization is:

$$\Delta C^{\circ}_{p,Born} = -T\left(\frac{\partial^2 \Delta G^{\circ}_{Born}}{\partial T^2}\right)_p = \omega_e T\varepsilon^{-1}\left[\left(\frac{\partial^2 \ln\varepsilon}{\partial T^2}\right)_p - \left(\frac{\partial \ln\varepsilon}{\partial T}\right)^2_p\right] = \omega_e TX \quad (1.6.9)$$

The equation of state for the standard partial molar isothermal compressibilities κ_T° can be obtained from the standard partial molar volume:

$$\kappa^{\circ}_T = \left(\frac{\partial V^{\circ}}{\partial p}\right)_T = \left(a_2 + \frac{a_4}{T-\Theta}\right)\left(\frac{1}{\Psi + p}\right)^2 + \omega_e N \quad (1.6.10)$$

where a_2 and a_4 are the coefficients determined from the partial molar volumes and N is the pressure derivative of the Born function Q:

$$N = \left(\frac{\partial Q}{\partial p}\right)_T = \frac{1}{\varepsilon^2}\left[\left(\frac{\partial^2 \varepsilon}{\partial p^2}\right)_T - \frac{2}{\varepsilon}\left(\frac{\partial \varepsilon}{\partial p}\right)^2_T\right] \quad (1.6.11)$$

The terms in the equations derived from the Born equation dominate at high temperatures where the Born model is most satisfactory. The remaining terms in each equation are purely empirical and are most important at low temperatures where the Born model is least satisfactory. As a result, the HKF treatment is well suited for the extrapolation of low temperature data to predict the standard partial molar thermodynamic properties of ionic organic species to elevated temperatures and

pressures. Helgeson and co-workers have intensively analyzed the experimental data for a wide class of electrolytes using the HKF approach. The model has considerable predictive power although problems arise due to the inadequate assumption that water is a continuous dielectric fluid (especially near an ion, where molecular size effects occur) and to uncertainties in assigning the ionic radii to solutes in water. Generally, these radii are larger than the crystallographic radii and are denoted "effective" aqueous radii. The dielectric constant of water decreases as the temperature is increased and it is expected that because of this decrease (due mainly to the breakdown of ordered water structure because of increased thermal motion) the Born equation will become better at representing thermodynamic properties at elevated temperatures.

The revised HKF model, as modified by Shock and Helgeson (1990), allows for the prediction of the standard partial molar thermodynamic properties of neutral aqueous organic species up to a temperature of 1273 K and a pressure of 500 MPa. To give the revised HKF model predictive capabilities it was first fitted to all available temperature and pressure dependent experimental data for neutral aqueous organic species. The values of the fitting parameters were then correlated with the low temperature thermodynamic data for each species. For organic species ω_e is a fitting parameter and can be either positive or negative. If ω_e is negative then either the effective radius of the dissolved species is negative or the effective charge on the dissolved species Z_e is an imaginary number. Consequently, equation 1.6.5 has no physical meaning when ω_e is

negative. The validity of the HKF model for neutral species is questionable since the predictive power of the model is based on no physical meaning and on a limited number of neutral aqueous species for which there are temperature and pressure dependent thermodynamic data.

1.7 The Density Model

Franck (1956,1961) observed that the ionization constants of water and of many aqueous solutes at elevated temperatures and pressures showed a remarkably linear behavior for a wide range of density when plotted as log K versus log ρ_1^*, where K is the ionization constant and ρ_1^* is the density of water. This observation led Marshall and Franck (1981) to develop the following equilibrium to represent the ionization constant of water at temperatures up to 1273 K and at pressures up to 1000 MPa :

$$\log K = \left(a + \frac{b}{T} + \frac{c}{T^2} + \frac{d}{T^3} \right) + k \log \rho_1^* \qquad (1.7.1)$$

where K is the ionization constant for an aqueous species; a, b, c, d, e, f, and g are fitting parameters, T is the temperature; ρ_1^* is the density of water and k is defined by:

$$k = \left(e + \frac{f}{T} + \frac{g}{T^2} \right) \qquad (1.7.2)$$

Mesmer *et al.* (1988) later demonstrated that equation 1.7.1 can be used to represent ionization reactions in general. This density-based model has relatively few parameters to

describe such widely ranging temperature-pressure conditions, and although it may not fit the data within experimental uncertainty everywhere it represents the principal variations accurately. Such an analytical function affords the opportunity for evaluating and examining the thermodynamic derivative quantities. The expression for log K in equation 1.7.1 was used to obtain expressions for a number of other thermodynamic quantities. An expression for the Gibbs free energy of ionization for an aqueous species ΔG° was obtained through the following relationship:

$$\Delta G^\circ = -RT \ln K \tag{1.7.3}$$

where R is the gas constant. Hence:

$$\Delta G^\circ = -2.303RT\left[\left(a+\frac{b}{T}+\frac{c}{T^2}+\frac{d}{T^3}\right)+\left(e+\frac{f}{T}+\frac{g}{T^2}\right)\log\rho_1^*\right] \tag{1.7.4}$$

Similarly, an expression for the enthalpy of ionization for an aqueous species ΔH° was obtained from the following relation:

$$\Delta H^\circ = \left(\frac{\partial\left(\Delta G^\circ/T\right)}{\partial\left(1/T\right)}\right)_p \tag{1.7.5}$$

Hence:

$$\Delta H^\circ = -2.303R\left(b + \frac{2c}{T} + \frac{3d}{T^2} + \left(f + \frac{2g}{T}\right)\log\rho_1^*\right) - RT^2k\alpha_1^* \qquad (1.7.6)$$

where α_1^* is the expansivity coefficient of water, $\alpha_1^* = -(1/\rho_1^*)(\partial\rho_1^*/\partial T)_p$. An expression for the entropy of ionization for an aqueous species ΔS° was obtained through the relation:

$$\Delta S^\circ = -\left(\frac{\partial \Delta G^\circ}{\partial T}\right)_p \qquad (1.7.7)$$

Hence:

$$\Delta S^\circ = 2.303R\left(a - \frac{c}{T^2} - \frac{2d}{T^3} + \left(e - \frac{g}{T^2}\right)\log\rho_1^*\right) - RTk\alpha_1^* \qquad (1.7.8)$$

Similarly, an expression for the standard partial molar heat capacity of ionization for an aqueous species ΔC_p° was obtained from the relation:

$$\Delta C_p^\circ = \left(\frac{\partial \Delta H^\circ}{\partial T}\right)_p \qquad (1.7.9)$$

Hence:

$$\Delta C_p^\circ = -2.303R\left(\frac{-2c}{T^2} - \frac{6d}{T^3} - \left(\frac{2g}{T^2}\right)\log\rho_1^*\right) - R\alpha_1^*\left(2eT - \frac{2g}{T}\right) - RT^2k\left(\frac{\partial \alpha_1^*}{\partial T}\right)_p \qquad (1.7.10)$$

Using the following relationship an expression for the standard partial molar volume of ionization for an aqueous species ΔV° was obtained:

$$\Delta V^\circ = \left(\frac{\partial \Delta G^\circ}{\partial p}\right)_T \tag{1.7.11}$$

Hence:

$$\Delta V^\circ = -RTk\beta_1^* \tag{1.7.12}$$

An expression for the standard partial molar isothermal compressibility was obtained from the pressure derivative of the partial molar volume:

$$\kappa_T^\circ = \left(\frac{\partial V^\circ}{\partial p}\right)_T = -RTk\left(\frac{\partial \beta_1^*}{\partial p}\right)_T \tag{1.7.13}$$

Equation 1.7.1 can be further simplified for data over restricted regions of temperature and pressure. Simpler forms having a reduced number of parameters have been successful in modeling several reaction types at temperatures up to about 573 K along the saturation pressure curve. This simple form requires only reference values for log K, ΔH° and ΔC_p° at 298 K and 100 kPa (Anderson *et al.*, 1991; Pitzer, 1991).

1.8 Excess Properties

There is a vast literature on the thermodynamic properties of mixtures of liquids where the nonideality is generally represented as excess quantities Y^{EX}. The excess

thermodynamic functions measure deviations from Raoult's Law and are calculated from the expression:

$$Y^{EX} = Y - X_1 Y_1^{\bullet} - X_2 Y_2^{\bullet} \tag{1.8.1}$$

where Y is the total property of the solution or mixture per total number of moles of components 1 and 2, $Y_i^{\bullet}$ is the molar property of pure component 1 or 2. This quantity gives an overall view of the magnitude of the nonideality in the solution and it is often used in conjunction with the Redlich-Kister equation (Redlich and Kister, 1948) to represent thermodynamic data for mixtures of liquids. The Redlich-Kister equation is an expanded Margules equation and has the form:

$$Y^{EX} = X_2(1-X_2)\sum_{i=0}^{p} A_i(2X_2 - 1)^i \tag{1.8.2}$$

where A_i are least-squares parameters. The Redlich-Kister equation is a flexible polynomial expression in mole fraction that provides a convenient method for representing the excess properties of a liquid mixture and classifying different types of liquid solutions (Prausnitz *et al.* 1986). In proposing this equation, the authors stated that the relation must contain the factor $X_2(1-X_2)$ while it is desirable to develop a series with respect to the mole fraction which is somehow symmetrical with respect to the two components. The first term in the expansion is symmetric in X_2 and gives a parabola when the excess property is plotted against X_2. The odd-powered correction terms [first (A_1), third (A_3),...] are asymmetric in X_2 and therefore skew the parabola either to the left

or right. The even-powered correction terms [second (A_2), fourth (A_4),...] which are symmetric in X_2, flatten or sharpen the parabola. For an equimolar mixture ($X_1 = X_2 = 0.5$), this expression gives $Y^{EX} = A_0$. Thus, regardless of the number of terms in the series, we can determine from just A_0 the correlated equimolar value of the scaled excess property (Sandler, 1994). In principle we can accommodate a variety of subtleties by including an adequate number of terms in a polynomial representation. However, so many terms may be needed in certain cases as to render the correlation meaningless. A general guideline is that if more than four terms are required, an alternative method for representing the data should be considered since the goal is always to represent data to within their precision by using as few empirical parameters as possible.

Optimal flexibility can be obtained by rational functions, i.e., by ratios of polynomials. Van Ness and Abbott (1982) discuss the rational function:

$$Y^{EX} = \frac{A_0 + \sum A_n (X_1 - X_2)^n}{1 + \sum D_m (X_1 - X_2)^m} \qquad (1.8.3)$$

which has been used extensively by Christensen and co-workers (1986, 1985, 1984) to fit excess molar enthalpies of binary mixtures containing carbon dioxide.

Although thermodynamic data on mixtures of liquids are usually expressed as excess quantities Y^{EX} this approach can in some cases be misleading because it can hide strong interactions at low concentrations. An alternative approach has been suggested by

Davis (1993) and Desnoyers and Perron (1997). The properties of solutes in dilute solutions are conveniently represented by apparent molar properties. The definition of an apparent molar quantity (equation 1.2.4) may be expressed as:

$$Y_{\phi,2} = \frac{\left(Y - X_1 Y_1^*\right)}{X_2}; Y_{\phi,1} = \frac{\left(Y - X_2 Y_2^*\right)}{X_1} \qquad (1.8.4)$$

From equation 1.8.1 it is apparent that there is a direct relationship between the apparent molar quantities of both components and the excess functions over the entire mole fraction range:

$$\frac{Y^{EX}}{X_1 X_2} = \frac{\left(Y_{\phi,2} - Y_2^*\right)}{X_1} = \frac{\left(Y_{\phi,1} - Y_1^*\right)}{X_2} \qquad (1.8.5)$$

Extrapolation of $Y^{EX}/(X_1X_2)$ to $X_2 = 0$ and $X_2 = 1$ will give the two excess partial molar quantities $Y_2^\circ - Y_2^*$ and $Y_1^\circ - Y_1^*$ which include Y_1° and Y_2°, the standard partial molar properties of both components at infinite dilution. These are, by definition, measures of the solute-solvent interactions of both components. These relations follow directly from the definitions of excess functions and apparent molar quantities and are independent of any model.

1.9 The Chemistry of Amines

Of all the hundreds of common neutral functional groups, only the amino groups are of sufficient basicity to be ionized by protonation within the pH range of acidity. An anomaly exists in the sequence of the relative base strengths of the amines (Jones and Arnett, 1974):

$$NH_3 < \text{Primary} < \text{Secondary} > \text{Tertiary}$$

According to Jones and Arnett, the anomalous base-strength order arises from the influence of two opposing effects, both of which operate more energetically on the ammonium ions than on the neutral amines. The ions are stabilized internally by the ability of alkyl groups to disperse positive charge (the inductive effect) and externally through solvation by the hydrogen bonding of water with its acidic protons. Through a given series of amines from ammonia to the tertiary compound, the successive replacement of hydrogen atoms by alkyl radicals exerts an inductive base-strengthening influence, but the continued loss of hydrogen-bonding sites tends to destabilize the ion and hence weaken the ability of the base to accept a proton. The balance between the two energy terms is apparently quite close for the secondary ammonium ions since secondary amines are only slightly more basic than the corresponding primary amines. For the tertiary ions, however, the added inductive influence of the third substituent cannot compensate for the drop in solvation energy arising from the decreased number of hydrogen bonds with water; thus the net base strength of tertiary amines is depressed.

1.10 Thermodynamic Data in the Literature

Jones and Arnett (1974) have reviewed the literature on methyldiethanolamine and other amines before 1972 and have provided a critical compilation of data on the thermodynamics of solution and ionization for the amines in water. More recent work in several laboratories has determined new values for enthalpies of ionization (Christensen *et al.*,1985; Kim *et al.*, 1987; Oscarson *et al.*, 1989), viscosities (Teng *et al.*, 1994; Rinker *et al.*, 1994) , densities (Rinker *et al.*, 1994; Maham *et al.*, 1995; Hsu and Li, 1997), and surface tension (Rinker *et al.*, 1994) of aqueous methyldiethanolamine. Maham *et al.* (1997) and Chiu *et al.*(1999) have measured the molar heat capacities of pure liquid methyldiethanolamine over a range of temperatures. Maham *et al.* (1985) have also reported volumetric data leading to the standard partial molar volumes of methyldiethanolamine for the temperature range 298 K to 353 K. Cobble and Turner (1985) have measured apparent molar heat capacities for methyldiethanolamine and its salt, methyldiethanolammonium chloride ($MDEAH^+Cl^-$) at 298.15 K. The literature values for methyldiethanolamine and methyldiethanolammonium chloride are summarized in Table 3.2.3 and Table 3.2.4 respectively.

1.11 Goals and Objectives

As described in Section 1.1, thermodynamic properties of amine species are needed to model speciation and vapor-liquid equilibria, and for developing predictive

models for their behavior at elevated temperatures and pressures. Partial molar heat capacities and volumes of aqueous methyldiethanolamine in its neutral and ionized forms are important parameters because they define the temperature and pressure dependence of the ionization constant, enthalpy of ionization and activity coefficients. Although volumetric data have been reported for the neutral amine below 373 K (Maham *et al.*, 1995), no measurements for the salt exist in the literature. Aside from the limited data at 298 K reported by Cobble and Turner, there are no measurements of the apparent molar heat capacities of aqueous methyldiethanolamine and its salt. In addition, no measurements of compressibilities or excess heat capacities of either aqueous species have been reported in the literature.

The goals of the work are (i) to obtain accurate thermodynamic data for dilute aqueous solutions of the amine and its salt over a range of conditions which is applicable to power stations and (ii) to obtain thermodynamic data below 373 K for the neutral species at finite concentrations which is applicable to gas processing. The significance of this work lies in the diversity of complementary thermodynamic data obtained using various instrumentation (microcalorimetry, densimetry, and solution acoustics) in order to construct a complete thermodynamic characterization of the chemical systems. The main theme is the study of thermodynamic functions corresponding to first and second derivatives (with respect to p and T) of the Gibbs free energy. While the first derivative properties can reveal some of the peculiarities of aqueous solutions, the singularities of

water and dilute aqueous systems are best evidenced in second derivative functions.

Thus, the objectives of this work are:

(1) Measurement of the apparent molar volumes V_ϕ, apparent molar heat capacities $C_{p,\phi}$, and apparent molar compressibilities κ_ϕ for methyldiethanolamine and its salt.

(2) Calculation of the standard partial molar volumes $V°$, heat capacities $C_p°$, and compressibilities $\kappa_T°$ for each species.

(3) Measurement of molar heat capacities of methyldiethanolamine over the entire mole fraction range within the temperatures 273 K to 373 K and calculation of the excess and reduced excess heat capacities; and the application of appropriate fitting equations such as the Redlich-Kister equation to the data.

(4) Fitting of the density model and the revised HKF model to the experimentally determined data and comparison of the experimentally determined values to those predicted from the models.

Chapter 2: Experimental

2.1 Materials and Solution Preparation

Methyldiethanolamine [$CH_3N(C_2H_4OH)_2$, "MDEA"] was obtained from Aldrich Chemical Company (certified A.C.S.) and was used without further purification. Prior to preparation of the aqueous methyldiethanolamine solution, the nanopure water (resistivity > 17 MΩ·cm) was boiled for 15 to 20 minutes to drive out any dissolved carbon dioxide. A stock solution of methyldiethanolamine was prepared by mass and then standardized by titration with hydrochloric acid. The results agreed to within 0.1 mol percent. Hydrochloric acid solutions were obtained by diluting a 15 mol·kg^{-1} stock solution (Fisher A.C.S. certified reagent grade) and standardized by titration against TRIS [tris(hydroxymethyl)aminomethane; Aldrich, certified A.C.S.]. The various aqueous methyldiethanolamine stock solutions were kept from exposure to CO_2 in air by mixing only one litre at a time, and by minimizing the time of exposure to the surroundings. To further minimize exposure of the solutions to the atmosphere, the solutions were not filtered. More dilute solutions were prepared from the stock solution by mass, using the boiled nanopure water.

A stock solution of methyldiethanolammonium chloride [$CH_3NH(C_2H_4OH)_2Cl$, $MDEAH^+Cl^-$] was prepared by adding an excess weighed amount of standard HCl to the diluted methyldiethanolamine solutions as to obtain a 1 mol per cent excess in order to suppress the deionization of $MDEAH^+Cl^-$ (pH ≈ 2.3).

Aqueous solutions of NaCl (Fisher Scientific, certified A.C.S., crystal) were prepared by mass after drying the salt at 473 K for 24 hours and had a molality of approximately 1 $mol \cdot kg^{-1}$.

2.2 Picker Flow Calorimeter

The Picker flow calorimeter represented in Figure 2.2.1 consists of a tubular sample cell and a reference cell (twin symmetrical cells). Zener diodes (heaters) are attached to the two cells in the up-stream region of the tubes and sensitive thermistors (temperature sensors) in the down-stream area so that the temperature increase generated by the heater in solution can be detected. The heat capacity of a solution in each cell can be determined by:

$$c_p = \frac{W}{f_m \Delta T} \tag{2.2.1}$$

where c_p is the specific heat capacity, W is the electric power input to the heater, f_m is the mass flow rate of the liquid through the cell, and ΔT is the temperature rise produced by the combination of flow rate and electric power. The calorimeter design allows two liquids at the same temperature, which are flowing in twin cells at the same volumetric flow rate, to be heated simultaneously so that the difference in the applied power ΔW necessary to maintain the final temperature of both liquids constant can be recorded. The outlet of the sample cell is connected to the inlet of the reference cell by a teflon tube, the "delay line", so that liquids flow sequentially through the two cells. The electronically

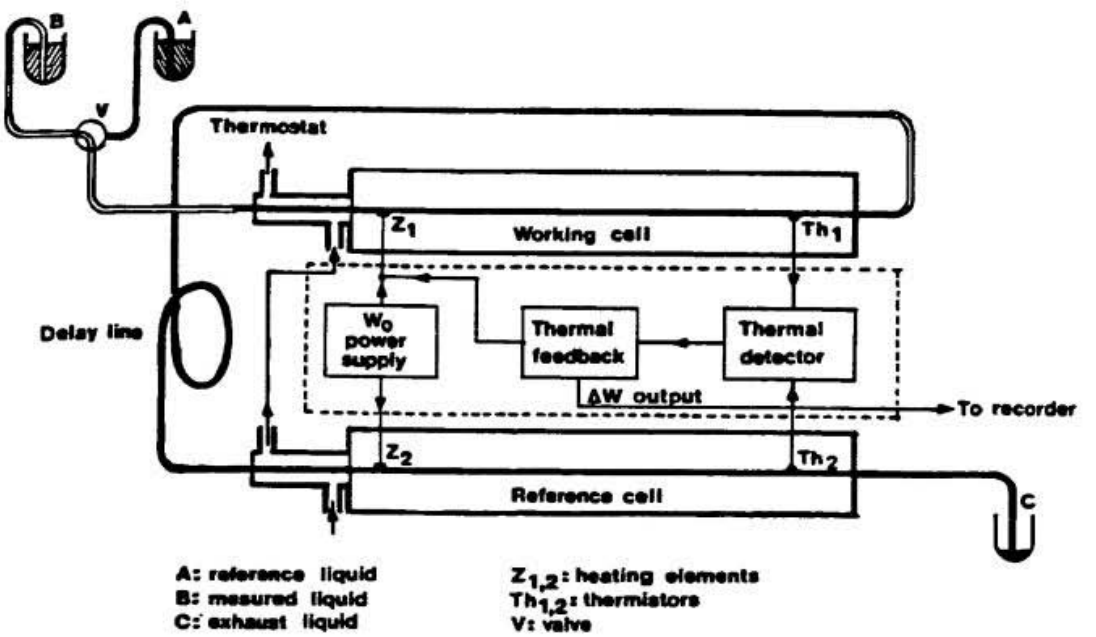

Figure 2.2.1 Schematic diagram of Picker flow calorimeter

controlled thermal feedback and control unit maintains the exact temperature rise in both cells by matching differences in thermistor output resistance through changes in the ratio of the power delivered to the heaters.

Thus, the ratio of the powers supplied to the heaters is proportional to the ratio of heat capacity fluxes through the cells:

$$\frac{c_{p,sol}}{c_{p,l}^{*}} = \left(1 + \frac{ff\Delta W}{W_o}\right)\left(\frac{\rho_l^{*}}{\rho_{sol}}\right) \tag{2.2.2}$$

where $c_{p,sol}$ and $c_{p,l}^{*}$ are the specific heat capacities of the solution and water, respectively; ρ_{sol} and ρ_l^{*} are the densities of the solution and water at the temperature of the delay line, respectively; and ff is the heat leak correction described below.

Desnoyers *et al.* (1976) and White and Wood (1982) observed that the Picker flow calorimeter suffers from very small heat losses due to slight asymmetries in the two cell and loss of heating power through convection, radiation, and conduction through the leads and cell walls. The heat leak correction factor ff is defined by:

$$ff = \frac{(c_p\rho)_{std} - (c_{p,l}^{*}\rho_l^{*})}{(c_p\rho)_{expt} - (c_{p,l}^{*}\rho_l^{*})} \tag{2.2.3}$$

where $(c_p\rho)_{expt}$ and $(c_p\rho)_{std}$ are the product of the specific heat capacity and density for the standard NaCl solution measured in the calibration experiments and that calculated from the literature data (Archer, 1992), respectively.

The electronic circuit was designed in such a way that a constant power W_o is

supplied equally to both cells and a bias DC voltage (negative or positive) which is proportional to the bias power ΔW is applied to the heater on the sample cell. W_o is related to the voltages across the heater on the reference cell and the sample cell, and the total heating current I_o. The currents are determined by measuring the voltages across standard resistors that are connected in series with the heating circuits.

2.3 Low Temperature Density Measurements

The densities of all solutions were obtained by the use of a vibrating tube densimeter (Picker *et al.*, 1974). The measurement principle of the vibrating tube is based on the properties of a mechanical oscillator where the oscillation frequency of the tube is dependent on the total mass of the tube and thus the density of the liquid flowing through the tube (Kratky *et al.*, 1969). The tube is driven to vibrate by the force generated by the interaction between the permanent magnetic field and an alternating current through one of two metal bars located within the poles of the magnet. The AC current induced in the other bar serves to sense the period of vibration. The natural vibration period of the tube is related to the density of the liquid according to the relationship: $\rho = A + K \tau^2$ where A and K are constants unique to the mechanical characteristics of the vibrating tube assembly.

The calibration constant K can be calculated by knowing the densities and time periods of two reference solutions:

$$K = \frac{\rho_2 - \rho_1}{\tau_2^2 - \tau_1^2} \tag{2.3.1}$$

Once the densimeter is calibrated (K is calculated), the density of an aqueous solution can be calculated relative to water by the equation:

$$\rho_{sol} = \rho_1^* + K(\tau_{sol}^2 - \tau_w^2) \tag{2.3.2}$$

where ρ_1^* and ρ_{sol} are the densities of water and the solution and τ_w and τ_{sol} are the corresponding time periods.

The densimeter was connected to a high stability temperature control unit and circulating pump (Sodev models PC-B and CT-L). The temperature was monitored by a thermistor placed in the circulating fluid lines from the temperature bath. Thermistor resistances were measured with a Hewlett-Packard multichannel multimeter (HP 3457A). Frequencies were recorded by a Hewlett-Packard universal counter (HP 5328A) with an integration time of 30 seconds.

2.4 High Pressure and Temperature Density Measurements

High pressure/temperature measurements were obtained using a platinum vibrating-tube densimeter constructed in our laboratory by Xiao (1996) according to the design of Albert and Wood (1984), as modified by Corti and Fernandez-Prini (1990), shown in Figure 2.4.1

The densimeter consists of a alloy U-tube (90% platinum + 10% iridium),

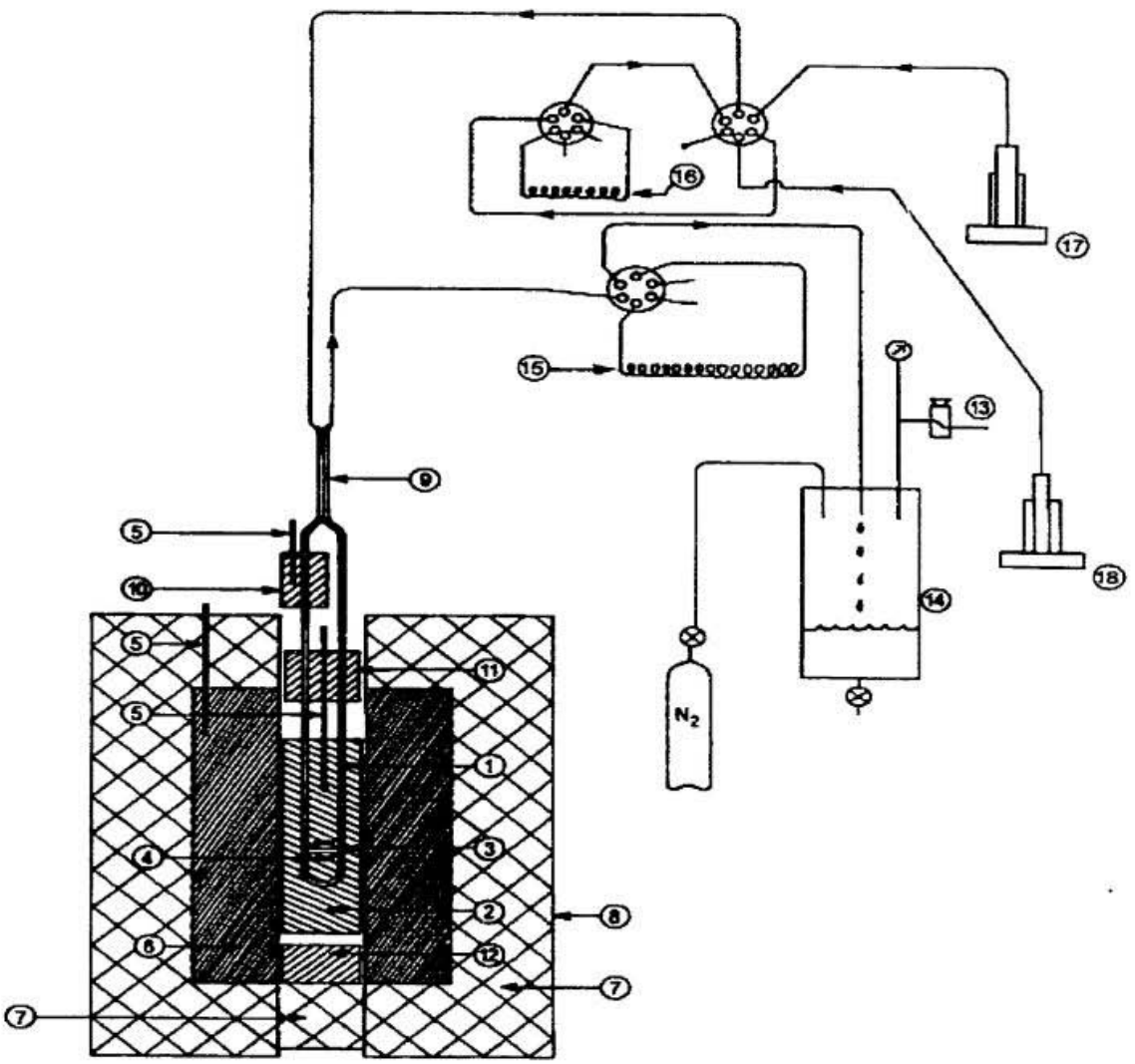

Figure 2.4.1 Schematic diagram of the densitometer. 1, platinum U-shaped vibrating tube; 2, densitometer cell body; 3, Inconel rods for sensing and driver current; 4, permanent magnet; 5, RTD; 6, brass oven; 7, thermal insulation; 8, stainless steel container; 9, heat exchanger; 10, aluminum preheater; 11, aluminum heat shield; 12, brass heat shield; 13, back-pressure regulator; 14, stainless steel reservoir; 15, sampling loop; 16, injection loop; 17, pump; 18, pre-pressurizing pump.

mounted in a cylindrical copper block, so that a permanent horseshoe magnet rests between the two arms of the tube. Two inconel rods positioned between the poles of the magnet are connected to a feedback amplifier using fine silver wires. One of the rods carries the electrical current which drives the vibration of the U-tube while the other carries the induced current which is measured to sense the frequency of vibration. The temperature of the brass cylinder was measured by a 100 Ω platinum RTD and monitored by a Hewlett-Packard 3478A multimeter. The RTD was calibrated to an estimated accuracy of 0.02 K by measuring the ice point of water and the freezing points of tin and lead (supplied by NIST as standard reference materials).

The oven temperature was controlled by an Omega CN2011P2-D3 temperature controller and measured by a 100 Ω platinum RTD located near the outer circumference of the large brass cylinder. Stable temperature control was provided by both the large thermal mass of the large brass cylinder and the insulation surrounding it. The temperature fluctuation measured by the 100 Ω platinum RTD was less than 0.03 K at 523 K.

The exposed inlet and outlet ends of the densimeter U-tube are located outside of the entrance to the oven core. The inlet tube passes through a small aluminum cylinder which serves as a preheater. The aluminum cylinder is surrounded by a Chromalox heater which is controlled independently to 0.2 K by an Omega nozzle heater (HBA - 103027) and an Omega CN7600 PID temperature controller. The heat exchanger,

preheater, and tubing are wrapped in insulation to prevent heat loss.

The sample injection system consisted of an Isco 260D high pressure pump used to deliver water at a constant volumetric flow rate (0.07 ml/min at 298 K). A two-position six-port valve was used to direct the flow of water either directly into the densitometer to act as a reference or into a 15 cm^3 injection loop to force the sample solution into the densimeter. The sample solution was loaded into the injection loop using a second two-position six-port valve and a filling syringe and was pre-pressurized to the system pressure by an HPLC pump. The pressure of the flow system was maintained by nitrogen cylinder and a back-pressure regulator (Tescom model 26-1700). The system pressure was measured by an Omega PX9510 pressure transducer traceable to NIST standards and an Omega DP41-E process indicator. The RTDs were monitored with a Hewlett-Packard 34401A digital voltmeter.

The design for the electronic circuit was based on the phase-locked loop described by Wood *et al.* (1989). Frequencies were measured with a Hewlett-Packard 5316A universal counter. Aqueous NaCl solutions and water were used to calibrate the densitometer at all temperatures and pressures using the literature values of Archer (1992) and Hill (1990), respectively.

2.5 Speed of Sound Measurements

Speed of sound measurements were made on a NUSONIC velocimeter (Mapco,

Model 6080) at 4 MHz based on the sing-around technique (Millero and Kubinski, 1975). The velocimeter is a precision, microprocessor-based laboratory instrument designed to measure the velocity at which ultrasonic pulses (sound waves) travel through a wide variety of liquids. The ultrasonic velocities are obtained by the period of the ultrasonic wave between a transducer and reflector. Use of the NUSONIC velocímeter is limited to liquids that are sonically transparent and the degree of transparency depends on the amount of absorption and scattering, which depends on both the particle (solute) and liquid carrier (solvent).

The electronic portion of the velocimeter consists of three printed-circuit board assemblies (pcb) and a modular subassembly. The printed-circuit board assemblies, shown in block diagram in Figure 2.5.1, are the sound velocity (sv) printed-circuit board, the micro/power supply printed-circuit board, and the LCD printed-circuit board. The electronics primarily consist of solid-state components mounted on the printed-circuit boards contained in a small, portable, metal housing. The housing dimensions are: 5.5 inches wide, 6.5 inches high, and 11 inches deep.

The sample temperature was maintained by circulating water from a Haake temperature controller through the thermostating chamber of the cell. The solution to be analyzed was added to the insulated double-walled glass cell and the transducer element was lowered into the solution and the velocity was recorded. The transmit/receive cycle of the instrument (sing-around technique) involves a piezoelectric crystal element in the

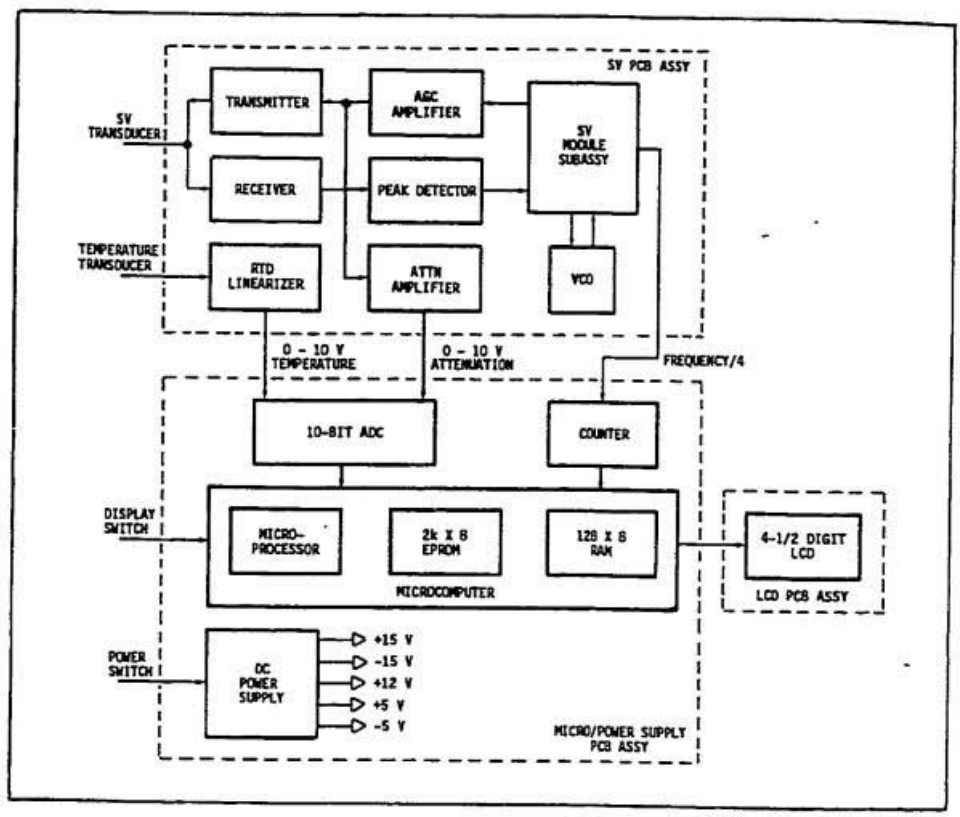

Figure 2.5.1 Block diagram of printed-circuit board assembly of electronic portion of velocimeter

sound velocity transducer which is subjected to a narrow electrical pulse from the transmitter on the sound velocity transducer. Excitation of the element results in the emission of sonic compression waves into the surrounding liquid. These high-frequency waves (in the megahertz region) form a sonic pulse that travels through the liquid to the transducer reflector and back (Figure 2.5.2). The sonic pulse is converted to an electrical signal by the receiving element, amplified in the receiver section, and applied to a peak detector. As soon as the received pulse amplitude reaches an appropriate level, the peak detector produces an output that controls the frequency of a VCO (voltage-controlled oscillator). Thus, the time required for the sonic pulse to travel through the liquid and the temperature govern the VCO frequency. Thus, the sound velocity, in units of $m \cdot s^{-1}$ is obtained from the average round-trip period of the ultrasonic wave in the fixed path length between the piezoelectric transducer and reflector and is computed in the microcomputer of the instrument by solving the equation:

$$u = \frac{fA(1+\alpha T)}{7-(fB*10^{-6})} \qquad (2.5.1)$$

where u is sound velocity ($m \cdot s^{-1}$), A is the sonic path length (0.085157 m), B is the electronic time delay (2.27855 μs), f is the VCO frequency in Hertz, α is the coefficient of thermal expansion of the transducer holder, T is the solution temperature in degrees Celsius, and 7 is a multiplier factor for greater resolution. The values of A, B and α are

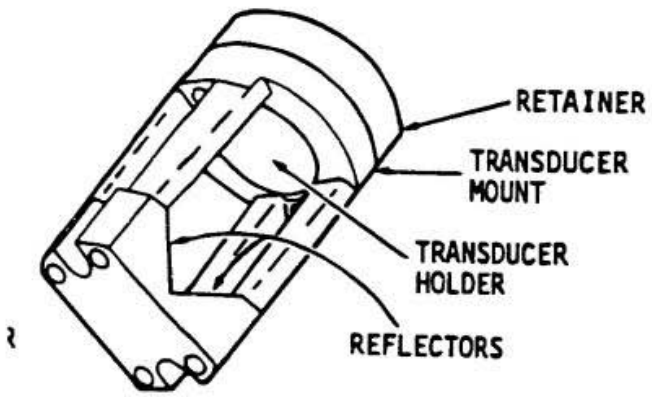

Figure 2.5.2 Schematic of standard velocimeter transducer assembly

determined for each transducer assembly during instrument calibration and stored in the ROM of the electronics system. Experimental investigation of the error was also performed by measuring the molar sound velocity number, [U], of NaCl in the concentration range from 0.04 to 0.18 M defined by $[U]=(U-U_o)/(U_oC)$ where U and U_o are the sound velocities in the solution and solvent, respectively, and C is the molar concentration of the solute. Linear extrapolation to infinite dilution in coordinates [U] vs $C^{1/2}$ yielded $[U]^\circ = 43.2\ cm^3 \cdot mol^{-1}$ which coincides with literature data obtained from independent techniques: 43.3 $cm^3 \cdot mol^{-1}$ (Kharakoz, 1991), 43.4 $cm^3 \cdot mol^{-1}$ (Millero *et al.*, 1977). The estimated error in the measurement of ultrasonic velocity is $\pm 0.02\ m \cdot s^{-1}$.

2.6 Differential Scanning Calorimeter

A CSC Model 4100 programmable differential scanning calorimeter was used to determine heat capacities over the entire mole fraction range for the methyldiethanolamine/water system. The DSC uses semiconductor thermo-electric devices (TED) as detectors and a 1 ml sample volume to achieve a 100X sensitivity over classical DSC instruments. The DSC (Figure 2.6.1) consists of four TED detectors (G) mounted to a common heat sink (A). This sink is isothermally controlled by the RTD temperature control sensor (B) or scanned by the scan TED (C). A 1000 ohm platinum RTD (F) is used to monitor the DSC temperature. The adiabatic shield reduces (by an order of magnitude) the losses from the heat sink to the environment, thus reducing

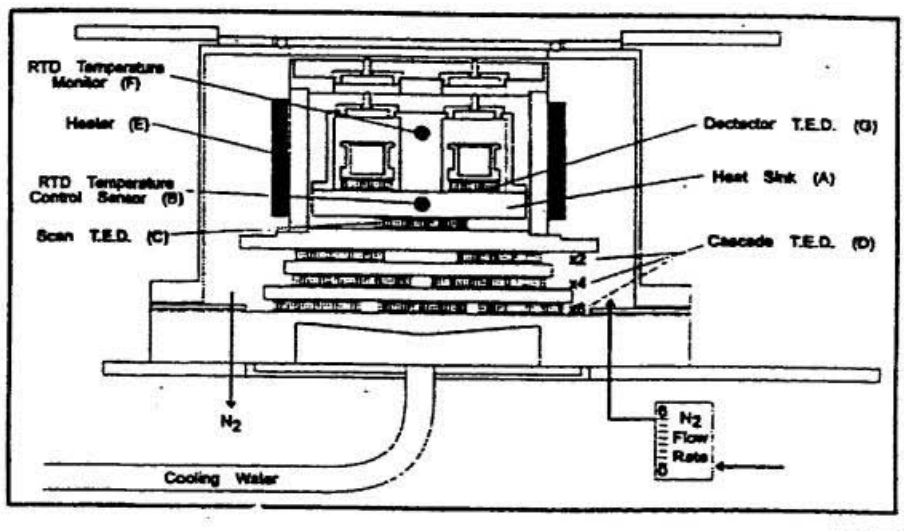

Figure 2.6.1 Cross-section of differential scanning calorimeter measuring unit.

the high sensitivity detectors thermal noise. Dry nitrogen is used to keep moisture from condensing on the measurement area when the DSC is operating below the ambient temperature. The heater (E) and TED cascade (D) are used to allow sufficient heating to scan to 110°C and the TED cascade (D) is used to cool 30°C below bath temperature.

The detector TEDs (G) have a sensitivity near 3 microwatts per microvolt. A high quality four channel DC amplifier (50 nanovolt noise level and gain of 400) is used to allow the DSC to measure 100 milliwatts to a sensitivity of 1 microwatt. Temperature measurement is accomplished using an AC bridge with lock-in amplifier technology. This allows the 1000 ohm platinum film sensor (F) to have low noise while providing linearity of 1 millikelvin over the operating range of the DSC.

A Thaler 22-Bit A/D converter with a CMOS multiplexer is used to convert the analog signal to a digital level. It has a 5 microvolt sensitivity and a ±10 volt input range. The device interfaces to an external personal computer workstation. The workstation uses a high capacity hard disk drive to store collection programs and raw data in the event of a power failure. The data is displayed in columns of temperature, raw data (as differential sensor voltages), and elapsed time. The output signal of the calorimeter is power in μW, or $\mu J \cdot s^{-1}$.

The Hastelloy-C reusable ampoules provided are a matched set of four whose weight were determined to be within 0.1 g of each other during assembly. For each experimental preparation, the ampoules were handled with tweezers to prevent

contamination by fingerprint oils and the sample was accurately weighed into the ampoule. To determine a molar heat capacity throughout the temperature range of interest, two tests must be performed under identical experimental conditions. In the first test, the sample under study is placed in a measurement ampoule and an empty ampoule is placed in the reference chamber. In the second test, referred to as the reference run, the ampoules (all empty) are subjected to the same experimental procedure. Subtracting the calorimetric signal of the reference run from the signal obtained in the first test allows for the correction for the very slight mass differences between the sample and reference ampoules and negates any instrument effects from the experimental data prior to the heat capacity measurements. In a scanning calorimeter, the sample and reference are subjected to the same temperature change and the heat capacity of the sample is determined with respect to the reference from the observed differential calorimetric signal. After completion of the scans, the sample ampoules were removed and reweighed to check for material loss or leakage during the run.

Although the DSC had been calibrated at the factory, the calibration was periodically verified by determining the enthalpy of fusion of ice. The heat of fusion of ice is 333.9 $J \cdot g^{-1}$. During calibration procedures the values obtained were always within 1% of this value (between 330.6 to 337.2 $J \cdot g^{-1}$).

2.7 Calculations

2.7.1 Young's Rule

It is necessary to subtract the contribution of additional solute species from the measured properties of aqueous solutions that contain more than one species in order to obtain the desired property for the solute. For this study, a small amount of excess standardized HCl was added to control speciation. Further, other species can form if the solute dissociates. When dealing with mixed electrolytes, the experimental apparent molar property is defined by

$$Y_{\phi}^{exp} = \frac{Y_{sol} - n_1 Y_1^*}{n_2 + n_3} \tag{2.7.1}$$

in which Y_{sol} is the extensive property of a specified quantity of solution, n_1 is the amount of substance of solvent in this specified quantity of solution, Y_1^* is the property of pure solvent, and n_2 and n_3 are the amounts of substance of each of the solutes in the specified quantity of solution. The presence of the additional species in solution must be accounted for in analyzing the values that come directly from the calorimetric and densimetric measurements. The experimental apparent molar properties of the solution have been separated into terms representing each of the two solutes by using Young's Rule (Young and Smith, 1954):

$$Y_{\phi}^{exp} = \frac{m_2}{m_2 + m_3} Y_{\phi,2} + \frac{m_3}{m_2 + m_3} Y_{\phi,3} + \delta \tag{2.7.2}$$

Here, $Y_{\phi,2}$ and $Y_{\phi,3}$ are the values for the hypothetical solution of the pure components with speciation and ionic strength identical to that of the total solution, and δ is an excess mixing term. Because of the large ratio of m_2 to m_3 and the presence of a common anion, the excess mixing term is ignored in subsequent calculations due to its small value.

2.7.2 Chemical Relaxation

The calculation of apparent molar heat capacities for aqueous solutions containing partially dissociated solutes requires an additional term to account for the shift in the dissociation caused by the temperature increment in the heat capacity measurement, the "chemical relaxation" effect $C_{p,\phi,2}^{exp}$ described by Randall and Taylor (1941), Woolley and Hepler (1977) and Mains *et al.* (1984). For example, if a particular dissociation reaction is more complete at a higher temperature than at a lower, the heat corresponding to the additional fraction of dissociated solute at the higher temperature will be measured as though it were a part of the heat capacity of the solution. The effect is not only limited to reactions that are more complete at higher temperatures (endothermic) but also those that are less complete (exothermic).

When interpreting the effect of chemical relaxation on heat capacities, it is useful to express the heat capacity in terms of the total enthalpy of a mixture (Woolley and Hepler, 1977):

$$C_p^{sol} = \left(\frac{\partial H}{\partial T}\right)_p = \sum_k n_k \left(\frac{\partial H_k}{\partial T}\right)_p + \sum_k H_k \left(\frac{\partial n_k}{\partial T}\right)_p \qquad (2.7.3)$$

The two terms in equation 2.7.3 represent contributions from the species "sp" and the change in the number of moles of each species present (the chemical relaxation effect "rel") so that:

$$C_p^{sol} = \left(\frac{\partial H}{\partial T}\right)_p^{sp} + \left(\frac{\partial H}{\partial T}\right)_p^{rel} \qquad (2.7.4)$$

Thus, the experimental apparent molar heat capacity is calculated from the expression:

$$C_{p,\phi}^{exp} = \frac{\left[\left(\frac{\partial H}{\partial T}\right)_p^{sp} + \left(\frac{\partial H}{\partial T}\right)_p^{rel} - n_1 C_{p,1}^{*}\right]}{n_2} \qquad (2.7.5)$$

The apparent molar heat capacity of the species from solutions containing partially dissociated solutes can be calculated using:

$$C_{p,\phi}^{sp} = C_{p,\phi}^{exp} - \frac{\left(\frac{\partial H}{\partial T}\right)_p^{rel}}{m} \qquad (2.7.6)$$

The relaxation term must be evaluated carefully and can be written as:

$$\left(\frac{\partial H}{\partial T}\right)_p^{rel} = \left(\frac{\partial H^{rel}}{\partial \alpha m}\right)_p \times \left(\frac{\partial \alpha m}{\partial T}\right)_p \qquad (2.7.7)$$

where α represents the fractional extent of the reaction. The quantity $(\partial H/\partial \alpha m)_p$ is directly related to the enthalpy of reaction:

$$\left(\frac{\partial H^{rel}}{\partial \alpha m}\right)_p = \Delta H_{rxn} \qquad (2.7.8)$$

where ΔH_{rxn} corresponds to the enthalpy of the reaction at the ionic strength of interest. The expression for the contribution of chemical relaxation to apparent molar heat capacities can be obtained by substituting Equation 2.7.8 into Equation 2.7.7 and combining with Equation 2.7.6:

$$C_{p,\phi} = C_{p,\phi}^{exp} - \Delta H_{rxn}\left(\frac{\partial \alpha}{\partial T}\right)_p \qquad (2.7.9)$$

In the current study, hydrolysis or dissociation and chemical relaxation effects for aqueous MDEA and its salt are considered and calculations are described in Chapter 3.

2.7.3 Uncertainty of Measurements

For low temperature calorimetric measurements, the error estimates were calculated from the sensitivity limit in determining the ratio of the electric power which includes contributions from fluctuations in heat response, flow rate, cell temperature,

and the accuracy of the calibration factor. According to Picker *et al.* (1971), the overall uncertainty in $\Delta W/W$ and consequently on the relative specific heat capacity is 0.5 per cent. With a ΔT of 1.6 K, the limit of detectability of a change in C_p is 7×10^{-5} $J\cdot K^{-1}\cdot g^{-1}$.

The errors associated with the density measurements using the vibrating tube densimeters come from the random errors associated with the fluctuations of temperature and pressure, the calibration constant, and periods of frequencies measured for water and the solution. It was determined (Xiao and Tremaine, 1997) that the error limits of densities through the temperature range of interest is $\pm$ 0.1 $kg\cdot m^{-3}$ for a 0.1m solution and $\pm$ 0.2 $kg\cdot m^{-3}$ for a 1 molal solution which results in uncertainties in V_ϕ of 1.5 $cm^3\cdot mol^{-1}$ and 0.3 $cm^3\cdot mol^{-1}$, respectively.

One of the main objectives of the work is to determine the standard partial molar properties of the aqueous neutral amine and its salt. The accuracy with which the standard partial molar properties were determined is limited by experimental uncertainty (random and systematic errors) and by the reliability of the extrapolation procedure. Weighted least squares curve fitting techniques have been used to fit equations to the isothermal data obtained at each experimental temperature and then to a "global" model in which temperature dependent parameters were fitted to all the experimental data. The purpose of the global fit was to provide equations for interpolating standard partial molar properties within the range of experimental data. Uncertainties in C_p° and V° were assigned as twice the standard deviation from isothermal fits and twice the estimated

uncertainty in the experimental measurements for the 95 % confidence limit.

2.8 Thermal Decomposition

Féron and Lambert (1992) examined the thermal decomposition of selected aqueous amines at elevated temperatures but unfortunately, methyldiethanolamine was not investigated. To test the thermal stability, or more directly, to detect species that would indicate sample decomposition, proton nuclear magnetic resonance spectroscopy (NMR) was used for the samples which were collected from the densitometer. NMR indicated only methyldiethanolamine with no other species for all samples collected below 523 K (detection limit ~2 percent). Since the measurements involve sample residence times in the high temperature region of the densimeter of less than 6 minutes, we have concluded that no significant decomposition occurred. The aqueous methyldiethanolamine solutions collected at 573 K were a bright orange color (as opposed to the original pale yellow color) which suggested significant decomposition. NMR of these solutions depicted a wide array of peaks which were not present in the original NMR of the pure methyldiethanolamine sample which confirmed decomposition. Solutions of the aqueous methydiethanolammonium chloride solutions were stable up to 573 K.

Chapter 3: Thermodynamics of Dilute Aqueous Methyldiethanolamine (MDEA) and Methyldiethanolammonium Chloride ($MDEAH^+Cl^-$) Solutions: Apparent Molar Volumes, Heat Capacities, and Compressibilities

3.1 Introduction

A continuing program in our laboratory is the investigation of the properties of electrolytes and non-electrolytes at elevated temperatures both because of technological interest and the desire to understand the phenomena of high-temperature hydration effects. As mentioned in Section 1.1, methyldiethanolamine is of interest since its thermodynamic properties are of importance to the electrical power industry, as it is widely used in steam generators as a volatile additive for pH control. Experimental values for apparent molar properties of MDEA in its neutral and ionic forms provide thermodynamic parameters that can be used to estimate the degree of ionization and volatility at elevated temperatures and pressures as well as insight into solvation effects.

In this chapter, we report apparent molar volumes for aqueous solutions of MDEA and $MDEAH^+Cl^-$ at temperatures up to 573 K, as a means of examining the effect of ionization on hydration and the success of various models used to extrapolate standard partial molar properties to elevated temperatures. Apparent molar heat capacities measured over the range 283.15 to 328.15 K are reported, as well as apparent molar isothermal compressibilities calculated from speed of sound measurements over the range 283.15 to 313.15 K.

3.2 Experimental Results

3.2.1 Apparent Molar Volumes

The relative densities of the sample fluids in the vibrating-tube densimeter were determined from the expression:

$$\rho_{sol} - \rho_1^* = K(\tau_{sol}^2 - \tau_w^2) \qquad (3.2.1)$$

where ρ_{sol} and ρ_1^* are the densities of the solution and water, respectively; τ_{sol} and τ_w are the resonance periods for the solution and water, respectively. The calibration constant K was determined by the calibration with water and aqueous NaCl (1 mol·kg^{-1}) using values for the densities of water and NaCl taken from the compilations by Hill (1990) and Archer (1992), respectively.

Both the high temperature and the Sodev vibrating tube densimeters yield experimental data for the relative densities (ρ-ρ_1^*) from which V_ϕ can be calculated. Apparent molar volumes, V_ϕ, were calculated from this function according to the relation:

$$V_\phi = \left(\frac{1000(\rho - \rho_1^*)}{m\rho\rho_1^*}\right) + \left(\frac{M}{\rho}\right) \qquad (3.2.2)$$

where M is the molar mass (119.16 g·mol^{-1} for methyldiethanolamine and 155.62 g·mol^{-1} for methyldiethanolammonium chloride) and m is the molality of the solution.

The ionization constants calculated from the thermodynamic data of Jones and Arnett (1974) indicate the formation of methyldiethanolamine is negligible in the methyldiethanolammonium chloride solutions over the temperature and molalities used in this investigation, in part because of the presence of excess HCl. The effect of the small amount of excess HCl was subtracted by applying Young's rule (equation 2.7.2). The $V_{\phi,3}$ values from $283.15 \leq T \leq 328.15$ K were calculated as functions of ionic strength and temperature from the equations for HCl reported by Tremaine *et al.* (1986). Excess NaOH was not used to suppress the ionization of the neutral species in the methyldiethanolamine solutions. The degree of dissociation in the aqueous methyldiethanolamine solutions was small but significant, and the effect on V_ϕ must be taken into account. Therefore, the resulting V_ϕ values for methyldiethanolamine were corrected for the reaction:

$$CH_3N(C_2H_4OH)_2(aq) + H_2O(l) \rightleftharpoons [CH_3NH(C_2H_4OH)_2]^+(aq) + OH^-(aq) \qquad (3.2.3)$$

using Young's rule.

The experimentally determined relative densities are listed in Table A.1.1 for aqueous methyldiethanolamine and Table A.1.2 for methyldiethanolammonium chloride for the temperature range studied. The tables also tabulate the experimental apparent molar volumes for both aqueous systems. The values of the average temperature and

pressure were calculated from the values recorded under experimental conditions. The values for $V_{\phi,2}$ are plotted as functions of molality in Figures 3.3.1 to 3.3.3 for methyldiethanolamine, and as functions of ionic strength in Figures 3.3.4 to 3.3.6 for methyldiethanolammonium chloride with the Debye-Hückel slope subtracted. The values for $V_{\phi,3}$ up to 573 K needed for the relatively minor Young's rule correction, were estimated from the approximation $V_{\phi,3}(HCl,aq) \approx V^{\circ}(HCl,aq)$ from the compilation of Shock and Helgeson (1992) as calculated with the SUPCRT software package (Johnson *et al.*, 1992).

3.2.2 Apparent Molar Heat Capacities

The Picker flow microcalorimeter yields experimental data for the function $[c_p\rho/(c_{p,1}^{\bullet}\rho_1^{\bullet})-1]$ from which $C_{p,\phi}$ can easily be calculated. Here, $c_p\rho$ and $c_{p,1}^{\bullet}\rho_1^{\bullet}$ are the specific heat capacity and density of the solution and water, respectively. The experimental values of $[c_p\rho/(c_{p,1}^{\bullet}\rho_1^{\bullet})-1]$ for the standard solution of NaCl(aq) were compared with literature values compiled by Archer and Wang (1990) to correct for a small heat leak effect, according to the method of Desnoyers *et al.* (1976). The experimental values of the heat capacity ratios $[c_p\rho/(c_{p,1}^{\bullet}\rho_1^{\bullet})-1]$ of the solutions are listed in Table A.1.3 for methyldiethanolamine and Table A.1.4 for methyldiethanolammonium chloride. The tables also tabulate the experimental apparent molar heat capacities. Young's rule was used to subtract the excess acid using the $C_{p,\phi,3}$ values from 283.15 to

328.15 K calculated from the equations by Tremaine *et al.* (1986). In addition, the calculation for the $C_{p,\phi,2}$ values requires an additional term to account for the shift in the dissociation caused by the temperature increment in the heat capacity, the chemical relaxation effect $C_{p,\phi,2}^{rel}$, described in Section 2.7.2; to yield the expression:

$$C_{p,\phi}^{expt} = (1-\alpha)C_{p,\phi,2}[CH_3N(C_2H_4OH)_2, aq] + \alpha\, C_{p,\phi}[CH_3NH(C_2H_4OH)_2Cl, aq] + \alpha C_{p,\phi}[NaOH, aq] - \alpha C_{p,\phi}[H_2O, l] - \alpha C_{p,\phi}[NaCl, aq] + C_{p,\phi,2}^{rel} \quad (3.2.4a)$$

where $$C_{p,\phi,2}^{rel} = (\Delta H_r)^2\alpha(1-\alpha)/\{RT^2(2-\alpha)\} \quad (3.2.4b)$$

Here α is the fraction of stoichiometric methyldiethanolamine that is dissociated and ΔH_r represents the partial molar enthalpy of dissociation of methyldiethanolamine at the molality of the $C_{p,\phi}^{expt}$ measurement. Equation 3.2.4 is based on the generalized analysis by Mains *et al.* (1984) for equilibria of the form $AB \rightleftharpoons A+B$. The partial molar properties of the minor species in equation 3.2.1 were approximated by the values at infinite dilution, $Y_\phi = Y^\circ$ because α is small under our experimental conditions. ΔH_r° at 298.15 K was taken from Jones and Arnett (1974) and values for other temperatures were determined using $\Delta C_{p,r}^\circ$ at 298.15 K where:

$$\Delta C^{\circ}_{p,r} = C^{\circ}_p[CH_3NH(C_2H_4OH)_2Cl, aq] - C^{\circ}_p[Cl^-, aq] + C^{\circ}_p[OH^-, aq]$$
$$- C^{\circ}_p[CH_3N(C_2H_4OH)_2, aq] - C^{\circ}_p[H_2O, l] \qquad (3.2.5a)$$

and: $$\Delta H_r = \Delta H^{\circ}_{298.15} + \Delta C^{\circ}_{p,r} \Delta T \qquad (3.2.5b)$$

For the purposes of this investigation $\Delta C_{p,r}^{\circ}$ was assumed constant over the temperature range. Values for $C^{\circ}_p[(HOC_2H_4)_2NCH_3,aq]$ and $C^{\circ}_p[(HOC_2H_4)_2NHCH_3Cl,aq]$ were obtained from the data in this investigation, $C^{\circ}_p[Cl^-,aq]$ and $C^{\circ}_p[OH^-,aq]$ were obtained from Hovey *et al.* (1988) and $C^{\circ}_p[H_2O,l]$ was obtained from Hill (1990). The relaxation corrections $C_{p,\phi,2}^{rel}$ for the aqueous solutions are listed in Tables A.1.3 along with the corrected values for $C_{p,\phi,2}$. The $C_{p,\phi,2}$ results for methyldiethanolamine are plotted in Figure 3.3.7 while the values for methyldiethanolammonium chloride are plotted in Figure 3.3.8 with the Debye-Hückel slope subtracted.

3.2.3 Apparent Molar Isothermal Compressibilities

The sound velocities of methyldiethanolamine and methyldiethanolammonium chloride have been measured within a temperature range of $283.15 \leq T \leq 313.15$ K at p = 0.1 MPa. A key experimentally-measurable parameter is the relative molar increment of sound velocity, $[U] = (U-U_0)/(U_0C)$, where U and U_0 are the sound velocities in the solution and solvent, respectively, and C is the molar concentration of the solute.

Significantly, the experimentally measurable parameter [U], is related to the apparent molar volume, V_ϕ, and the apparent molar adiabatic compressibilities, $\kappa_{\phi,S}$, by means of the following expression:

$$\kappa_{s,\phi} = \beta_1^{\bullet}\left(2V_\phi - 2[U] - \frac{M}{\rho_1^{\bullet}}\right) \tag{3.2.6}$$

where $\beta_1^{\bullet}$ and $\rho_1^{\bullet}$ are the adiabatic compressibility and density of water, respectively and M is the molecular weight of the solute. This relationship is valid for dilute solutions when $(U-U_0)/U_0 \leq 1$. If the apparent molar volume of a solute is determined as a function of temperature, then the apparent molar expansivity E_ϕ can be calculated as the temperature slope of the apparent molar volume: $E_\phi = (\partial V_\phi / \partial T)_P$. To determine the apparent molar expansivity, the experimentally measured temperature dependencies of the apparent molar volume of methyldiethanolamine and methyldiethanolammonium chloride at atmospheric pressure were fit to second-order polynomial functions from which first and second temperature derivatives were calculated. For both compounds the fits were excellent with the correlation coefficients higher than 0.998. If the value for $C_{p,\phi}$ is known one can calculate the apparent molar isothermal compressibility κ_T° of the solute using the following expression:

$$\kappa_{T,\phi} = \kappa_{S,\phi} + \left(\frac{T(\alpha_1^{\bullet})^2}{\rho_1^{\bullet} C_{p,1}^{\bullet}}\right)\left[\left(\frac{2E_\phi}{\alpha_1^{\bullet}}\right) - \left(\frac{C_p}{\rho_1^{\bullet} C_{p,1}^{\bullet}}\right)\right] \tag{3.2.7}$$

Apparent molar adiabatic compressibilities, $\kappa_{S,\phi}$, and isothermal compressibilities, $\kappa_{T,\phi}$, were calculated at atmospheric pressure from the data for [U], V_ϕ, E_ϕ, and $C_{p,\phi}$ using equations 3.2.6 and 3.2.7, respectively. Tables A.1.5 and A.1.6 present the resulting data for methyldiethanolamine and methydiethanolammonium chloride.

The concentration dependence of the apparent molar isothermal compressibilities were modeled with simple linear expressions similar in form to those employed by Hershey *et al.*(1984). For methyldiethanolamine, the following equation was employed:

$$\kappa_{\phi,T} = \kappa_T^\circ + km \tag{3.2.8}$$

where the temperature dependence of the standard partial molar isothermal compressibility was described as $\kappa_T^\circ = a_0 + a_1T + a_2T^2$; k is a fitting parameters described as $k = k_0 + k_1T + k_2T^2$, and m is the molality. The apparent molar isothermal compressibility for methyldiethanolammonium chloride was well represented by an extended Debye-Hückel equation:

$$\kappa_{\phi,T} = \kappa_T^\circ - 1.5(Z_-Z_+)A_\kappa[I-2I^{1/2} + 2\ln(1 + I^{1/2})]/I + kI \tag{3.2.9}$$

where I is the ionic strength, $I = \frac{1}{2}\sum m_iZ_i^2$. The value for the Debye-Hückel limiting slope ($A_\kappa = -3.3586\times10^{-3}$ $cm^3\cdot kg^{0.5}\cdot mol^{-1.5}\cdot MPa^{-1}$) for $\kappa_{\phi,T}$ was taken from the compilation by

Archer and Wang (1992).

Isothermal forms of equations 3.2.8 and 3.2.9 were fitted to the experimental results at each temperature by the Marquardt-Levenberg non-linear least-squares algorithm. The entire array of values at all temperatures and all concentrations was then used to optimize the parameters in the equations in order to obtain a global fit to the data. As will be explained in the next section, a weighting factor equivalent to the concentration for each data point was used in the fits.

The fitted parameters are listed in Table 3.2.1 along with their standard deviations. The values of the apparent molar isothermal compressibilities at infinite dilution for the amine and its salt, κ_T° are listed in Table 3.2.2 for each temperatures studied. The results are plotted as functions of molality in Figure 3.2.1 for methyldiethanolamine and as functions of ionic strength in Figure 3.2.2 for methyldiethanolammonium chloride. The Debye-Hückel slopes have been subtracted from the compressibilities of methydiethanolamine hydrochloride in Figure 3.3.2 to linearize the behavior of this apparent molar property. Relaxation corrections were not performed for the compressibilities due to the small fraction of stoichiometric $CH_3N(C_2H_4OH)_2$ that is dissociated.

Table 3.2.1 Fitting parameters for apparent molar isothermal compressibilities (equations 3.2.8 and 3.2.9) for methyldiethanolamine and methyldiethanolammonium chloride.

Parameter	Methyldiethanolamine	Methyldiethanolammonium Chloride
a_0	-0.7449	-1.8477
$a_1 \cdot 10^{-3}$	4.2023	11.6724
$a_2 \cdot 10^{-5}$	-0.5719	-1.8462
k_0	-3.876e-4	0.1536
$k_1 \cdot 10^{-4}$	-0.2481	-11.876
$k_2 \cdot 10^{-6}$	0.1107	2.2148

Table 3.2.2 Standard partial molar isothermal compressibilities κ_T° of methyldiethanolamine and methyldiethanolammonium chloride

	Methyldiethanolamine
T (K)	κ_T° ($cm^3 \cdot MPa^{-1} \cdot mol^{-1}$)
283.15	-0.01355
298.15	-0.000387
313.15	0.01020

	Methyldiethanolammonium Chloride
T (K)	κ_T° ($cm^3 \cdot MPa^{-1} \cdot mol^{-1}$)
283.15	-0.02283
298.15	-0.00872
313.15	-0.00292

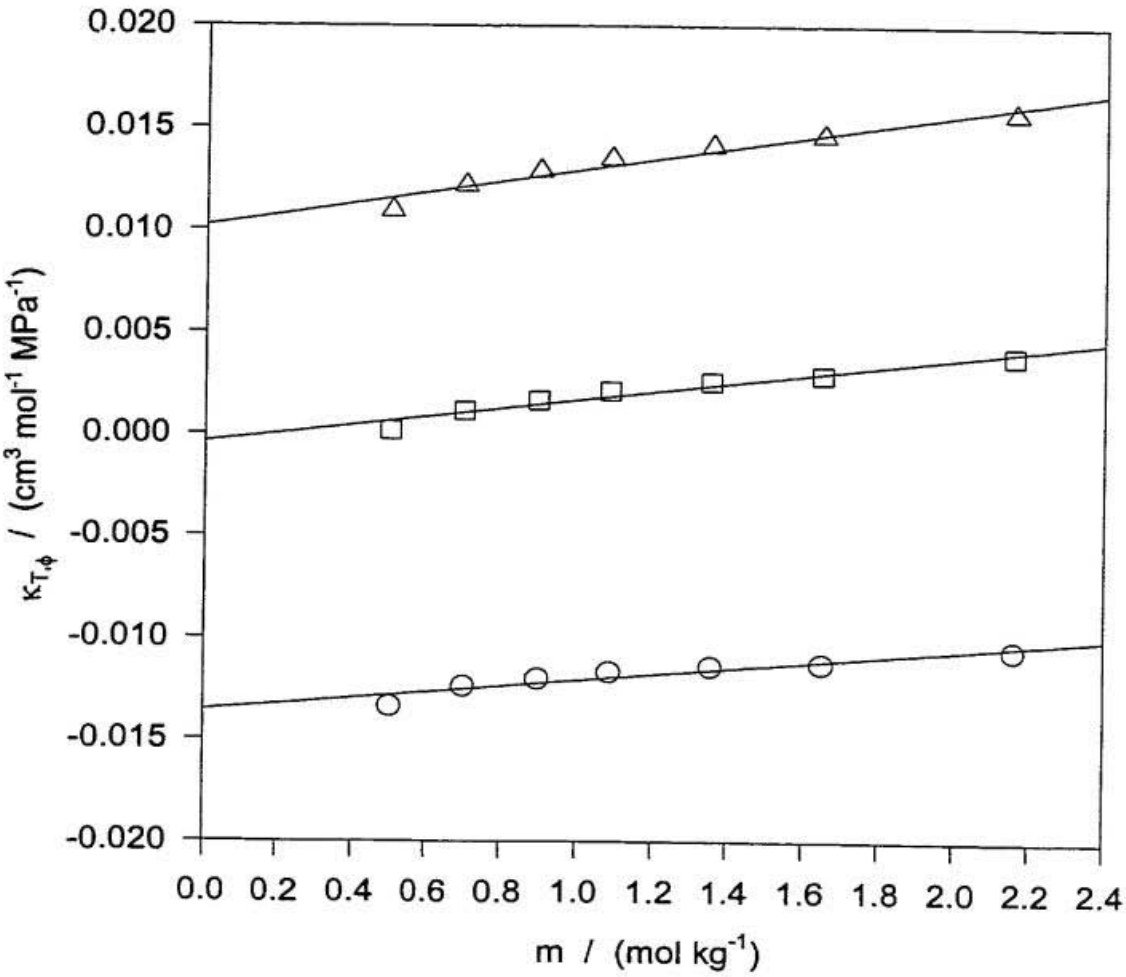

Figure 3.2.1 Apparent molar isothermal compressibilities $\kappa_{T,\phi}$ of methyldiethanolamine at 0.1 MPa plotted against molality. Symbols are experimental results: ○ 283.15 K; □ 298.15 K; Δ 313.15 K. Lines represent global fit of equation 3.2.8

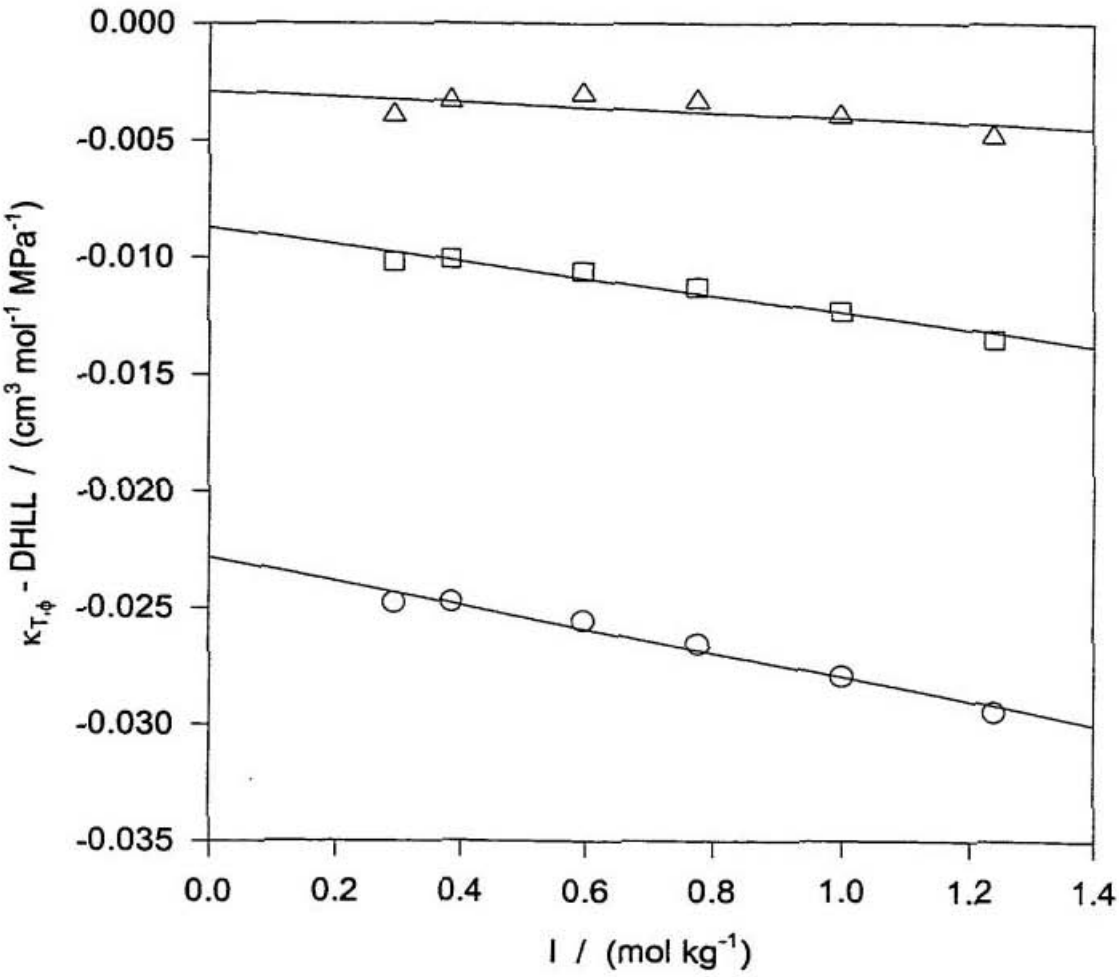

Figure 3.2.2 Apparent molar isothermal compressibilities $\kappa_{T,\phi}$ of methyldiethanolammonium chloride at 0.1 MPa plotted against molality after subtraction of Debye-Hückel limiting law term. Symbols are experimental results: ○ 283.15 K; □ 298.15 K; Δ 313.15 K. Lines represent global fit of equation 3.2.9

In Sections 3.3 and 3.4, fitting equations based on the density and HKF models used in this thesis are described. Although both models include expressions for the standard partial molar isothermal compressibility, the experimentally determined standard partial molar isothermal compressibilities from this section were not directly used in the global fits. Instead, the apparent molar compressibilities determined at 0.1 MPa were used with the low-temperature apparent molar volumes at 0.1 MPa to calculate values of V_ϕ at elevated pressures. Since the fitting expressions for the V_ϕ and $\kappa_{T,\phi}$ contain the same fitting parameters, these parameters were used to observe how adequately the models reproduced the standard partial molar isothermal compressibilities.

3.2.4 Comparison of Experimental and Literature Results

Although there are no reported high temperature studies on aqueous methyldiethanolamine, the low temperature experimental data can be compared to those in the available literature. A selection of literature values for methyldiethanolamine and methyldiethanolammonium chloride are summarized in Tables 3.2.3 and 3.2.4, respectively. The standard partial molar volumes of methyldiethanolamine were determined by Maham *et al.* (1995) at temperatures from 298.15 to 353.15 K. The value of 109.5 $cm^3 \cdot mol^{-1}$ for the standard partial molar volume at 298.15 K compares well with the value of 109.9 ± 0.5 $cm^3 \cdot mol^{-1}$ determined in our study.

The standard partial molar heat capacity of methyldiethanolamine determined by .

Table 3.2.3 Standard partial molar volumes (Mather *et al.*, 1995), standard partial molar heat capacities (Cobble and Turner, 1985), and molar heat capacities (Maham *et al.*, 1997) of methyldiethanolamine (MDEA) as reported in literature.

Maham *et al.* (1995)		Cobble and Turner (1995)		Maham *et al.* (1997)	
T (K)	V° ($cm^3 \cdot mol^{-1}$)	T (K)	C_p° ($J \cdot K^{-1} \cdot mol^{-1}$)	T (K)	$C_{p,m}$ ($J \cdot K^{-1} \cdot mol^{-1}$)
298.15	109.5	298.15	380.9	299.1	270.9
303.15	110.0			322.8	281.9
313.15	110.7			348.5	298.2
323.15	111.4			373.2	314.6
333.15	112.5			397.8	329.4
343.15	113.1				
353.15	113.8				

Table 3.2.4 Standard partial molar heat capacity (Cobble and Turner, 1985) of methyldiethanolammonium chloride ($MDEAH^+Cl^-$) as reported in literature.

T (K)	C_p° ($J \cdot K^{-1} \cdot mol^{-1}$)
298.15	198.8

Cobble and Turner (1985) is 380.9 $J \cdot K^{-1} \cdot mol^{-1}$ compared to 384.9 ± 4.2 $J \cdot K^{-1} \cdot mol^{-1}$ from this study.

Our value of C_p° = 194.3 ± 5.3 $J \cdot K^{-1} \cdot mol^{-1}$ for methyldiethanolammonium chloride compares well with the value of 198.8 $J \cdot K^{-1} \cdot mol^{-1}$ reported by Cobble and Turner (1985). Since Cobble and Turner investigated numerous amines, they obtained amines from various sources that were not of uniformly high purity and they failed to explicitly report the specific purity of the methyldiethanolamine used.

One of the aims of systematic studies of organic solutes is to devise methods of predicting the thermodynamic properties of large molecules from additivity rules. Therefore, it is possible to compare the experimental results at 298.15 K to those predicted by group additivity models such as those developed by Guthrie (1977), Perron and Desnoyers (1979), and Gianni and Lepori (1996). The predicted values for the standard partial molar volumes, $V^\circ\{CH_3N(C_2H_4OH)_2, aq\}$ = 110.0 $cm^3 \cdot mol^{-1}$ and $V^\circ\{CH_3NH(C_2H_4OH)_2Cl, aq\}$ = 123.5 $cm^3 \cdot mol^{-1}$, are in excellent agreement with the experimental values of 109.9 ± 0.5 $cm^3 \cdot mol^{-1}$ and 123.3 ± 0.6 $cm^3 \cdot mol^{-1}$, respectively. The predicted values for the standard partial molar heat capacities are less accurate: $C_p^\circ\{CH_3N(C_2H_4OH)_2, aq\}$ = 377.0 $J \cdot K^{-1} \cdot mol^{-1}$ compares somewhat poorly with the experimental value of 384.9 ± 4.2 $J \cdot K^{-1} \cdot mol^{-1}$. There is no literature value for the group contribution of $C_p^\circ\{>NHCl,aq\}$ so it was not possible to calculate $C_p^\circ\{CH_3NH(C_2H_4OH)_2Cl, aq\}$. Errors may be introduced by the fact that group additivity

schemes do not take into account the arrangement of these atoms or groups in a molecule. It is believed that C_p° is sensitive to secondary solvation effects, while V° primarily reflects the intrinsic volume of the solute molecule and effects in the primary solvation sphere. The presence and location of the functional groups attached to the nitrogen may affect their contribution to the overall partial molar heat capacities and perturb the secondary solvation sphere. Thus, it is difficult to assign parameters for atomic contributions to C_p° since the hybridization state and hydrogen bonding ability of the groups are important to the effect of the solute upon the organization of water molecules.

3.3 "Equations of State" for Aqueous Methyldiethanolamine and Methyldiethanolammonium Chloride: The Density Model

The molality dependence of the apparent molar volume and apparent molar heat capacity data for methydiethanolamine could be described closely by simple linear expressions:

$$V_\phi = V^\circ + vm \tag{3.3.1}$$

$$C_{p,\phi} = C_p^\circ + cm \tag{3.3.2}$$

whereas, the apparent molar volumes and heat capacities of methyldiethanolammonium chloride were described adequately by the Guggenheim form of the extended Debye-Hückel equation:

$$V_\phi = V^\circ + 1.5(Z_-Z_+)A_c\left[I - 2I^{1/2} + 2\ln(1+I^{1/2})\right]/I + vI \qquad (3.3.3)$$

$$C_{p,\phi} = C_p^\circ + 1.5(Z_-Z_+)A_v\left[I - 2I^{1/2} + 2\ln(1+I^{1/2})\right]/I + cI \qquad (3.3.4)$$

Here, V_ϕ and $C_{p,\phi}$ are the apparent molar volume and heat capacity, respectively, V° and C_p° are the standard partial molar volume and heat capacity, respectively; m and I ($I = 1/2 \cdot \Sigma m_i Z_i^2$) are the molality and ionic strength of the aqueous amine solutions, respectively, and v and c are functions which depend on temperature and pressure. Values for the Debye-Hückel limiting slopes, A_c and A_v, were calculated from the formulation reported by Archer and Wang (1992).

The model used to fit the temperature and pressure dependencies of the data is an extension of the density model used by Mesmer *et al.* (1988) to describe the behavior of log K under hydrothermal conditions (Section 1.7):

$$V^\circ = a_0 - \left(a_1T^2 + a_2T + a_3 + \frac{a_4}{T} + \frac{a_5}{T^2}\right)\left(R\beta_1^*\right) \qquad (3.3.5)$$

$$\Delta C_p^\circ = -2.303R\left[\left(\frac{-2a_6}{T^2} - \frac{6a_7}{T^3} + 2a_8T\right) + \left(-2a_1T - \frac{-2a_4}{T^2} - \frac{6a_5}{T^3}\right)\log\rho_1^*\right]$$
$$-R\alpha_1^*\left(2a_2T - \frac{2a_4}{T} - \frac{4a_5}{T^2} + 4a_1T^2\right) - RT^2k\left(\frac{\partial\alpha_1^*}{\partial T}\right)_p \qquad (3.3.6)$$

$$\kappa_T{}^\circ = R\left(a_1T^2 + a_2T + a_3 + \frac{a_4}{T} + \frac{a_5}{T^2}\right)\left(\frac{\partial\beta_1^*}{\partial p}\right)_T \qquad (3.3.7)$$

$$k = a_1 T + a_2 + \frac{a_3}{T} + \frac{a_4}{T^2} + \frac{a_5}{T^3} \tag{3.3.8}$$

$$v = v_1 + (v_2 + v_3 T)(R\beta_1^*) \tag{3.3.9}$$

$$c = (c_1 + c_2 T)R\left(\frac{\partial \alpha_1^*}{\partial T}\right)_p \tag{3.3.10}$$

The fitting parameters are a_0 - a_8, v_1, v_2, v_3, c_1, c_2, and c_3. The compressibility coefficient, β_1^*, is equal to $-(1/\rho_1^*)(\partial\rho_1^*/\partial p)_T$ while the expansitivity coefficient, α_1^* is equal to $-(1/\rho)(\partial\rho_1^*/\partial T)_p$ where ρ_1^* is the density of water. Mesmer *et al.*(1991) observed that acid-base equilibrium constants at constant density are linear functions of reciprocal temperatures over a very wide range which yields the terms containing β_1^* and $(\partial\alpha_1^*/\partial T)$ upon differentiation. Values of α_1^* and β_1^* were calculated from the Hill (1990) equation of state. Statistical mechanics also show that solute partial molar volumes should be related to $\beta_1^* T$, and that partial molar heat capacities should be related to $(\partial\alpha_1^*/\partial T)_p T$ as required by the density model (Levelt Sengers, 1991). The parameters that were absent in the original model (a_0, a_1, a_4, a_5, and a_8) were needed to increase the versatility of the model in fitting the temperature and pressure dependence of the experimental data and to include the standard partial molar compressibility results.

Equations 3.3.1 to 3.3.4 were fitted to the experimental results by the Marquardt-Levenberg least squares algorithm within the commercial software package Sigma-Plot©.

The entire array of values at all temperatures and molalities was then used to optimize the parameters in equations 3.3.5 to 3.3.10 by the least squares curve-fitting program. The variety of the data required that each data point be assigned a weight. It was observed by Xiao and Tremaine (1996) that the uncertainty associated with experimental apparent molar properties increases as the molality or ionic strength of the aqueous solution decreases. Therefore, the apparent molar volumes and heat capacities measured were given a weight equal to the molality of the solution. For the standard partial molar properties at each temperature and pressure the weight assigned was equal to the combined sum of the concentrations of the aqueous solutions. The overall standard deviation of the apparent molar volumes of MDEA and $MDEAH^+Cl^-$ are 0.42 and 0.63 $cm^3 \cdot mol^{-1}$, respectively. The standard deviations of the apparent molar heat capacities of MDEA and $MDEAH^+Cl^-$ are 2.4 and 1.9 $J \cdot K^{-1} \cdot mol^{-1}$, respectively. It is estimated that the combined statistical and estimated uncertainty lead to an uncertainty of $\pm$ 1.0 $cm^3 \cdot mol^{-1}$ or less in V° and $\pm$ 6 $J \cdot K^{-1} \cdot mol^{-1}$ or less in C_p°.

Table 3.3.1 contains the values obtained from fitting equations 3.3.1 and 3.3.2 for methyldiethanolamine and fitting equations 3.3.3 and 3.3.4 for methydiethanolammonium chloride to each set of isothermal data. The fitting parameters obtained using the density model are tabulated in Table 3.3.2 along with their standard deviations. The fitted apparent molar volumes of methyldiethanolamine are shown in Figures 3.3.1 to 3.3.3 and the fitted isotherms of the apparent molar heat capacities are

shown in Figure 3.3.7. In Figures 3.3.4 to 3.3.6, the fitted apparent molar volumes of methydiethanolammonium chloride are plotted while the fitted apparent molar heat capacities are plotted in Figure 3.3.8.

Table 3.3.1 Values of V°, v, C_p°, and c obtained from fitting equations 3.3.1 and 3.3.2 for methydiethanolamine and fitting equations 3.3.3 and 3.3.4 for methyldiethanolammonium chloride to each set of isothermal data.

T K	*p* MPa	V° $cm^3 \cdot mol^{-1}$	v $cm^3 \cdot kg \cdot mol^{-2}$	C_p° $J \cdot K^{-1} \cdot mol^{-1}$	c $J \cdot kg \cdot K^{-1} \cdot mol^{-2}$
			Methyldiethanolamine		
283.15	0.100	108.91 ± 0.05	-0.67 ± 0.05	374.81 ± 2.45	-22.38 ± 2.12
298.15	0.100	109.92 ± 0.04	-0.39 ± 0.03	384.92 ± 0.56	-11.13 ± 0.51
313.15	0.100	111.01 ± 0.03	-0.23 ± 0.03	396.76 ± 0.74	-6.73 ± 0.68
328.15	0.100	112.03 ± 0.04	-0.21 ± 0.03	411.30 ± 1.67	-8.53 ± 1.36
337.47	10.186	112.43 ± 0.09	-0.01 ± 0.03		
425.94	10.322	122.64 ± 0.07	0.12 ± 0.02		
523.34	10.400	141.13 ± 0.15	-0.03 ± 0.02		
335.21	20.190	111.12 ± 0.52	0.38 ± 0.02		
384.00	20.216	116.81 ± 0.07	0.14 ± 0.03		
424.37	20.182	121.98 ± 0.15	0.11 ± 0.06		
475.67	20.088	129.34 ± 0.18	0.20 ± 0.07		
524.57	20.083	139.69 ± 0.13	-0.04 ± 0.02		
			Methyldiethanolammonium Chloride		
283.15	0.100	121.41 ± 0.04	0.35 ± 0.05	171.16 ± 2.22	1.87 ± 0.32
298.15	0.100	123.32 ± 0.04	0.10 ± 0.05	194.31 ± 0.52	5.78 ± 0.75
313.15	0.100	124.39 ± 0.02	0.11 ± 0.05	217.31 ± 0.46	3.62 ± 0.66
328.15	0.100	125.43 ± 0.07	-0.21 ± 0.05	228.7 ± 1.19	3.78 ± 1.50
422.91	10.253	127.41 ± 0.24	-1.84 ± 0.05		
522.98	10.377	105.49 ± 0.53	0.58 ± 0.05		
334.22	20.049	126.02 ± 0.43	0.75 ± 0.05		
377.10	20.204	127.58 ± 0.13	-0.05 ± 0.05		
426.72	20.220	126.89 ± 022	-1.36 ± 0.05		
475.06	20.179	122.52 ± 0.35	1.30 ± 0.05		
523.78	20.161	109.19 ± 0.10	0.27 ± 0.05		
576.35	20.201	65.25 ± 0.31	-1.80 ± 0.05		

Table 3.3.2 Fitting parameters for density model (equations 3.3.5 to 3.3.10) where the standard deviation for each parameter is given in parentheses.

Parameter	Methyldiethanolamine	Methyldiethanolammonium Chloride
a_0 / $cm^3 \cdot mol^{-1}$	114.038 (2.112)	132.558 (3.502)
a_1 / K^{-1}	0.35312 (0.1418)	-0.23311 (.08149)
a_2	-475.581 (22.08)	443.543 (13.57)
$a_3 \cdot 10^{-5}$ / K	2.1889 (1.27)	-2.88458 (0.816)
$a_4 \cdot 10^{-7}$ / K^2	-4.177 (0.318)	7.8189 (0.211)
$a_5 \cdot 10^{-9}$ / K^3	2.9079 (0.294)	-7.3604 (0.2008)
$a_6 \cdot 10^{-6}$ / K^2	1.8535 (0.0548)	-1.6486 (0.4551)
$a_7 \cdot 10^{-7}$ / K^3	-9.4276 (0.0415)	15.2729 (3.448)
$a_8 \cdot 10^{4}$ / K^{-1}	-2.664 (0.00485)	244.63 (40.26)
v_1 / $cm^3 \cdot kg \cdot mol^{-2}$	2.1773 (0.3012)	-1.0991 (0.891)
$v_2 \cdot 10^{-3}$ / $kg \cdot mol^{-1} \cdot K$	-1.353 (0.183)	0.6954 .0478)
v_3 / $kg \cdot mol^{-1}$	2.17977 (0.2953)	-1.1915 (0.753)
$c_1 \cdot 10^{-5}$ / $kg \cdot mol^{-1} \cdot MPa^2$	-5.141 (0.2685)	-2.612 (0.436)
$c_2 \cdot 10^{-3}$ / $kg \cdot mol^{-1} \cdot MPa^2 \cdot K^{-1}$	1.226 (0.908)	0.9634 (0.148)

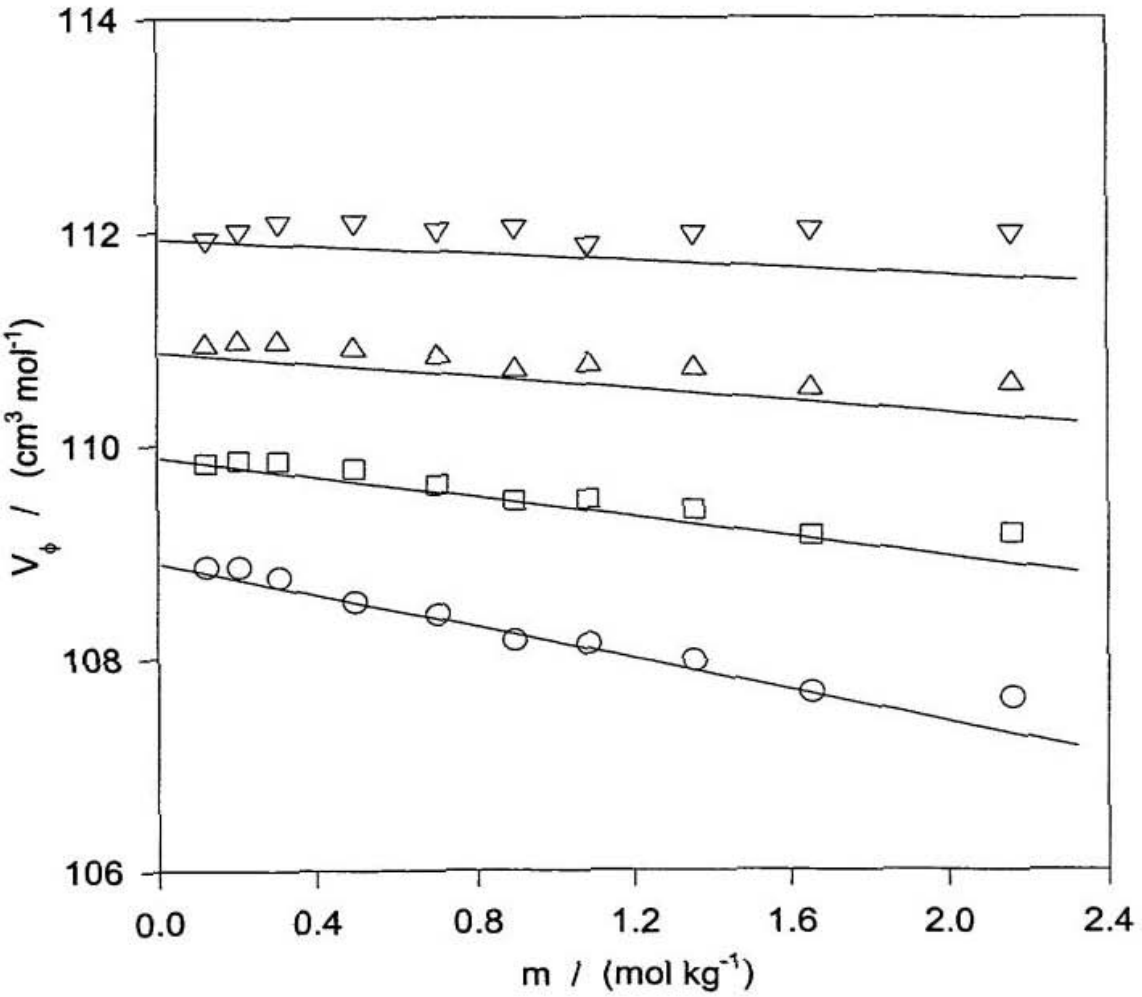

Figure 3.3.1 Apparent molar volumes V_ϕ of methyldiethanolamine at 0.1 MPa plotted against molality. Symbols are experimental results: ○ 283.15 K; □ 298.15 K; Δ 313.15 K; ▽ 328.15 K. Lines are fitted values from density model.

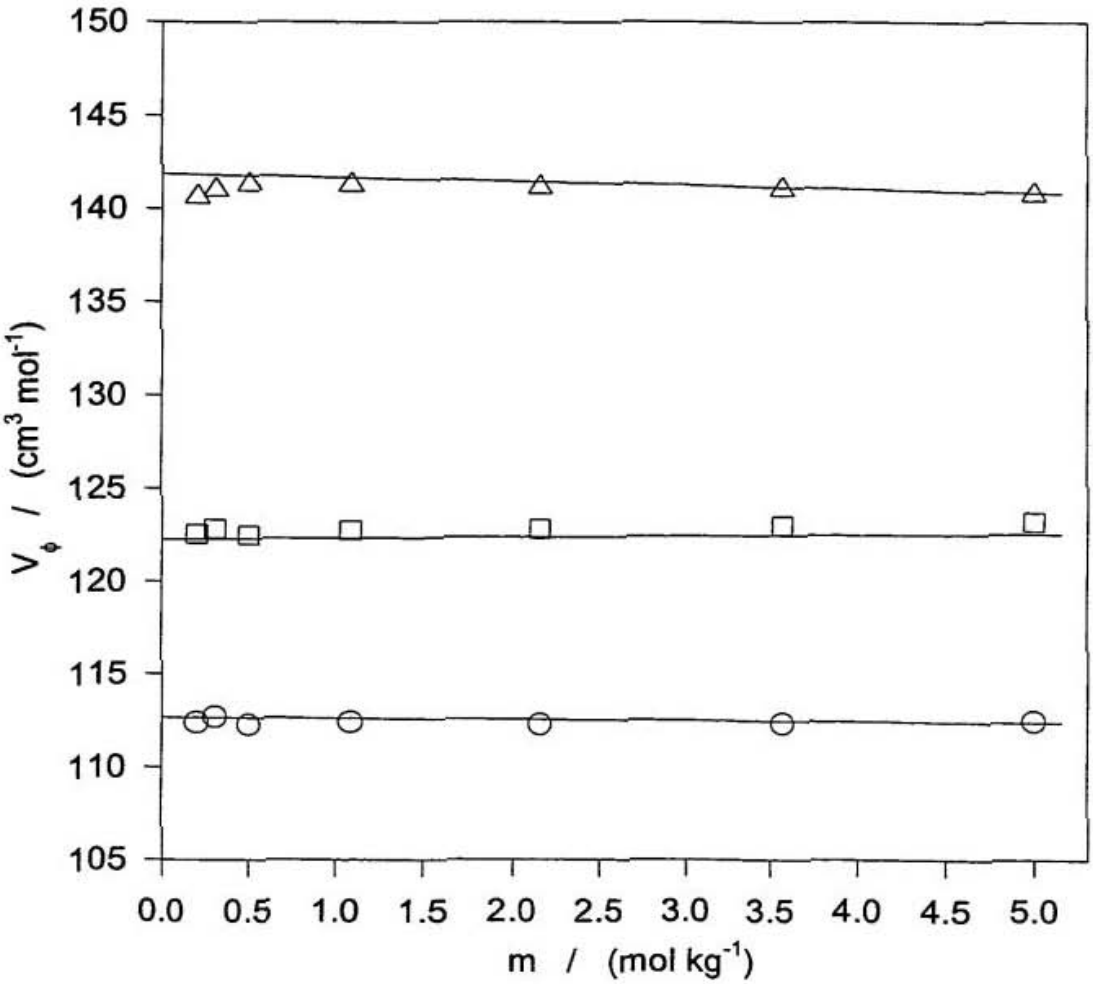

Figure 3.3.2 Apparent molar volumes V_ϕ of methyldiethanolamine at 10.3 MPa plotted against molality. Symbols are experimental results: ○ 337.47 K; □ 425.94 K; Δ 523.34 K. Lines are fitted values from density model.

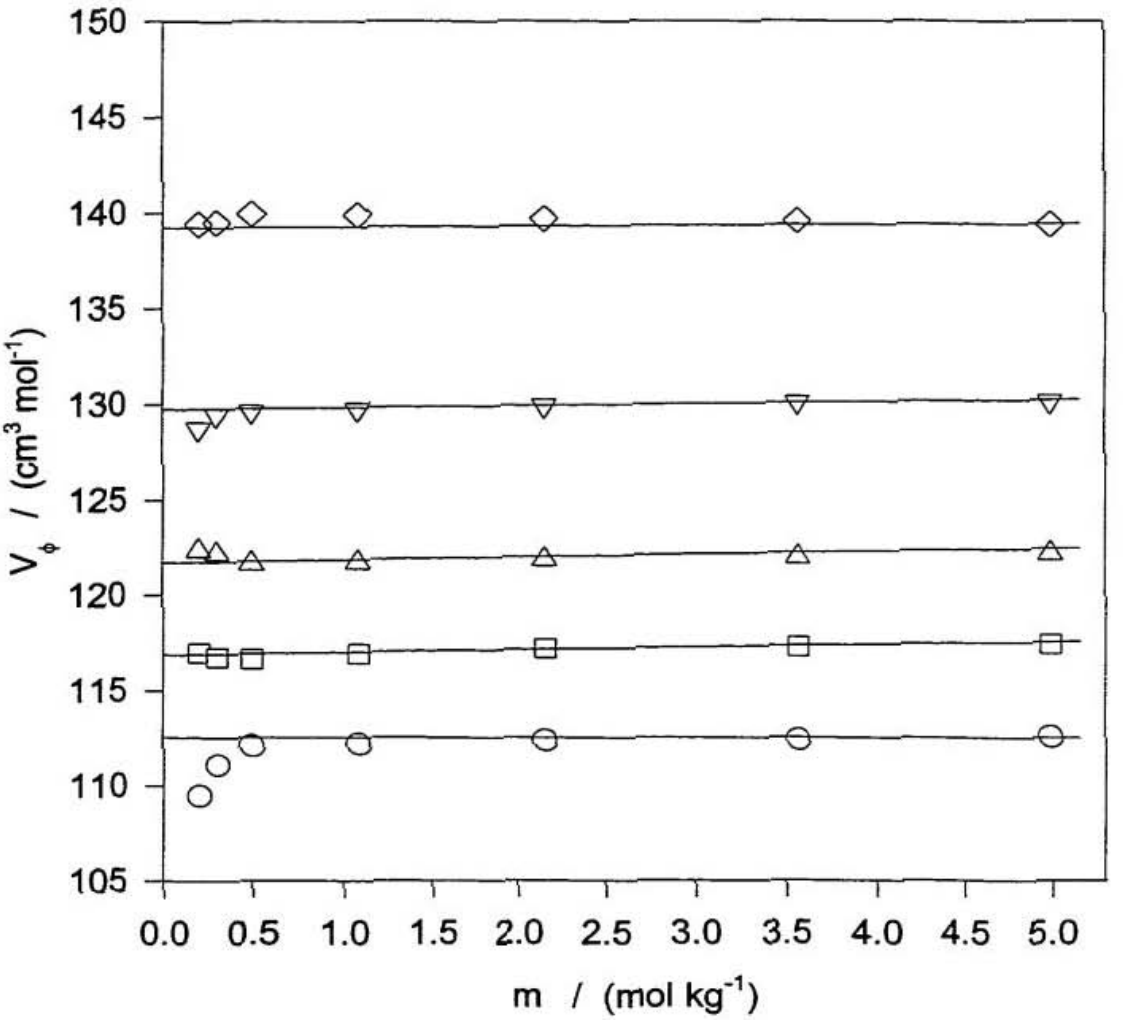

Figure 3.3.3 Apparent molar volumes V_ϕ of methyldiethanolamine at 20.1 MPa plotted against molality. Symbols are experimental results: ○ 335.21 K; □ 384.00 K; Δ 424.37 K; ∇ 475.67 K; ◇ 524.57 K. Lines are fitted values from density model.

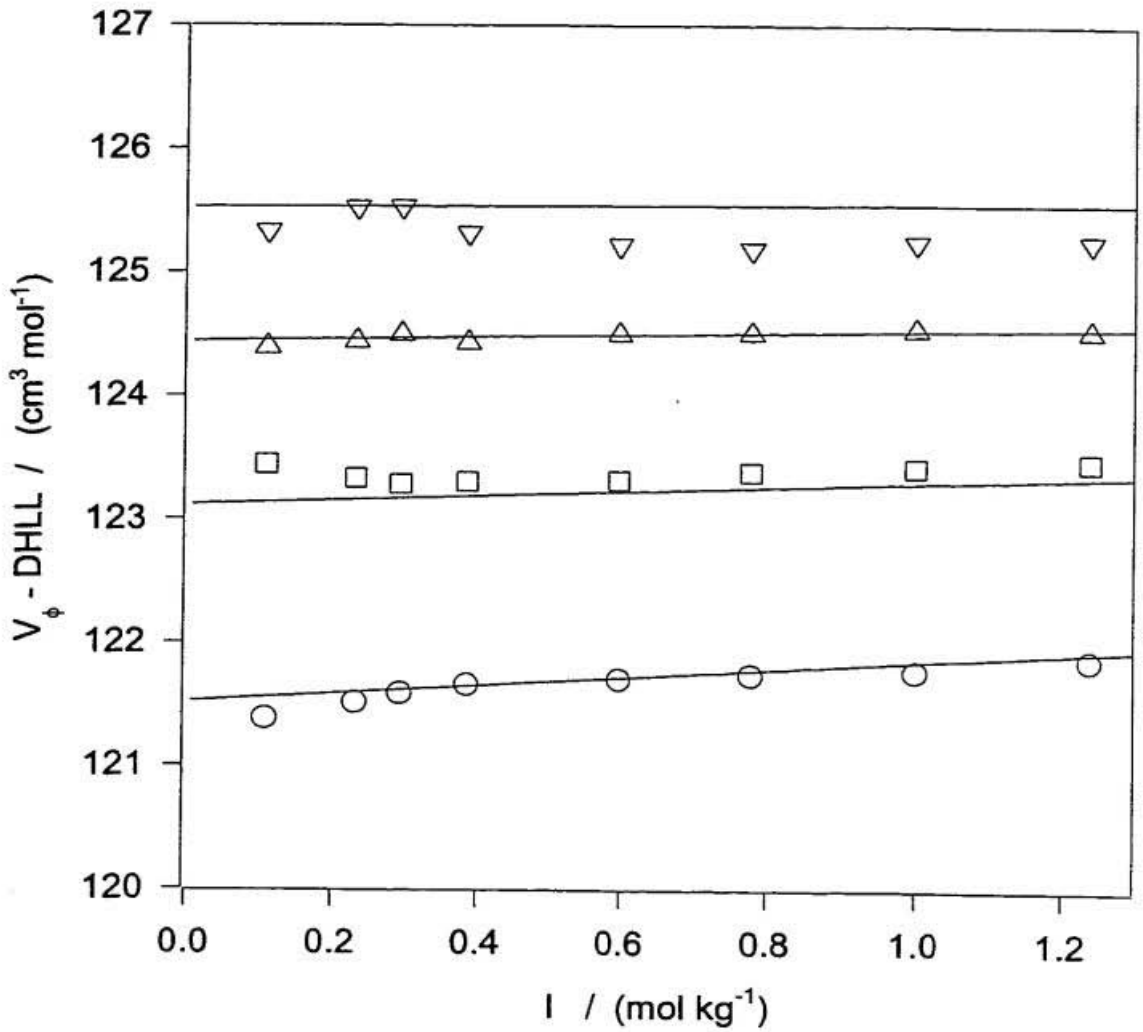

Figure 3.3.4 Apparent molar volumes V_ϕ of methyldiethanolammonium chloride at 0.1 MPa plotted against ionic strength after subtraction of the Debye-Hückel limiting law term. Symbols are experimental results: ○ 283.15 K; □ 298.15 K; Δ 313.15 K; ▽ 328.15 K. Lines are fitted values from density model.

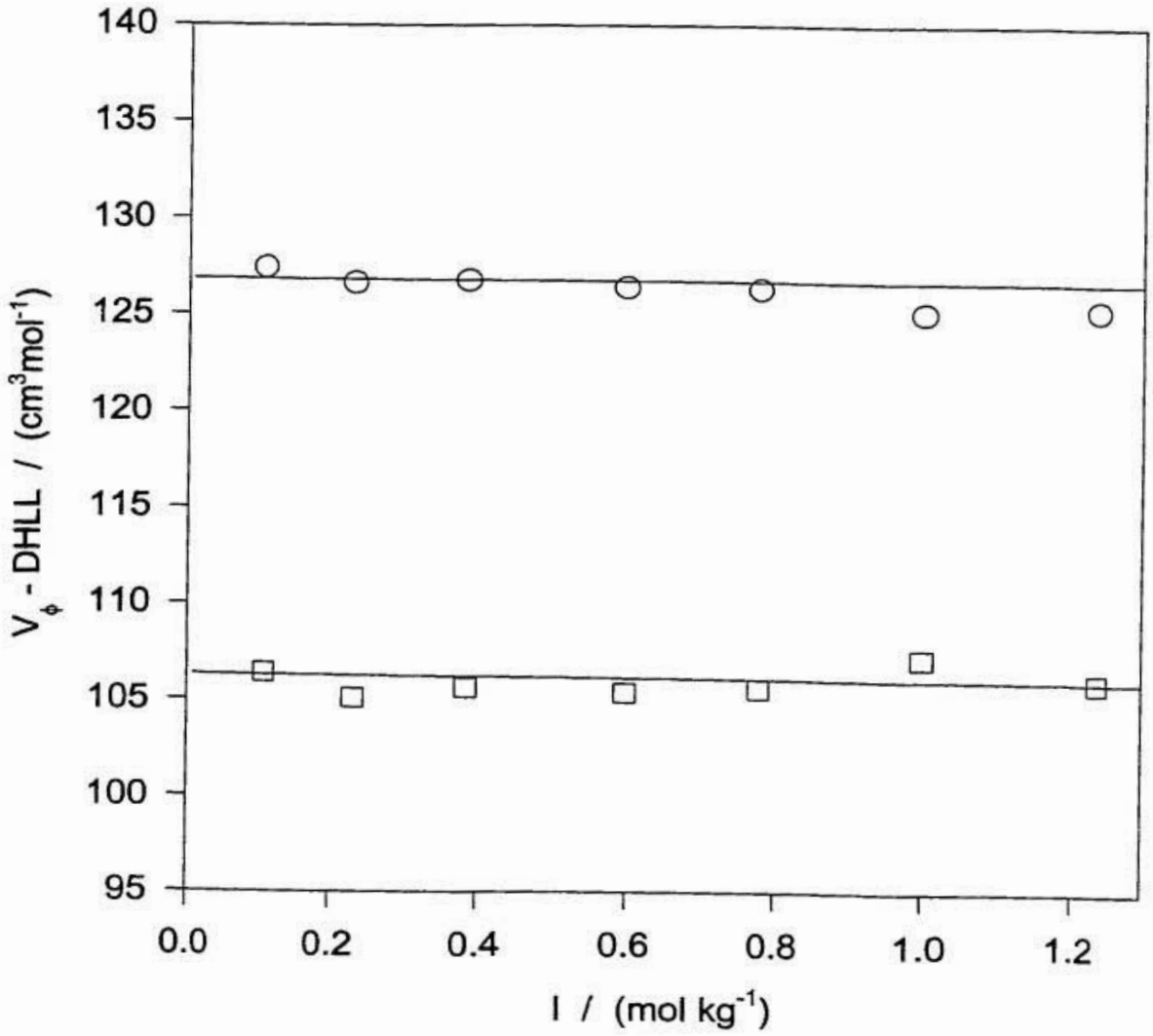

Figure 3.3.5 Apparent molar volumes V_ϕ of methyldiethanolammonium chloride at 10.3 MPa plotted against ionic strength after subtraction of the Debye-Hückel limiting law term. Symbols are experimental results: ○ 422.91 K; □ 522.98 K. Lines are fitted values from density model.

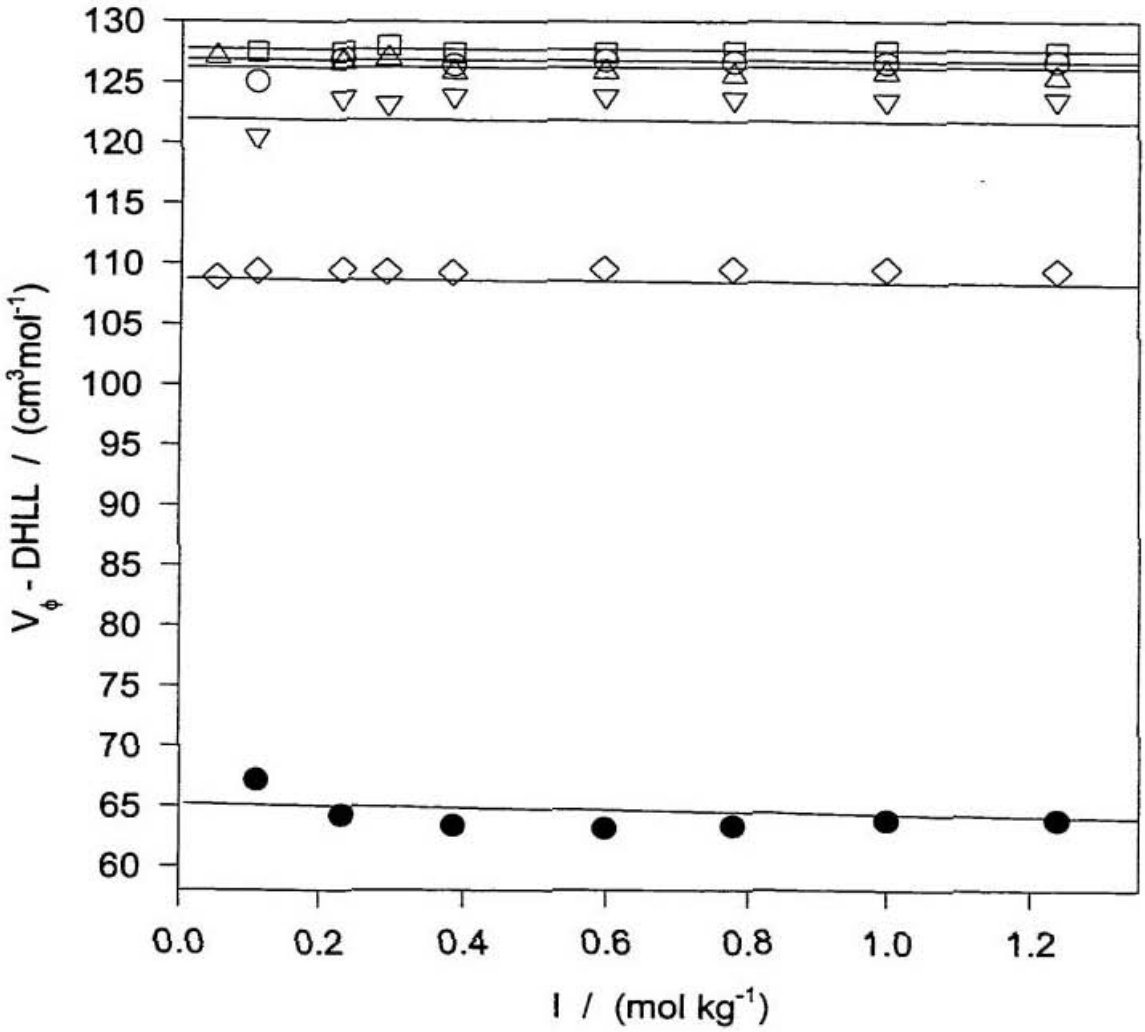

Figure 3.3.6 Apparent molar volumes V_ϕ of methyldiethanolammonium chloride at 20.2 MPa plotted against ionic strength after subtraction of the Debye-Hückel limiting law term. Symbols are experimental results: ○ 334.22 K; □ 377.10 K; Δ 426.76 K; ▽ 475.05 K; ◇ 523.78 K; ● 576.35 K. Lines are fitted values from density model.

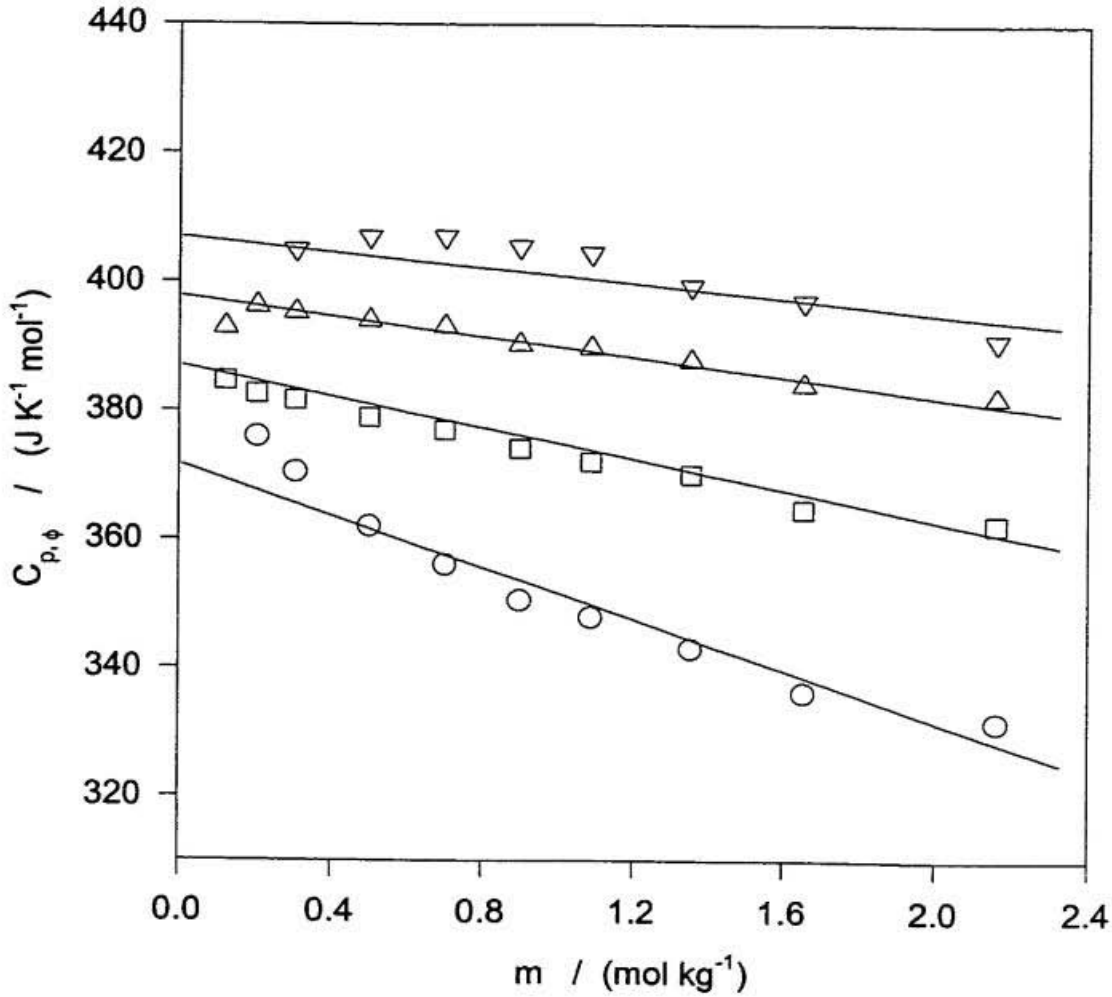

Figure 3.3.7 Apparent molar heat capacities $C_{p,\phi}$ of methyldiethanolamine at 0.1 MPa plotted against molality. Symbols are experimental results: ○ 283.15 K; □ 298.15 K; Δ 313.15 K; ▽ 328.15 K. Lines are fitted values from density model.

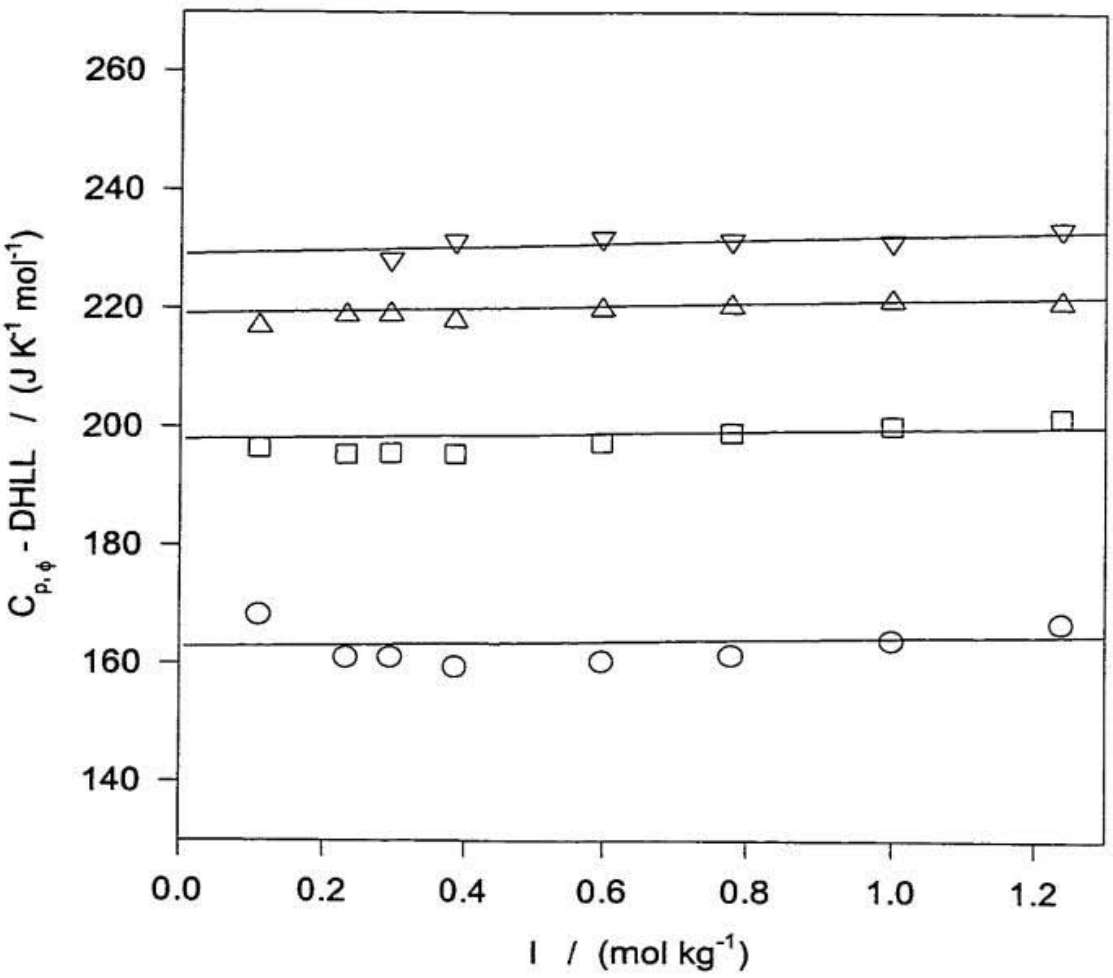

Figure 3.3.8 Apparent molar heat capacities $C_{p,\phi}$ of methyldiethanolammonium chloride at 0.1 MPa plotted against ionic strength after subtraction of the Debye-Hückel limiting law term. Symbols are experimental results: ○ 283.15 K; □ 298.15 K; Δ 313.15 K; ▽ 328.15 K. Lines are fitted values from density model.

3.4 "Equations of State" for Aqueous Methyldiethanolamine and Methyldiethanolammonium Chloride: The HKF Model

The revised Helgeson-Kirkham-Flowers model as adapted to organic species by Shock and Helgeson (1990) was employed to describe the standard state properties under widely varying temperatures and pressures:

$$V^{o} = v_1 + \frac{v_2}{\Psi + p} + \left(v_3 + \frac{v_4}{\Psi + p}\right)\left(\frac{1}{T - \Theta}\right) - \omega_e Q \tag{3.4.1}$$

$$C_p^{o} = c_1 + \frac{c_2}{(T-\Theta)^2} - \left(\frac{2T}{(T-\Theta)^3}\right)\left[v_3(p - p_r) + v_4 \ln\left(\frac{\Psi + p}{\Psi + p_r}\right)\right] + \omega_e TX \tag{3.4.2}$$

$$\kappa_T^{o} = \left[v_2 + v_4\left(\frac{1}{T-\Theta}\right)\right]\left(\frac{1}{(\Psi + p)}\right)^2 + \omega_e N \tag{3.4.3}$$

Here, v_1, v_2, v_3, v_4, c_1, c_2 are species-dependent fitting parameters; Ψ is a solvent parameter equal to 260 MPa; and Θ is a solvent parameter equal to 228 K. The terms $\omega_e Q$, $\omega_e TX$, and $\omega_e N$ are the electrostatic contributions to the standard partial molar volume, heat capacity, and compressibility according to the Born equation. The values $Q = (1/\varepsilon)(\partial\varepsilon/\partial p)_T$, $X = (1/\varepsilon)[(\partial^2 \ln \varepsilon/\partial T^2)_p - (\partial \ln \varepsilon/\partial T)_p^2]$, and $N = (\partial Q/\partial p)_T$ are Born functions where ε is the dielectric constant of water. Although Shock and Helgeson (1990) give

expressions for estimating the effective Born coefficient ω_e, it is used as a fitting parameter in this application of the revised HKF model. Table 3.4.1 contains the HKF parameters from equations 3.4.1 to 3.4.3 for methyldiethanolamine and methyldiethanolammonium chloride.

Table 3.4.1 HKF model parameters according to equations 3.4.1 and 3.4.2 for methydiethanolamine and methyldiethanolammonium chloride.

Parameter	$V°$ / ($cm^3 \cdot mol^{-1}$)	
	Methydiethanolamine	Methydiethanolammonium Chloride
v_1 / $cm^3 \cdot mol^{-1}$	168.2 ± 25.9	171.2 ± 16.2
$v_2 \cdot 10^{-4}$ / $MPa \cdot cm^3 \cdot mol^{-1}$	-1.4659 ± 0.69	-0.96731 ± 0.43
$v_3 \cdot 10^{-3}$ / $K \cdot cm^3 \cdot mol^{-1}$	-3.755 ± 0.19	-2.894 ± 1.21
$v_4 \cdot 10^{-5}$ / $MPa \cdot K \cdot cm^3 \cdot mol^{-1}$	9.0171 ± 0.51	6.0057 ± 0.32
$\omega_e \cdot 10^{-5}$ / $MPa \cdot cm^3 \cdot mol^{-1}$	-3.9047 ± 0.24	3.6642 ± 0.08

Parameter	$C_p°$ / ($J \cdot K^{-1} \cdot mol^{-1}$)	
	Methydiethanolamine	Methydiethanolammonium Chloride
c_1 / $J \cdot K^{-1} \cdot mol^{-1}$	374.8 ± 2.3	300.3 ± 2.9
$c_2 \cdot 10^{-5}$ / $J \cdot K \cdot mol^{-1}$	-0.92011 ± 0.11	-3.4527 ± 0.14

3.5 Discussion

3.5.1 Standard Partial Molar Properties and Behaviors at Elevated Temperatures and Pressures

The behavior of the standard partial molar volumes for methyldiethanolamine at elevated temperatures is similar to that observed for the few other aqueous nonelectrolytes that have been studied (Tremaine *et al.*, 1997; Shvedov and Tremaine, 1997; Fernandez-Prini *et al.*, 1992). As for other volatile organic solutes, methyldiethanolamine lowers the critical properties of water which will cause to lower the critical temperature and pressure of dilute aqueous solutions. This causes V°to rise towards a strong discontinuity near the critical temperature of water at steam saturation pressures as seen in Figures 3.5.1 and 3.5.2

The standard partial molar volume of methyldiethanolammonium chloride is typical of other aqueous electrolytes which approach a strong negative discontinuity at the critical temperature of water (Figures 3.5.3 and 3.5.4) due to the effects of long-range solvent polarization and the corresponding increase of the critical properties in the dilute aqueous solutions (Fernandez-Prini *et al.*, 1992; Mesmer *et al.*, 1991).

The opposite dependence of the behavior of V° on pressure is reversed for the amine and the amine salt and has been explained by Shvedov and Tremaine (1997) and Biggerstaff and Wood (1988). For the neutral amine, the presence of the solute expands the solvent, causing an increase in the standard partial molar volume. Since the

compressibility of water approaches infinity faster at steam saturation pressures, the ability of the neutral amine to expand the solvent is diminished at higher pressures which results in a smaller V°. For the amine salt, the greater compressibility of water at low pressures greatly enhances long-range solvent polarization by the ion. As the pressure is increased, the electrostriction effect is reduced causing the partial molar volume to increase.

As seen in Figure 3.5.5, the standard partial molar heat capacity of the neutral methydiethanolamine approaches a positive discontinuity at high temperatures which is consistent with similar organic molecules with amine groups (Tremaine *et al.*, 1997; Shvedov and Tremaine, 1997). The standard partial molar heat capacity of methyldiethanolammonium chloride (Figure 3.5.6) exhibits the typical inverted-U shape as a function of temperature which is a feature of aqueous electrolytes. The C_p° values for ions typically have a maximum in the neighborhood of 373.15 K and then approach negative infinity at the critical point (Anderson and Crerar, 1993).

For the HKF model, the standard state properties approach the Born equation at high temperatures so that, in principle, the model has considerable extrapolating power. The premise behind such extrapolations is that accurate standard state Gibbs energies can be calculated from even moderately accurate extrapolations of C_p° vs. T. Aside from fitting the concentration dependence of the data adequately, the density model is also valuable for estimating thermodynamic parameters since the variation of V° and C_p° with

β_1^* and $(\partial\alpha_1^*/\partial T)_p$ respectively for the solvent has been suggested from statistical mechanics.

The experimental apparent molar isothermal compressibilities as seen in Figures 3.2.1 and 3.2.2 show some regularities, an interpretation which may be offered in terms of two effects (Verrall and Conway, 1966): (a) a structural one, due to the influence of the uncharged hydrophobic functional groups at the nitrogen center of the amine, and (b) an electrostatic one. The lower (more negative) values of κ_T° for methyldiethanolammonium chloride in comparison with those of the corresponding neutral amine is the result of the ionic charge and the contribution of the chloride ion. Interpretation of the present results are made in terms of changes of the local compressibility of the solvent near the molecules. The bulkiness of the hydrophobic methyl group of the amine and the relatively large hydrophobic ethanol groups promote hydrophobic interactions with the surrounding water. These bonded water molecules may possess higher compressibility because they may be pushed together without hydrogen bond rupture and the main effect will be to decrease the void space between the molecules. The local solvent structure for methyldiethanolammonium chloride may be considered to be electrostricted water as the dipoles orient themselves toward the ions. The electrostricted water molecules will be expected to have low compressibility since the water molecules are constrained to approach each other around the ion. Figures 3.5.7 and 3.5.8 compare the experimentally determined κ_T° with the fitted values of κ_T° from

equations 3.3.7 and 3.4.3, respectively. The density fit to the standard partial molar isothermal compressibilities κ_T° is quite satisfactory for methydiethanolamine and methyldiethanolammonium chloride and is more successful than the HKF model. The HKF model fits the data at the temperatures 298.15 to 313.15 K adequately although it poorly represents the curvature of the data for both systems.

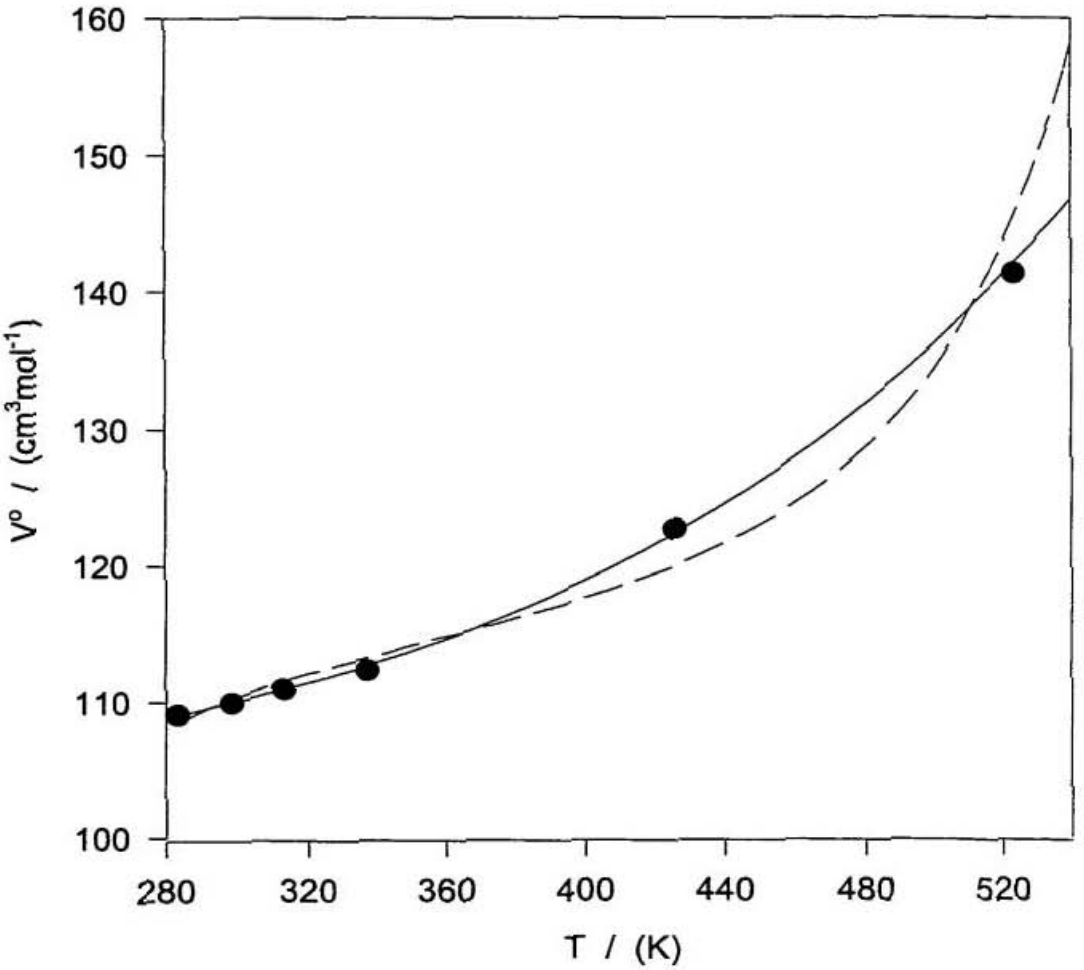

Figure 3.5.1 Standard partial molar volumes V° of methyldiethanolamine at 10.3 MPa plotted against temperature. Symbols are values obtained from isothermal fits of equation 3.4.1. Lines are fitted values : —— density model; ----- HKF model.

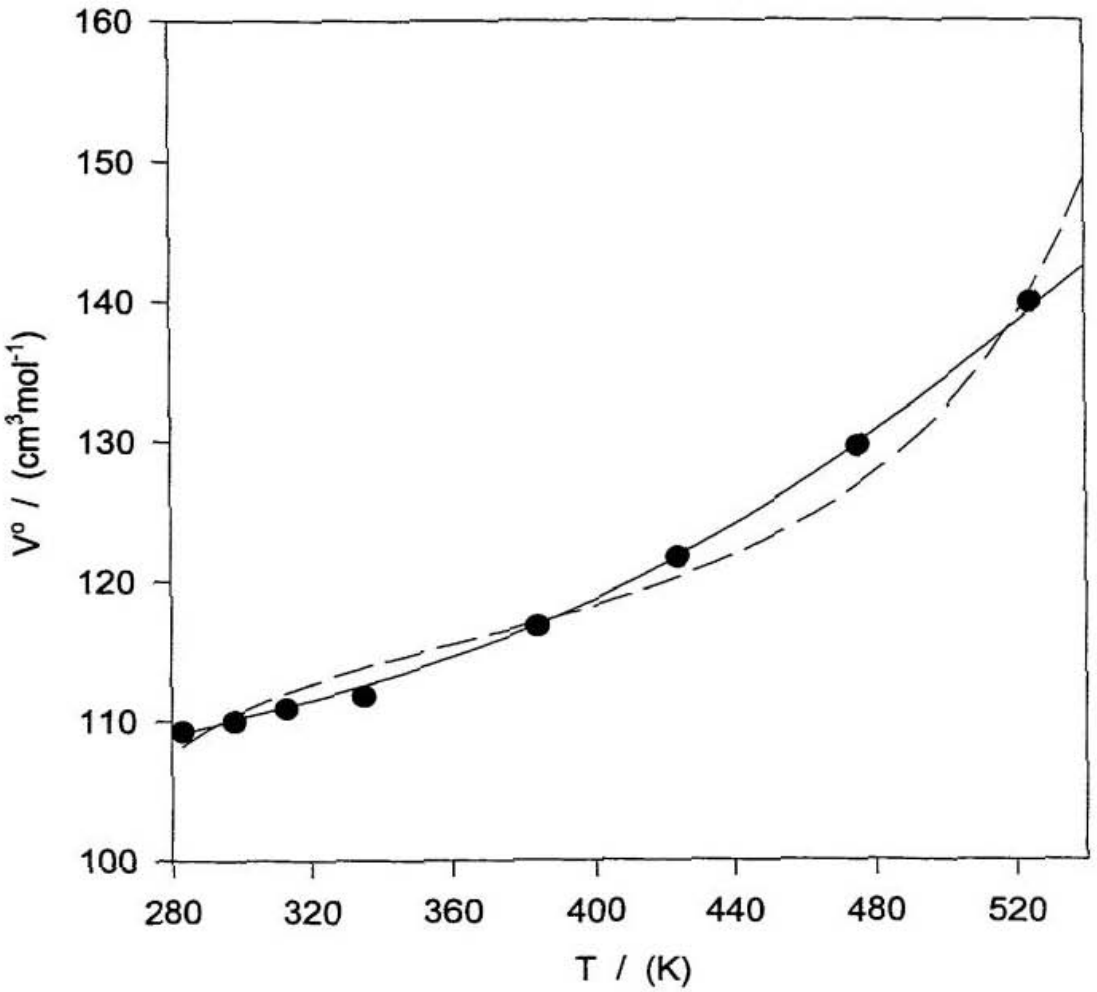

Figure 3.5.2 Standard partial molar volumes V° of methyldiethanolamine at 20.1 MPa plotted against temperature. Symbols are values obtained from isothermal fits of equation 3.4.1. Lines are fitted values : —— density model; ----- HKF model.

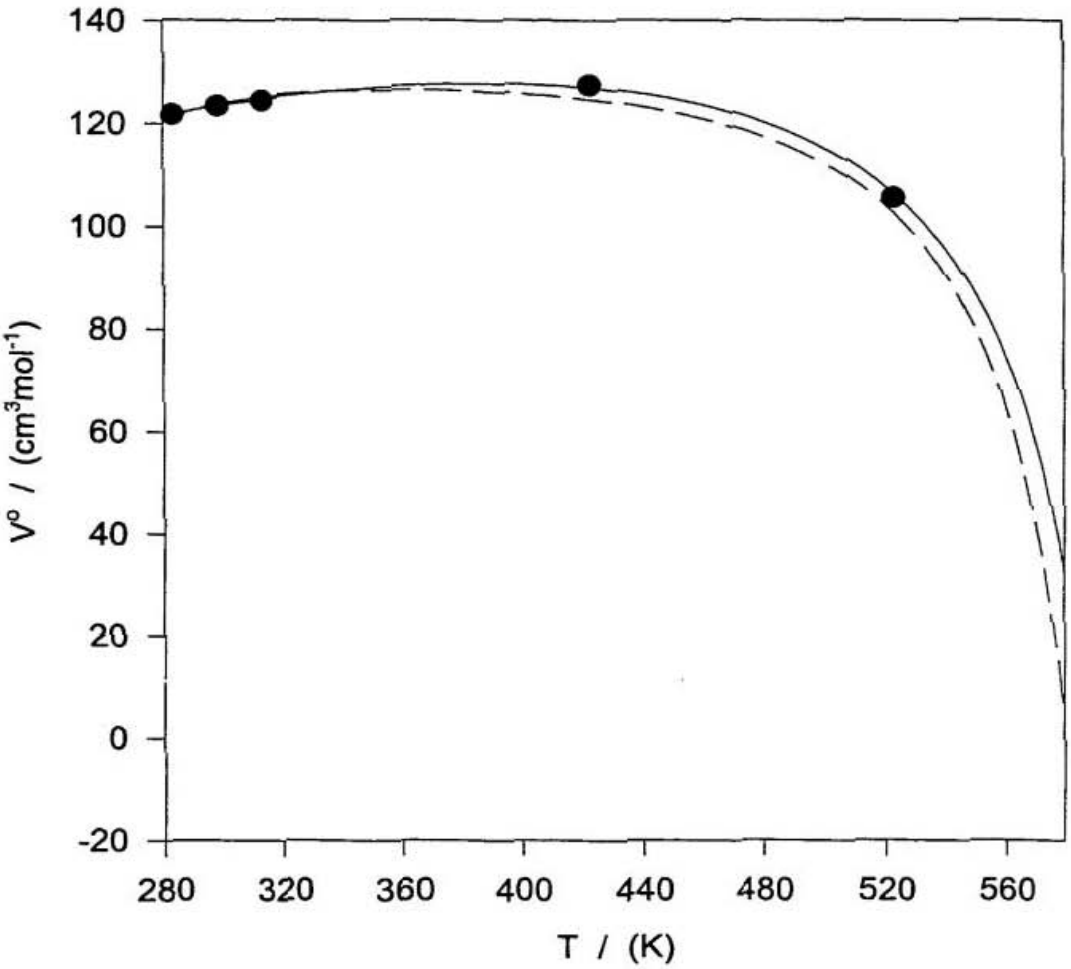

Figure 3.5.3 Standard partial molar volumes V° of methyldiethanolammonium chloride at 10.3 MPa plotted against temperature. Symbols are values obtained from isothermal fits of equation 3.4.3. Lines are fitted values : —— density model; ----- HKF model.

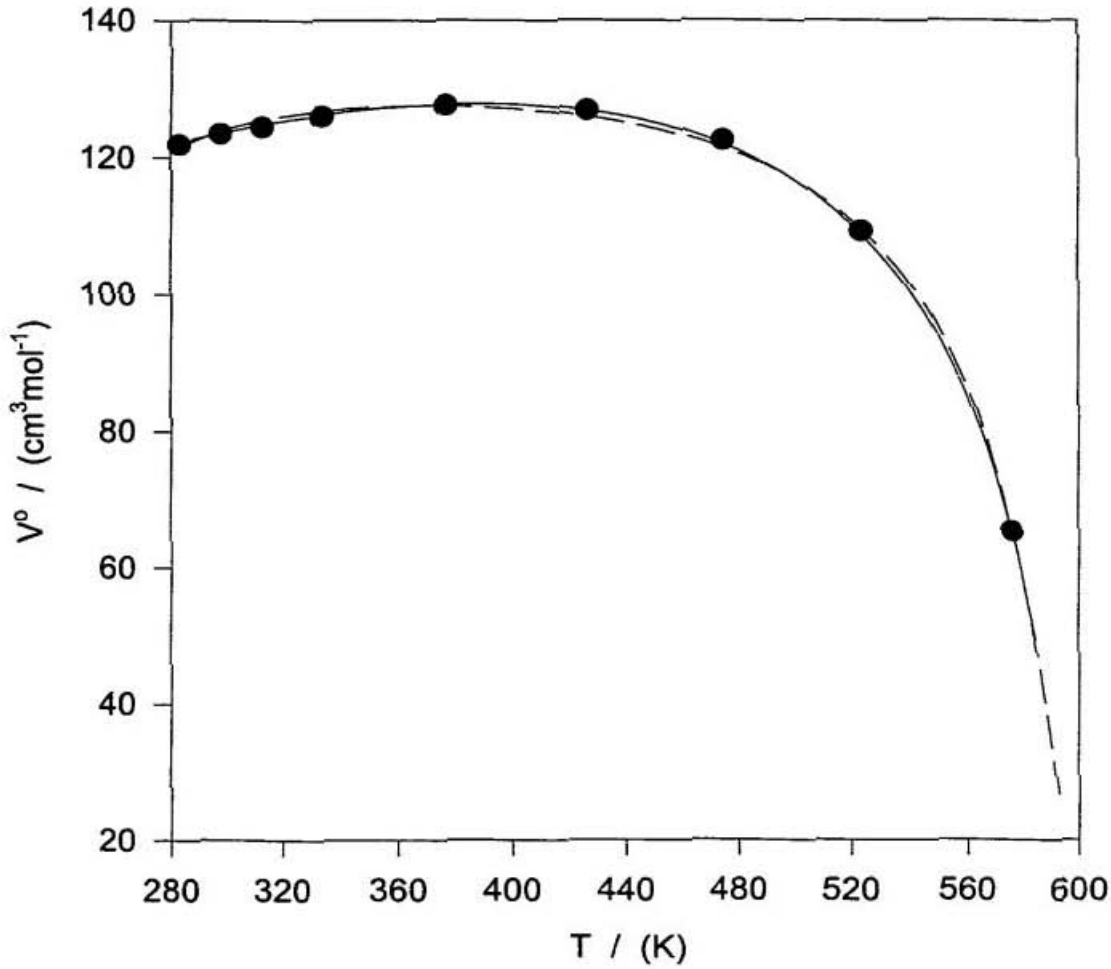

Figure 3.5.4 Standard partial molar volumes V° of methyldiethanolammonium chloride at 20.2 MPa plotted against temperature. Symbols are values obtained from isothermal fits of equation 3.4.3. Lines are fitted values : —— density model; ----- HKF model.

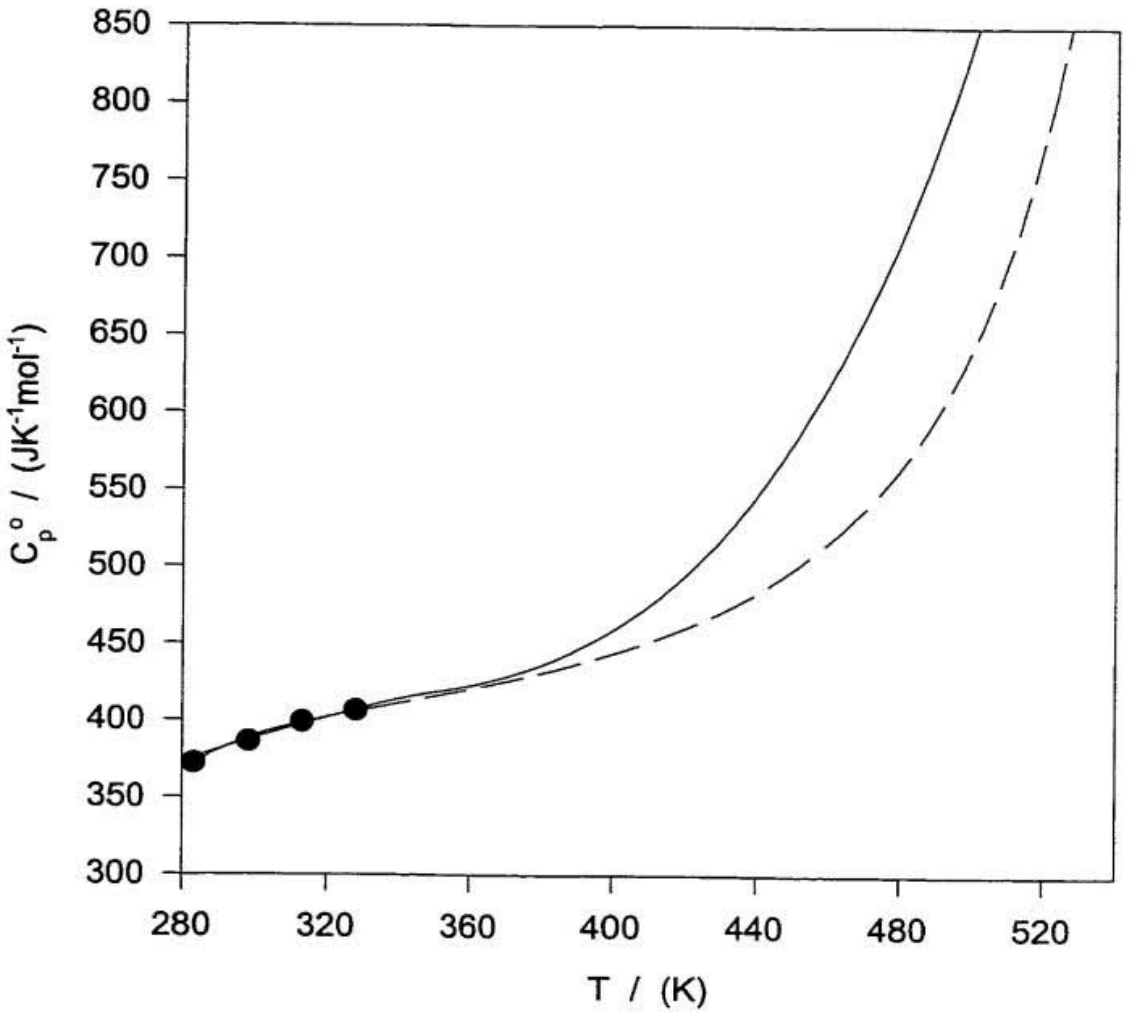

Figure 3.5.5 Standard partial molar heat capacities C_p° of methyldiethanolamine at 0.1 MPa plotted against temperature. Symbols are values obtained from isothermal fits of equation 3.4.2. Lines are fitted values : —— density model; ----- HKF model.

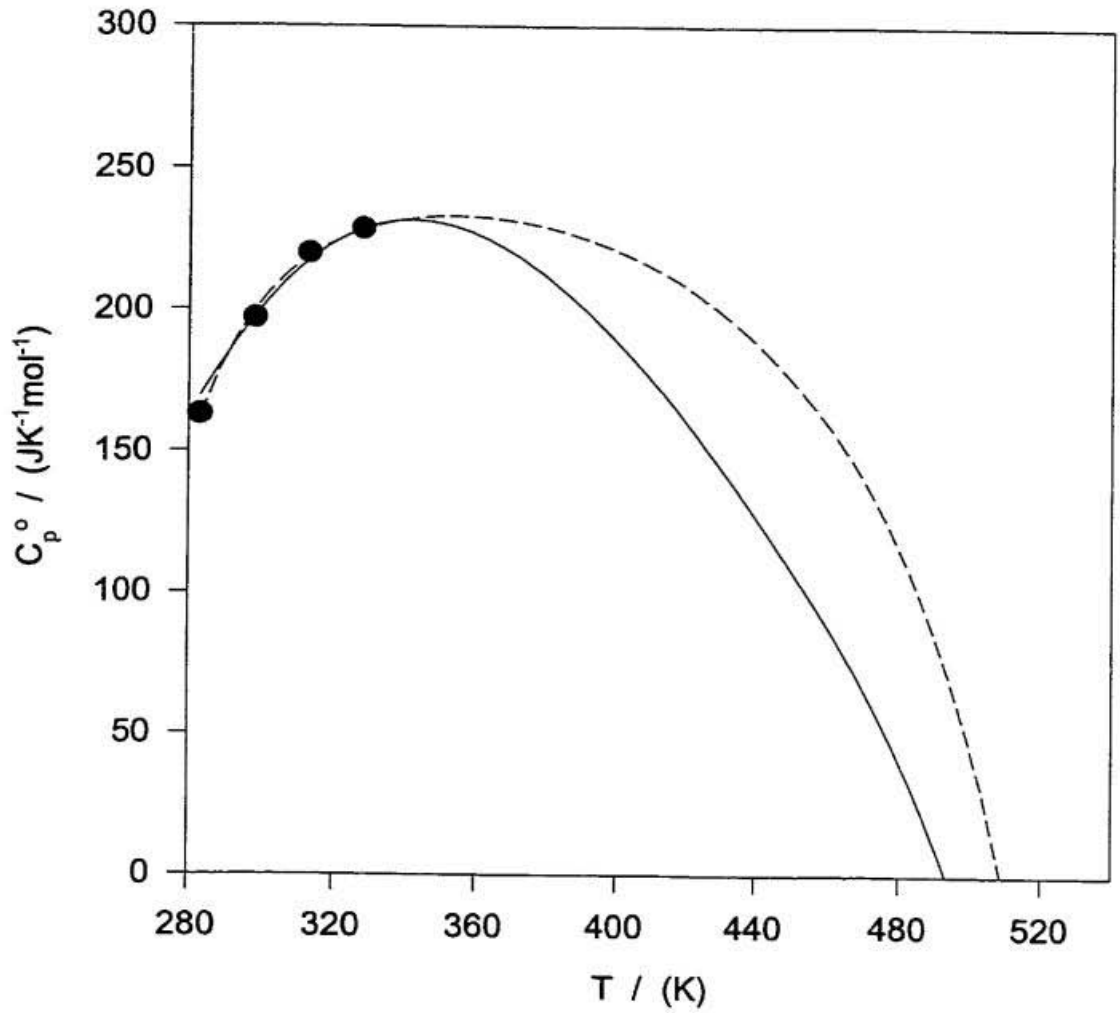

Figure 3.5.6 Standard partial molar heat capacities $C_p°$ of methyldiethanolammonium chloride at 0.1 MPa plotted against temperature. Symbols are values obtained from isothermal fits of equation 3.4.4. Lines are fitted values : —— density model; ----- HKF model.

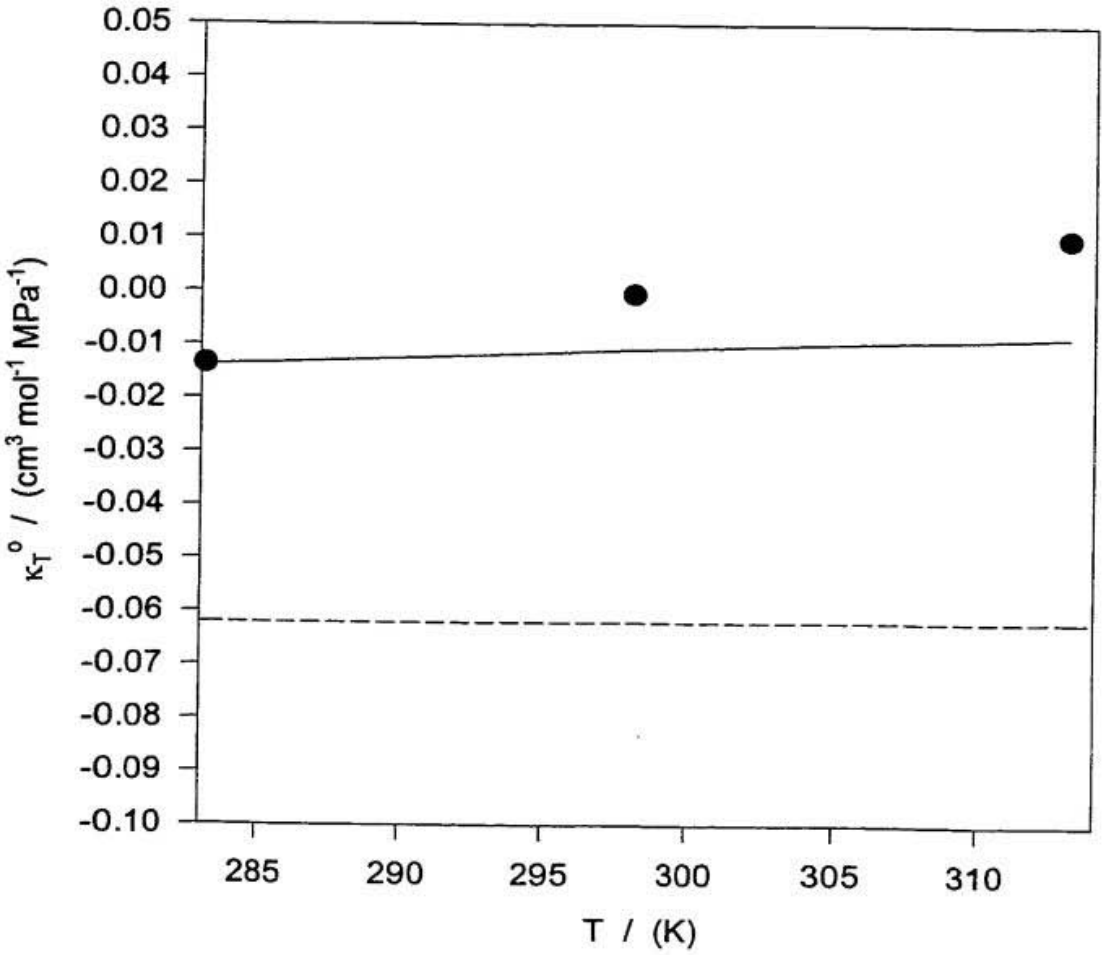

Figure 3.5.7 Standard partial molar isothermal compressibilities κ_T° of methyldiethanolamine at 0.1 MPa plotted against temperature. Symbols are experimental values. Lines are fitted values : —— density model; ----- HKF model.

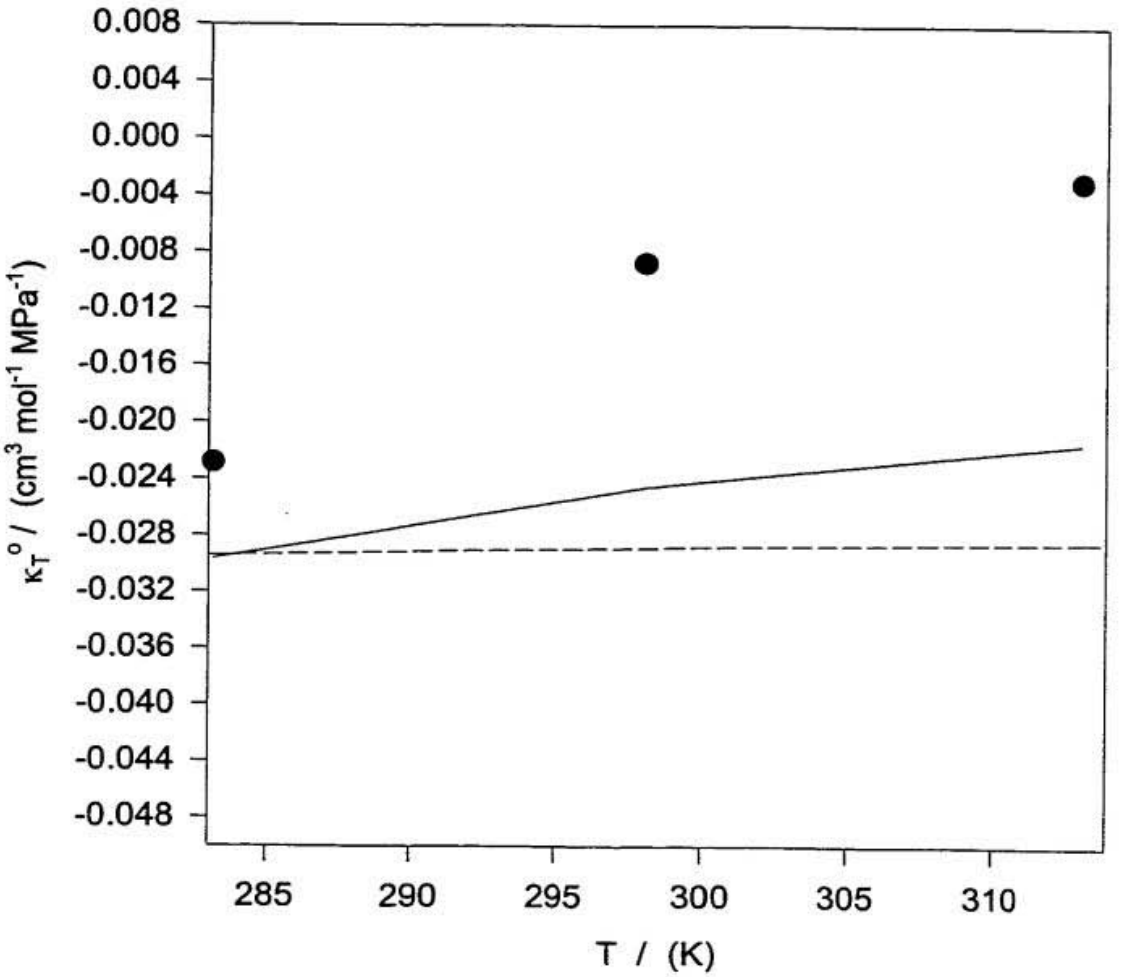

Figure 3.5.8 Standard partial molar isothermal compressibilities κ_T° of methyldiethanolammonium chloride at 0.1 MPa plotted against temperature. Symbols are experimental values. Lines are fitted values : —— density model; ----- HKF model.

3.5.2 The Density Model

The molality dependent apparent molar properties were represented by the model to within an overall standard deviation of 0.42 $cm^3 \cdot mol^{-1}$ and 1.2 $J \cdot K^{-1} \cdot mol^{-1}$ for the methyldiethanolamine, and 0.63 $cm^3 \cdot mol^{-1}$ and 1.0 $J \cdot K^{-1} \cdot mol^{-1}$ for the methyldiethanolammonium chloride. The fitted curves lie within the statistical scatter of all the experimental data. The fitting was challenging due to the changes in the molality dependence of the apparent molar properties below 328.15 K, the quantity and diversity of the experimental data, and the number of equations that were being fit simultaneously. Equations 3.3.5 to 3.3.10 were chosen from several modifications of the density model as a compromise between the number of terms required to significantly reduce the standard deviation, and an acceptable fit in the low temperature region.

When fitting the standard partial molar volumes, the compressibility term of equation 3.3.5 is dominant at elevated temperatures and is used to model both the temperature and pressure dependence of the thermodynamic properties of the aqueous species in this region. The value of β_1^* approaches positive infinity as the critical and pseudo-critical temperatures of water are approached. The value of each thermodynamic quantity for an aqueous electrolyte or non-electrolyte approaches either positive or negative infinity as these temperatures are approached. The pressure dependence of β_1^* can easily account for the small pressure dependence observed in the aqueous solutions.

3.5.3 The HKF Model and the Born Term

The effective Born coefficient ω_e is a purely empirical fitting parameter and it usually has a negative value for non-polar molecules, implying that Z_e is a fractional imaginary number. The HKF model does represent the data adequately, although it is less accurate than the density model which has more adjustable parameters for the low-temperature region. It was not possible to reproduce the partial molar functions of the methyldiethanolammonium ion if it was assumed that the radius was equal to that of the neutral molecule. Thus, ω_e was used as an adjustable parameter and was determined by a least-squares fit to values for V°. Although the pressure influence was minimal, it was not possible to reproduce the pressure-dependent data at higher temperatures without using v_2 and v_4 in equation 3.4.11.

As mentioned, the fits obtained with equations 3.4.1 to 3.4.3 are less accurate than those from equations 3.3.5 to 3.3.7 which have more adjustable parameters. Nonetheless, the HKF model does adequately reproduce the data for V° and C_p° for methyldiethanolamine and its chloride salt.

3.5.4 Methyldiethanolamine Ionization

Jones and Arnett (1974) have reviewed thermodynamic data for the ionization of aqueous amines at 298.15 K. Very few experimental ionization constants or other thermodynamic properties of aqueous methyldiethanolamine and its chloride salt have

been reported in the literature. It is possible, using the density and HKF models, to estimate the standard partial molar volume change of the ionization equilibrium, $\Delta_r V°$, and the standard partial molar heat capacity change, $\Delta_r C_p^\circ$ at elevated temperatures for the reaction:

$$CH_3N(CH_2CH_2OH)_2(aq) + H^+(aq) \rightleftharpoons CH_3NH(CH_2CH_2OH)_2^+(aq) \qquad (3.10.1)$$

Values for $\Delta_r C_p^\circ$ and $\Delta_r V°$ were calculated from the expression:

$$\Delta_r Y° = Y°\{CH_3N(C_2H_4OH)_2, aq\} - Y°\{CH_3NH(C_2H_4OH)_2Cl, aq\} - Y°\{HCl, aq\} \quad (3.10.2)$$

The relative contributions of methyldiethanolamine, methyldiethanolammonium chloride, and HCl to $\Delta_r V°$ are plotted in Figure 3.5.9. The similarity in the plots for $V°\{CH_3NH(C_2H_4OH)_2Cl, aq\}$ and $V°\{HCl\}$ illustrates that much of the difference between $V°\{CH_3N(C_2H_4OH)_2, aq\}$ and $V°\{CH_3NH(C_2H_4OH)_2Cl, aq\}$ is due to the contribution of the chloride ion. This observation is also confirmed by the small values of $\Delta_r V°$ which are almost independent of temperature.

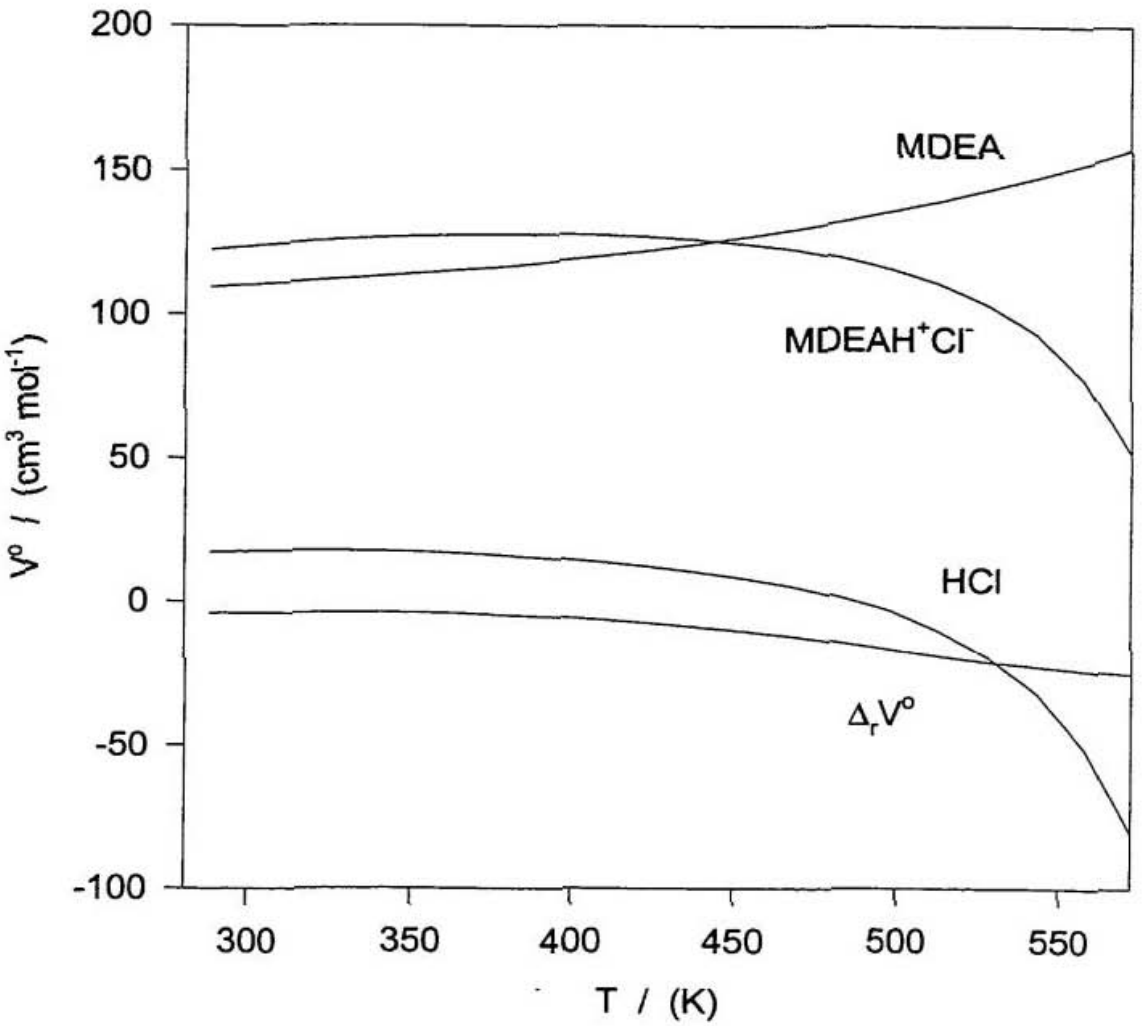

Figure 3.5.9 Contributions to the standard partial molar volume change $\Delta_r V°$ for the ionization of methyldiethanolamine

Oscarson *et al.* (1989) have determined values for the heat capacity changes for protonation of aqueous methyldiethanolamine $\Delta_r C_p^\circ$ by using calorimetric techniques. The results are plotted in Figure 3.5.10, along with the fitted curves corresponding to equation 3.3.6 and equation 3.4.2 calculated from the C_p° values for methyldiethanolamine and methyldiethanolammonium chloride. Values for $C_p^\circ\{HCl,aq\}$ for the calculation were taken from the expression reported by Shock and Helgeson (1988). Both the density and HKF models yield results which deviate significantly from each other above 425 K. The density and HKF models predict deviations in opposite directions which may be interpreted in a variety of ways. The density model contains a large number of fitting parameters in the low temperature region which may affect its ability to successfully extrapolate $\Delta_r C_p^\circ$. As well, the HKF model over-predicts the approach of the critical point of the high temperature V° for the neutral amine which may affect its description of $\Delta_r C_p^\circ$. Lastly, the magnitude of the contributions to C_p° from the ionic and neutral amine as illustrated in Figures 3.5.5 and 3.5.6 is so finely balanced over the temperature range that the deviations may arise from the slight differences in the fitted data at elevated temperatures. Although the predicted C_p° from the density and HKF model differ by almost 100 $J \cdot K^{-1} \cdot mol^{-1}$ at elevated temperatures, the differences in the values calculated for $\Delta_r C_p^\circ$ cancel out at temperatures up to 400 K.

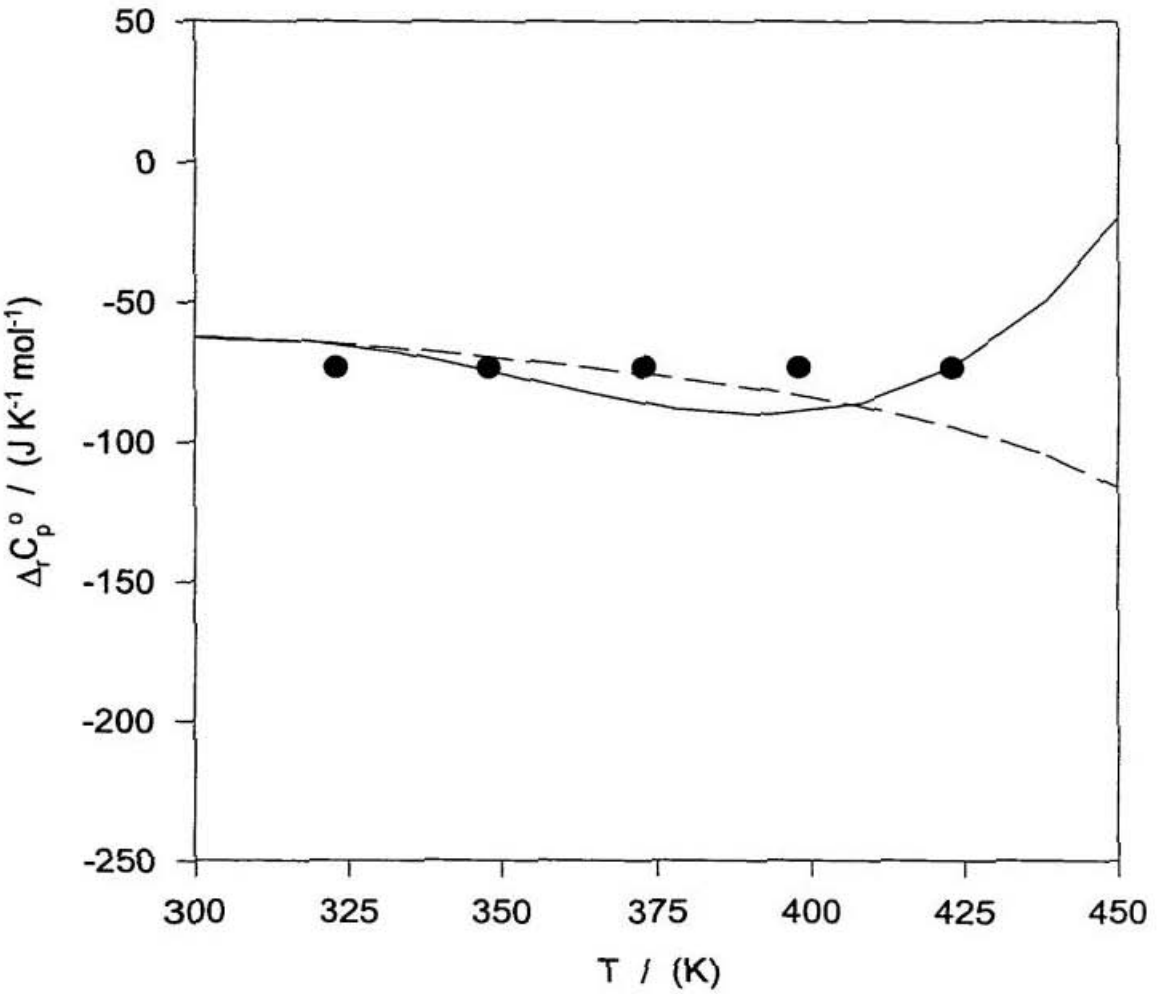

Figure 3.5.10 Standard partial molar heat capacity change $\Delta_r C_p^\circ$ for the ionization of methyldiethanolamine. Symbols are experimental results from Oscarson *et al.* (1989). Lines are predicted values : —— density model; ----- HKF model.

Chapter 4: Excess and Reduced Excess Heat Capacities of Aqueous Solutions of Methyldiethanolamine at Finite Concentrations from 273 to 373 K

4.1 Introduction

As noted in Section 1.1, aqueous solutions of MDEA are finding increasing use for the selective removal of H_2S from gas mixtures containing H_2S and CO_2. Methyldiethanolamine is a tertiary amine which does not form a carbamate and the rate of reaction with carbon dioxide is slow relative to that with hydrogen sulfide. Heat capacity data for methyldiethanolamine are required for the design of the heat-exchanger equipment used in the gas-treating processes. Little information on the heat capacity or related thermophysical properties of methyldiethanolamine is available in the literature. This chapter reports measurements of molar heat capacities over the entire water/MDEA mole fraction range made with a commercial biological differential scanning calorimeter from 278.15 to 368.15 K from which excess and reduced excess heat capacities were calculated

4.2 Experimental Results

4.2.1 Molar Heat Capacities and Vaporization Corrections

The DSC calorimeter cells are operated with a vapor space to accommodate the expansion of the sample during the heating process so that the experimental heat capacity is that of a liquid in equilibrium with a small amount of its vapor, which includes a

contribution from the heat of vaporization. Hence:

$$C_p^{exp} = n_{H2O(l)}C_{p,H2O(l)} + n_{H2O(g)}C_{p,H2O(g)} + \Delta H_{vap}\left(\frac{\partial n_{H2O(g)}}{\partial T}\right)_V \qquad (4.2.2)$$

While the contribution of the vapor is negligible at low vapor pressure, the correction for the enthalpy of vaporization is required at temperatures approaching the normal boiling point of the solutions. The vaporization corrections depend on the amount of each substance in the vapor phase. These depend in turn on the quantity of sample in the cell, the vapor pressure of the components, and the (vapor + liquid) equilibrium distribution of the mixture.

To determine the change in the number of moles of vapor with temperature, we use the simple relation:

$$\left(\frac{\partial n_{H2O(g)}}{\partial T}\right)_V = \left(\frac{\partial (pV_{gas}/RT)}{\partial T}\right)_V \qquad (4.2.3)$$

This expression can be expanded to:

$$\left(\frac{\partial (pV_{gas}/RT)}{\partial T}\right)_V = \left[\frac{V_{gas}}{RT}\left(\frac{\partial p}{\partial T}\right)_V + \frac{pV_{gas}}{R}\left(-\frac{1}{T^2}\right)\right] \qquad (4.2.4)$$

The Clausius-Clapeyron equation relates the temperature dependence of the vapor

pressure of a liquid to the heat of vaporization and assumes that $(\partial V_{gas}/\partial T)_V$ is small:

$$\left(\frac{\partial p}{\partial T}\right)_V = \frac{p\Delta H_{vap}}{RT^2} \tag{4.2.5}$$

Thus:

$$\left(\frac{\partial n_{H2O(g)}}{\partial T}\right)_V = \left[\frac{V_{gas}}{RT}\left(\frac{p\Delta H_{vap}}{RT^2}\right) + \frac{pV_{gas}}{R}\left(-\frac{1}{T^2}\right)\right] \tag{4.2.6}$$

The values used to calculate the vapor correction are listed in Table 4.2.1 based on constant value of 6.5×10^{-7} m^3 for the volume of the vapor in the calorimetric cells.

The experimental molar heat capacities for water and pure methyldiethanolamine are tabulated in Table 4.2.2 for the temperature range studied Selected experimental data points are plotted in Figure 4.2.1 for water after the appropriate corrections. Molar heat capacities for pure methyldiethanolamine were determined by Maham *et al.* (1997) at T = 299.1, 322.8, 348.5, 373.2, and 397.8 K and modeled using the equation: $C_p/(J\cdot K^{-1}\cdot mol^{-1})$ = (88.5 ± 6.8) + (0.604 ± 0.019)T. The molar heat capacities from our work lie within the combined statistical uncertainty of the data in Figures 4.2.1 and 4.2.2 which corresponds to an accuracy of ± 2 per cent or better.

Differential scanning calorimeters are increasingly used for determining the heat capacities of non-volatile liquids. For example, Mraw and O'Rourke (1980, 1981) have shown that the heat capacities can be accurate to ± 2 per cent at temperatures up to 700 K

Table 4.2.1 Vapor pressure correction for water

T (K)	p (Pa)	ΔH_{vap} ($J \cdot mol^{-1}$)	$\Delta H_{vap}(\partial n_{H2O(g)}/\partial T)$ ($J \cdot K^{-1}$)	$\Delta H_{vap}(\partial n_{H2O(g)}/\partial T)_V$ ($J \cdot K^{-1} \cdot mol^{-1}$)
283.15	1228	44608.6	9.586e-4	0.049
288.15	1706	44397.5	1.250e-3	0.064
293.15	2339	44186.4	1.610e-3	0.082
298.15	3170	43967.7	2.051e-3	0.105
303.15	4247	43757.4	2.586e-3	0.133
308.15	5629	43539.5	3.227e-3	0.166
313.15	7385	43329.1	3.990e-3	0.205
318.15	9595	43110.5	4.887e-3	0.251
323.15	12350	42892.6	5.934e-3	0.305
328.15	15760	42673.9	7.148e-3	0.368
333.15	19950	42456.1	8.547e-3	0.440
338.15	25040	42237.4	0.0101	0.522
343.15	31200	42010.5	0.0119	0.614
348.15	38600	41791.8	0.0139	0.719
353.15	47410	41564.1	0.0162	0.836
358.15	57870	41337.2	0.0188	0.966
363.15	70180	41102.0	0.0216	1.110
368.15	84610	40866.0	0.0246	1.268
373.15	101400	40630.7	0.0280	1.440

Table 4.2.2 Experimental molar heat capacities of water $C_{p,1}^{*}$ and methyldiethanolamine $C_{p,2}^{*}$ determined with the DSC where T denotes temperature

T / K	$C_{p,1}^{*}$ / $J \cdot K^{-1} \cdot mol^{-1}$	$C_{p,2}^{*}$ / $J \cdot K^{-1} \cdot mol^{-1}$
278.15	75.77	256.08
283.15	75.64	260.05
288.15	75.43	263.50
293.15	75.39	266.63
298.15	75.37	269.55
303.15	75.36	272.34
308.15	75.35	275.05
313.15	75.35	277.73
318.15	75.35	280.40
323.15	75.35	283.08
328.15	75.36	285.79
333.15	75.38	288.55
338.15	75.41	291.38
343.15	75.44	294.28
348.15	75.49	297.28
353.15	75.54	300.38
358.15	75.60	303.59
363.15	75.67	306.93
368.15	75.75	310.41

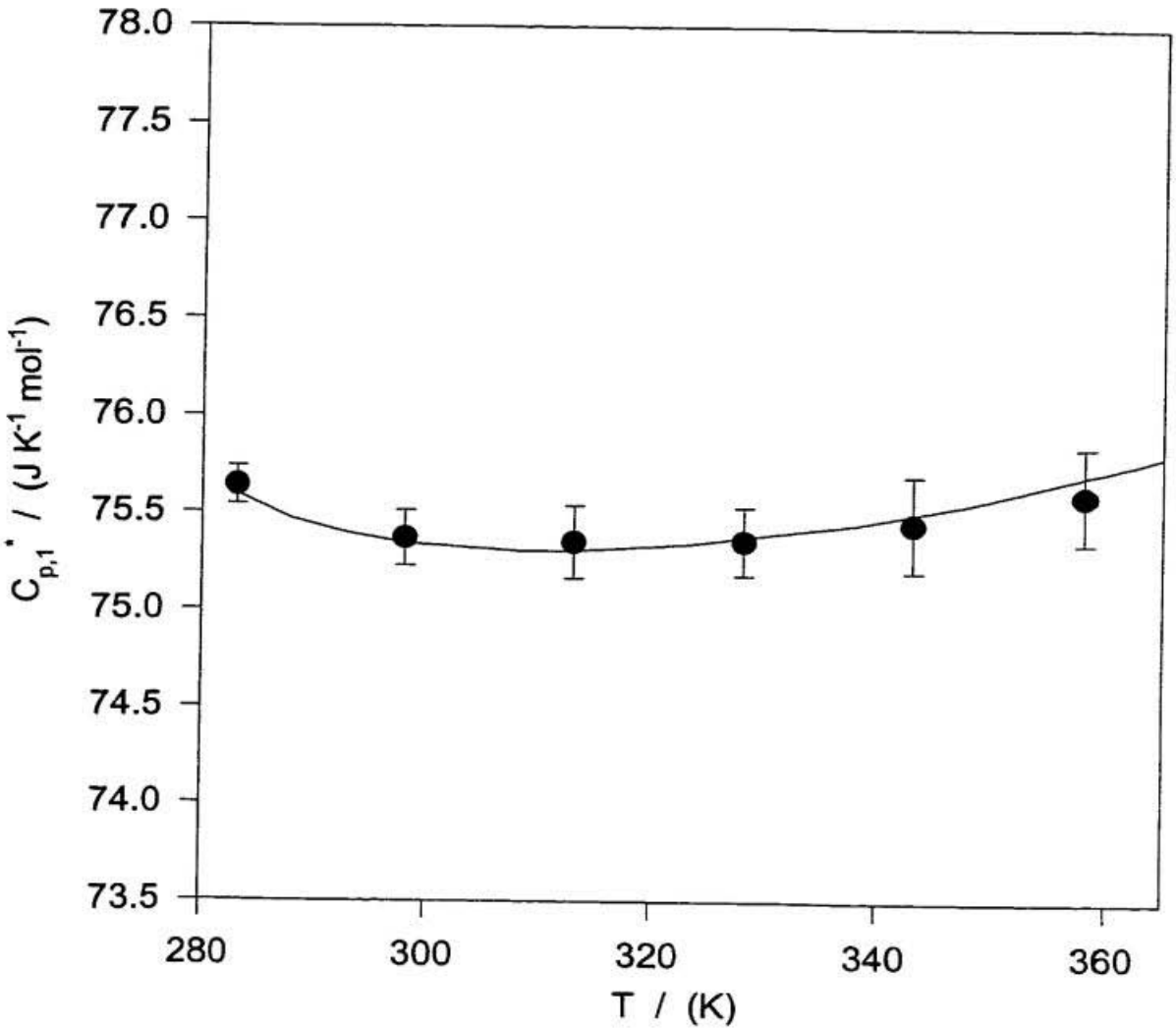

Figure 4.2.1 Molar heat capacities of water. The curve represents data from NIST while symbols and error bars were determined from experimental results.

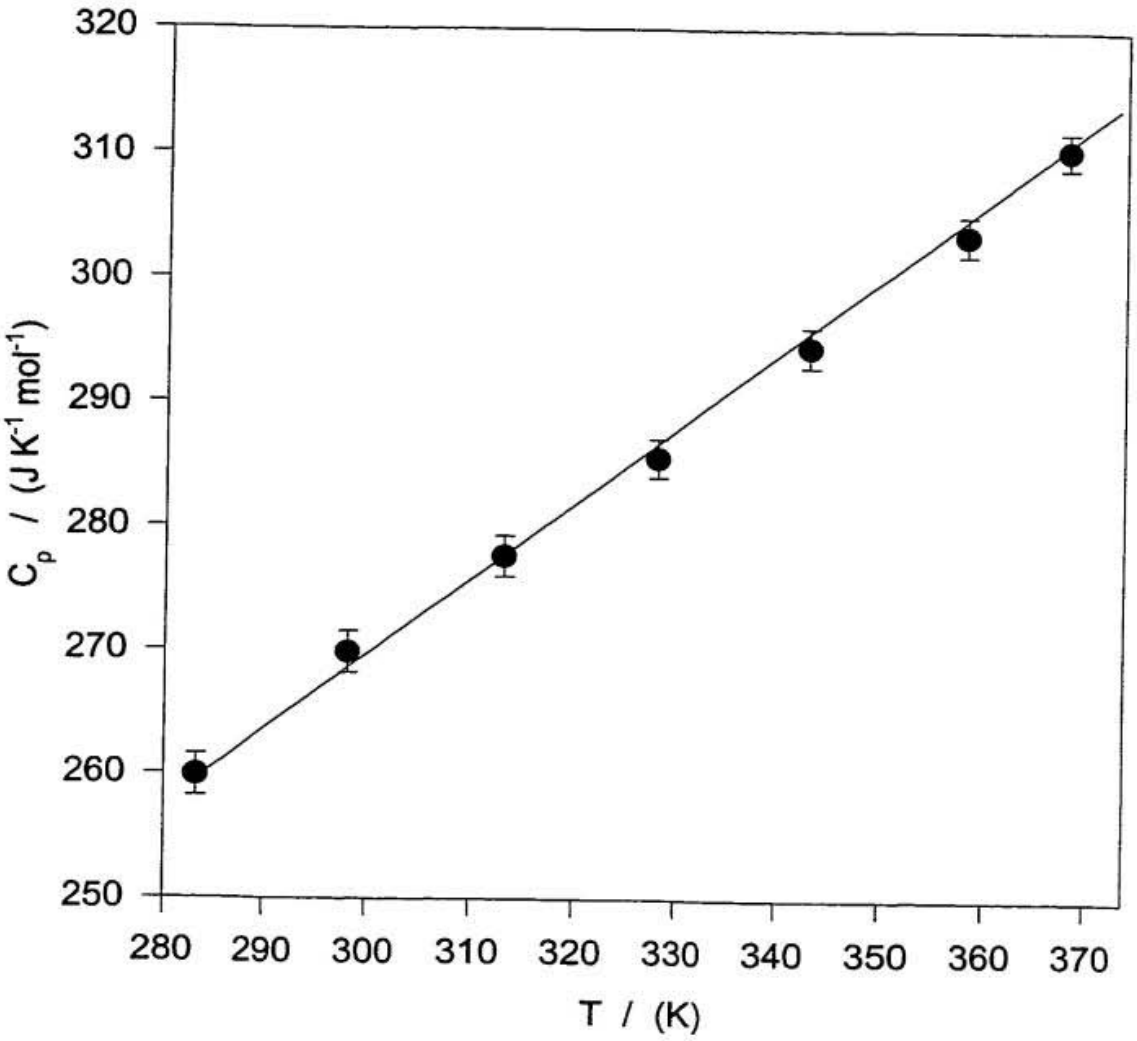

Figure 4.2.2 Molar heat capacities of liquid methyldiethanolamine. The curve represents data from Maham *et al.* (1997) while symbols and error bars were determined from experimental results.

with a specially constructed Calvet calorimeter. Recently, the constant-pressure heat capacities of hydrogen-containing propane and butane derivatives have been measured to within ± 3 % by differential scanning calorimetry at 313 K (Hwang *et al.*, 1992). Chiu *et al.* (1999) and Mather *et al.* (1997) used a DSC and a Setaram C80 Calvet calorimeter, respectively, to measure heat capacities of alkanolamines in the range 300 to 400 K with an estimated uncertainty of ± 3% or better.

Many of the differential scanning calorimeters used for measurements on biological systems have the accuracy required for measurements on volatile systems but have been rarely used for that purpose because of the large correction required for vaporization (Marsh and O'Hare, 1994). Grolier (1994) used a Setaram C80 differential scanning calorimeter to obtain $C_{p,\phi}$ of aqueous solutions at elevated temperatures using samples of ~10 cm^3 but avoided vapor corrections by filling a constant volume sample cell and allowing the liquid to escape through a small capillary tube as the temperature was increased. This method requires an accurate knowledge of the densities of the samples.

Our work shows that it is possible to successfully operate the CSC 4100 DSC up to temperatures approaching 373 K for aqueous solutions. The accuracy obtained in our work is comparable to Grolier's despite the smaller sample volume and the required vapor corrections, suggesting that the instrument may well be suitable for measurements at temperatures in the range 373 to 473 K.

4.2.2 Excess Heat Capacities

As noted in Section 1.8, the excess molar heat capacity is defined by equation 1.8.1:

$$C_p^{EX} = C_p - X_2 C_{p,2}^{\bullet} - (1 - X_2) C_{p,1}^{\bullet} \qquad (1.8.1)$$

where X_2 refers to the mole fraction of methyldiethanolamine, C_p refers to the molar heat capacity of the mixture and the subscripts 1 and 2 refer to the pure components, water and methyldiethanolamine, respectively. Calculations were made in accordance with water vapor corrections from equation 4.2.6 and Raoult's law. The molar heat capacities for aqueous solutions of methyldiethanolamine over the entire mole fraction range and the excess heat capacities calculated from them are tabulated in Table A.2.1 for the temperature range 278.15 to 368.15 K. Actual experimental temperatures are within 0.06 K of the reported temperatures.

The excess heat capacities of the water/methyldiethanolamine system were represented by two fitting equations. The first, the Redlich-Kister equation, is a simple series expansion (Section 1.8):

$$\begin{aligned} Y^{EX} = X_2 X_1 [A_0 + A_1(2X_2 - 1) + A_2(2X_2 - 1)^2 + \\ A_3(2X_2 - 1)^3 + A_4(2X_2 - 1)^4] \end{aligned} \qquad (4.2.7)$$

where X_1 and X_2 are the mole fractions of the water and methyldiethanolamine

respectively; and A_0, A_1, A_2, A_3, and A_4 are least-squares temperature-dependent parameters which must be determined from experimental data at each temperature. Each excess heat capacity was given a statistical weight equal to $1/(X_2X_1)$ so that the most dilute and most concentrated mole fractions were given the greatest weight since these regions are of greater importance. The Redlich-Kister fitting parameters for each temperature are listed in Table 4.2.3 along with their standard deviations. The plots of C_p^{EX} as a function of temperature using the Redlich-Kister fitting equation are shown in Figures 4.2.3 and 4.2.4. The Redlich-Kister interaction parameters were also used to plot $C_p^{EX}/(X_2X_1)$ to illustrate how the values fit this function in the limit as $X_2 \to 0$ and $X_1 \to 0$.

The second fitting equation is a modified Redlich-Kister equation which is a simply a ratio of polynomials (Section **1**.8):

$$C_p^{EX} = \left[\frac{X_2(1-X_2)}{1+\sum_{n=1}^{B} D_n(2X_2-1)^n}\right]\sum_{n=0}^{A} A_n(2X_2-1)^n \qquad (4.2.8)$$

The coefficients D_n and A_n are given in Table 4.2.4 together with standard deviations *s* for each isothermal fit. Equation 4.2.8 was fitted to the C_p^{EX} data at each temperature using the weighting factor $1/(X_1X_2)$ with four adjustable constants A_0, A_1, D_2, and D_3. Figures 4.2.5 and 4.2.6 illustrate this fit to the excess heat capacity data for the temperatures studied.

Table 4.2.3 Fitting parameters for excess heat capacities from the Redlich-Kister equation (equation 4.2.7) where *s* denotes the standard deviation ($J \cdot K^{-1} \cdot mol^{-1}$) for each isothermal fit.

Parameter					
	278.15 K	**283.15 K**	**288.15 K**	**293.15 K**	**298.15 K**
A_0	4.592	9.935	15.138	19.868	23.955
A_1	-3.558	-6.298	-7.326	-8.812	-11.375
A_2	-0.085	-0.453	1.212	0.962	5.238
A_3	-17.974	-19.548	-23.508	-26.593	-26.030
A_4	22.417	28.517	29.611	33.562	30.278
s	*0.278*	*0.178*	*0.133*	*0.330*	*0.321*
	303.15 K	**308.15 K**	**313.15 K**	**318.15 K**	**323.15 K**
A_0	27.915	31.722	35.286	38.603	41.755
A_1	-13.840	-15.707	-17.329	-19.149	-21.124
A_2	9.350	12.682	16.381	22.303	26.396
A_3	-23.732	-22.333	-21.131	-18.698	-16.143
A_4	27.275	24.830	21.120	12.565	6.726
s	*0.275*	*0.270*	*0.351*	*0.283*	*0.315*
	328.15 K	**333.15 K**	**338.15 K**	**343.15 K**	**348.15 K**
A_0	44.712	47.589	49.852	52.894	55.276
A_1	-22.854	-24.390	-26.897	-28.248	-30.456
A_2	31.619	35.733	41.408	42.274	43.756
A_3	-13.535	-11.307	-8.510	-7.334	-6.367
A_4	-0.950	-6.767	-15.020	-17.837	-20.281
s	*0.347*	*0.426*	*0.424*	*0.483*	*0.476*
	353.15 K	**358.15 K**	**363.15 K**	**368.15 K**	
A_0	58.141	60.208	63.056	65.298	
A_1	-32.031	-34.799	-36.177	-37.775	
A_2	41.218	40.942	33.544	25.266	
A_3	-6.923	-6.548	-10.099	-14.582	
A_4	-17.544	-15.828	-4.053	14.391	
s	*0.574*	*0.464*	*0.500*	*0.620*	

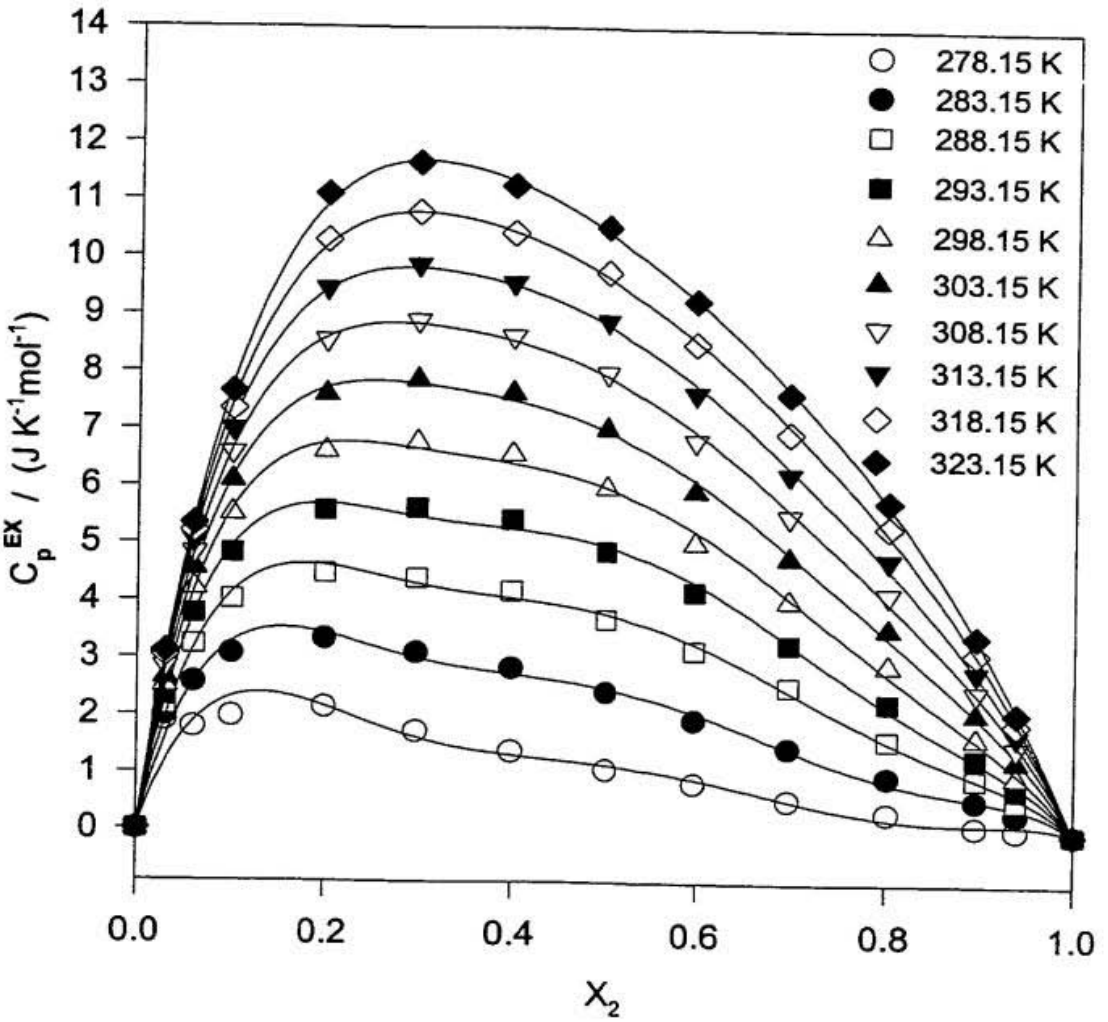

Figure 4.2.3 Excess heat capacities C_p^{EX} of methyldiethanolamine from 278.15 K to 323.15 K plotted against mole fraction. Lines are the fitted Redlich-Kister equation (equation 4.2.7).

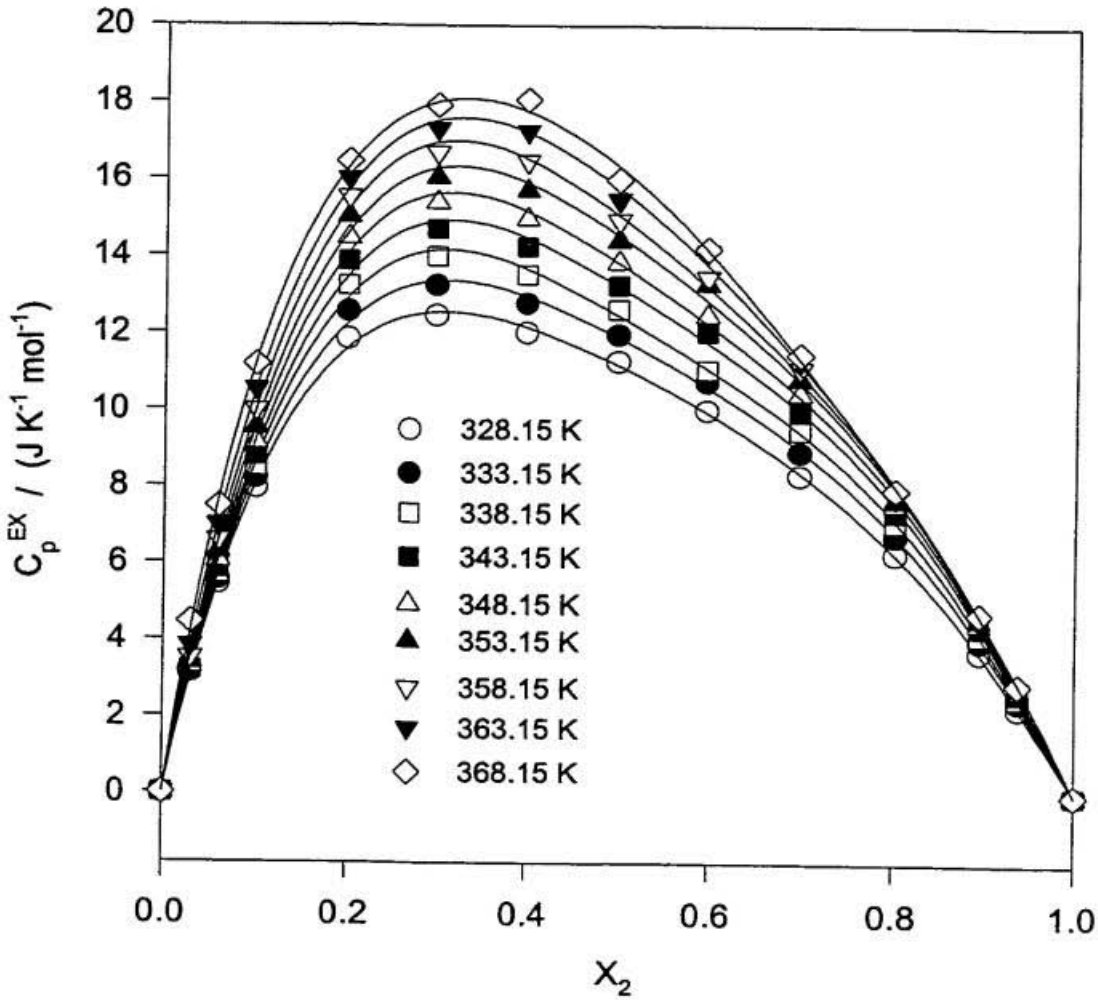

Figure 4.2.4 Excess heat capacities C_p^{EX} of methyldiethanolamine from 328.15 K to 368.15 K plotted against mole fraction. Lines are the fitted Redlich-Kister equation (equation 4.2.7).

Table 4.2.4 Fitting parameters for excess heat capacities from equation 4.2.8 where *s* denotes the standard deviation ($J \cdot K^{-1} \cdot mol^{-1}$) for each isothermal fit.

Parameter					
	278.15 K	**283.15 K**	**288.15 K**	**293.15 K**	**298.15 K**
D_2	-0.8638	-0.7609	-0.6516	-0.6127	-0.5863
D_3	-0.0995	-0.0877	-0.1149	-0.0885	-0.0654
A_0	4.7020	9.6237	14.7506	19.3075	23.5465
A_1	5.1885	7.9790	10.4049	12.8741	15.0534
s	*0.433*	*0.185*	*0.131*	*0.201*	*0.227*
	303.15 K	**308.15 K**	**313.15 K**	**318.15 K**	**323.15 K**
D_2	-0.5792	-0.5582	-0.5345	-0.5102	-0.4914
D_3	-0.0249	-0.0141	-8.4367e-3	0.0199	0.0452
A_0	27.6245	31.5500	35.2914	38.9694	42.3469
A_1	16.8942	18.2532	19.4792	21.1920	22.8821
s	*0.300*	*0.153*	*0.205*	*0.282*	*0.377*
	328.15 K	**333.15 K**	**338.15 K**	**343.15 K**	**348.15 K**
D_2	-0.4725	-0.4562	-0.4459	-0.4219	-0.4120
D_3	0.0719	0.0917	0.1239	0.1336	0.1457
A_0	45.6437	48.7821	51.4395	54.5093	56.9562
A_1	24.4950	25.8952	28.1996	29.7298	31.8847
s	*0.497*	*0.616*	*0.725*	*0.767*	*0.782*
	353.15 K	**358.15 K**	**363.15 K**	**368.15 K**	
D_2	-0.3963	-0.4020	-0.3950	-0.4158	
D_3	0.1395	0.1487	0.1112	0.0640	
A_0	59.5752	61.5289	63.7427	65.2183	
A_1	33.5887	36.1112	37.4079	38.0712	
s	*0.775*	*0.669*	*0.554*	*0.564*	

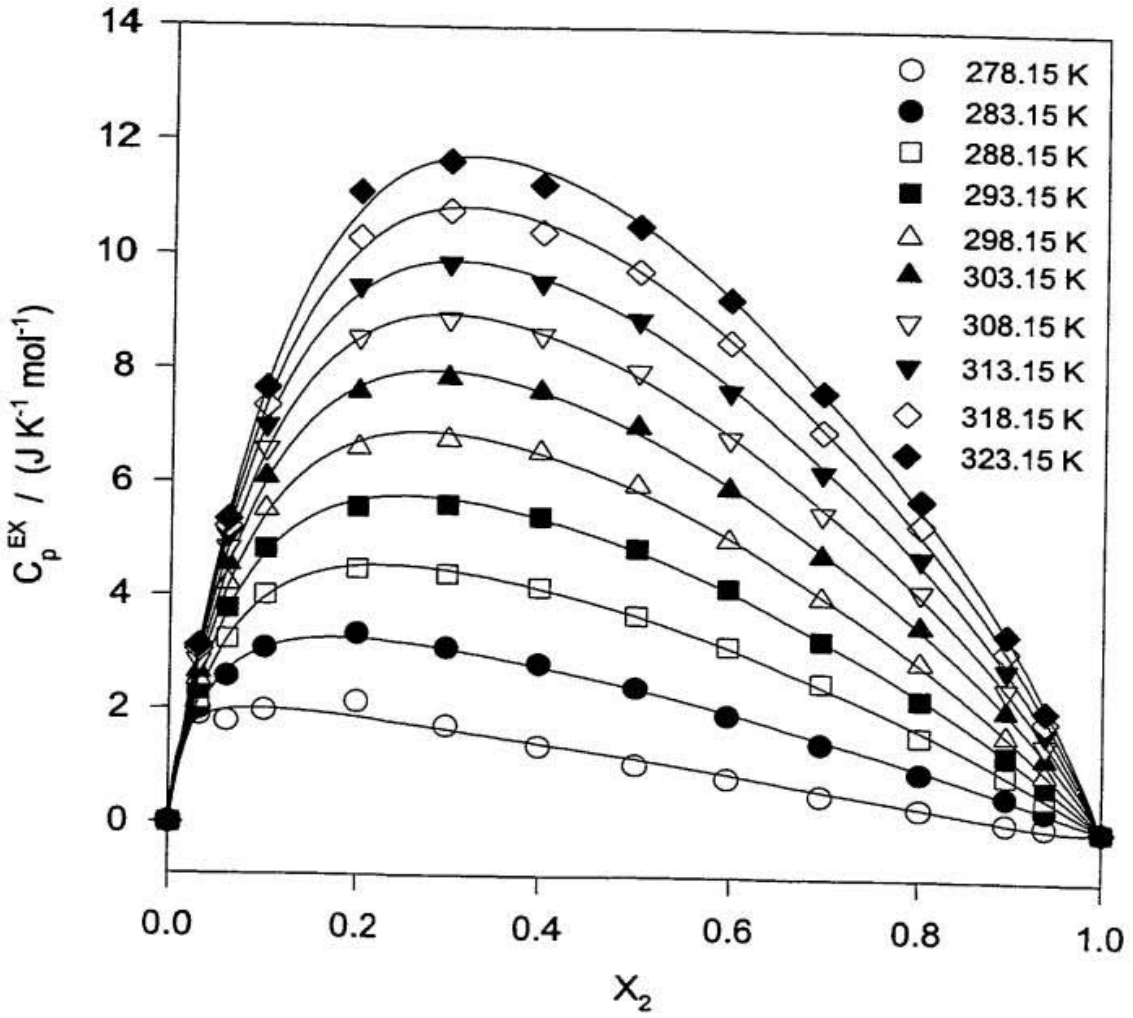

Figure 4.2.5 Excess heat capacities C_p^{EX} of methyldiethanolamine from 278.15 K to 323.15 K plotted against mole fraction. Lines are fitted values of equation 4.2.8.

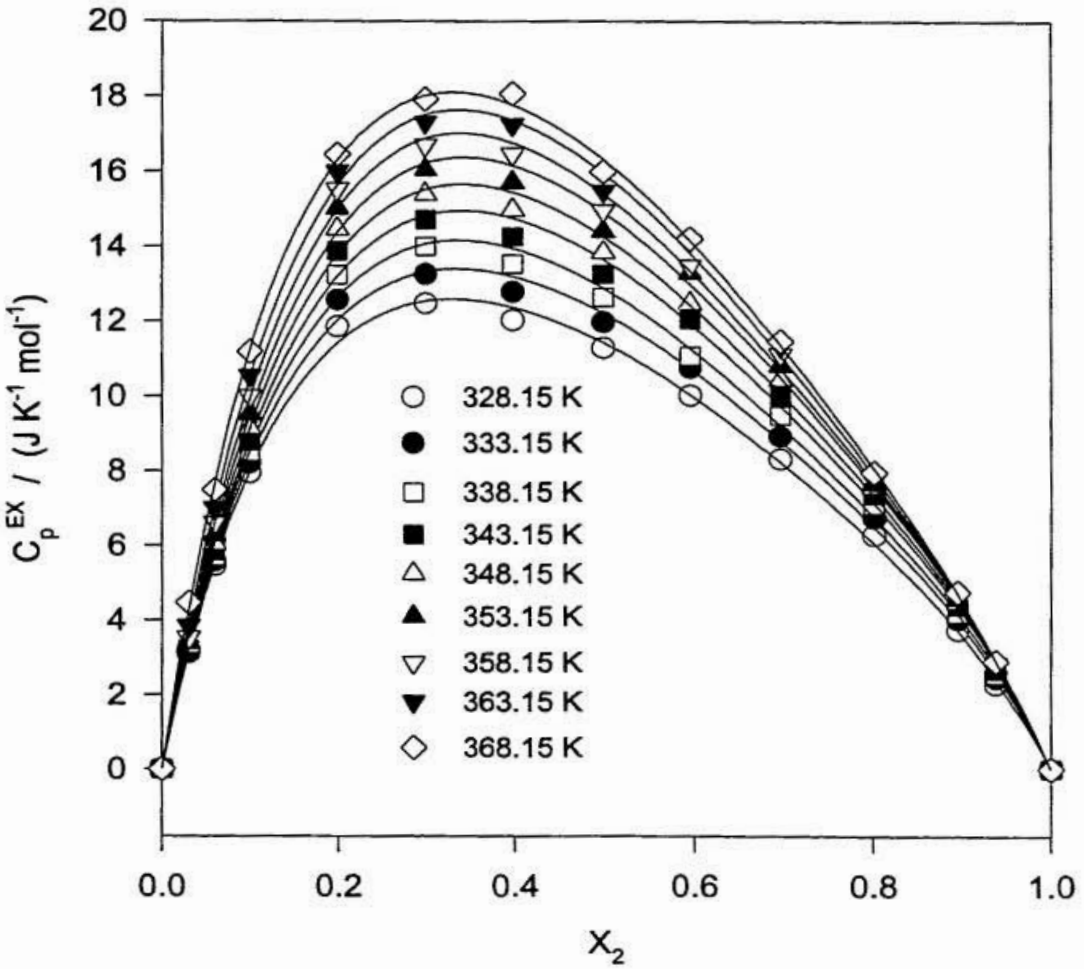

Figure 4.2.6 Excess heat capacities C_p^{EX} of methyldiethanolamine from 328.15 K to 368.15 K plotted against mole fraction. Lines are fitted values of equation 4.2.8.

4.3 Discussion

4.3.1 Excess Heat Capacities and Excess Volumetric Properties

The plots of excess heat capacities illustrated in Figures 4.2.3 to 4.2.6 indicate that the maximum deviation from ideality occurs at mole fractions below 0.5 for all temperatures. The maximum in C_p^{EX} is positive and large, and occurs at water-rich compositions with an approximate constant composition of $X_2 \approx 0.30$ at 298.15 K. The maximum increases to larger values and higher mole fractions with an increase in temperature. At $T < 298.15$ K, the maximum in C_p^{EX} shifts to lower concentrations reaching $X_2 = 0.01$ near 278.15 K.

Excess volumes and compressibilities were measured at 298.15 K as part of the author's undergraduate honors thesis (Hawrylak, 1997) and are illustrated in Figures 4.3.1 and 4.3.2. They were modeled by a Redlich-Kister equation with six parameters. The V^{EX} and κ_s^{EX} are negative over the mole fraction range which is common for other completely miscible water + polar organic species. The negative deviation indicates that the water/ MDEA mixtures result in solutions which are more dense, more compact, and less compressible than the individual contributions of the pure water and MDEA alone due to the geometrical fitting of one component into another caused by differences in the molar volume. At 298.15 K, the maximum deviation for both V^{EX} and κ^{EX} occurs at $X \approx 0.35$ which is comparable to the maximum deviation of C_p^{EX} at the same temperature.

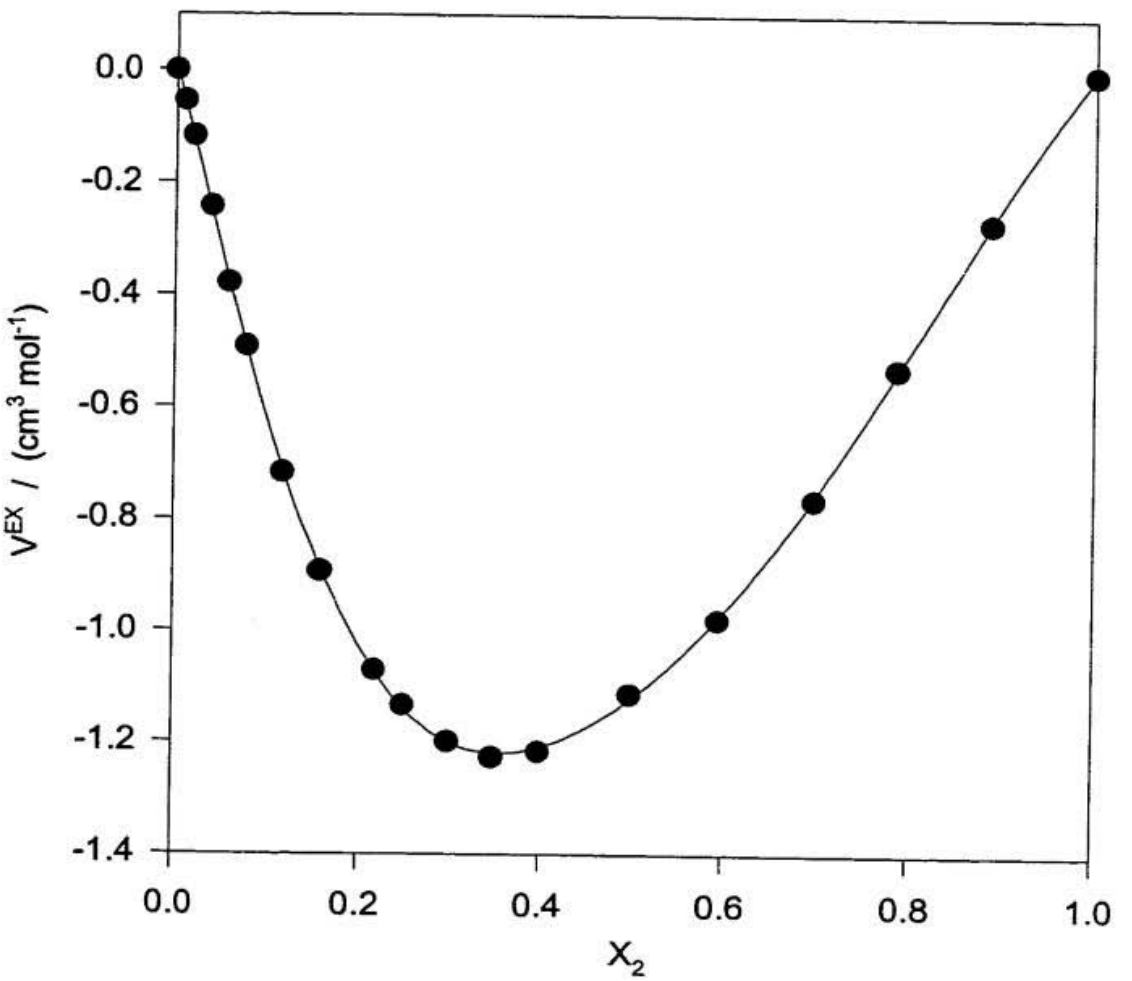

Figure 4.3.1 Excess volumes of methyldiethanolamine at 298.15 K.

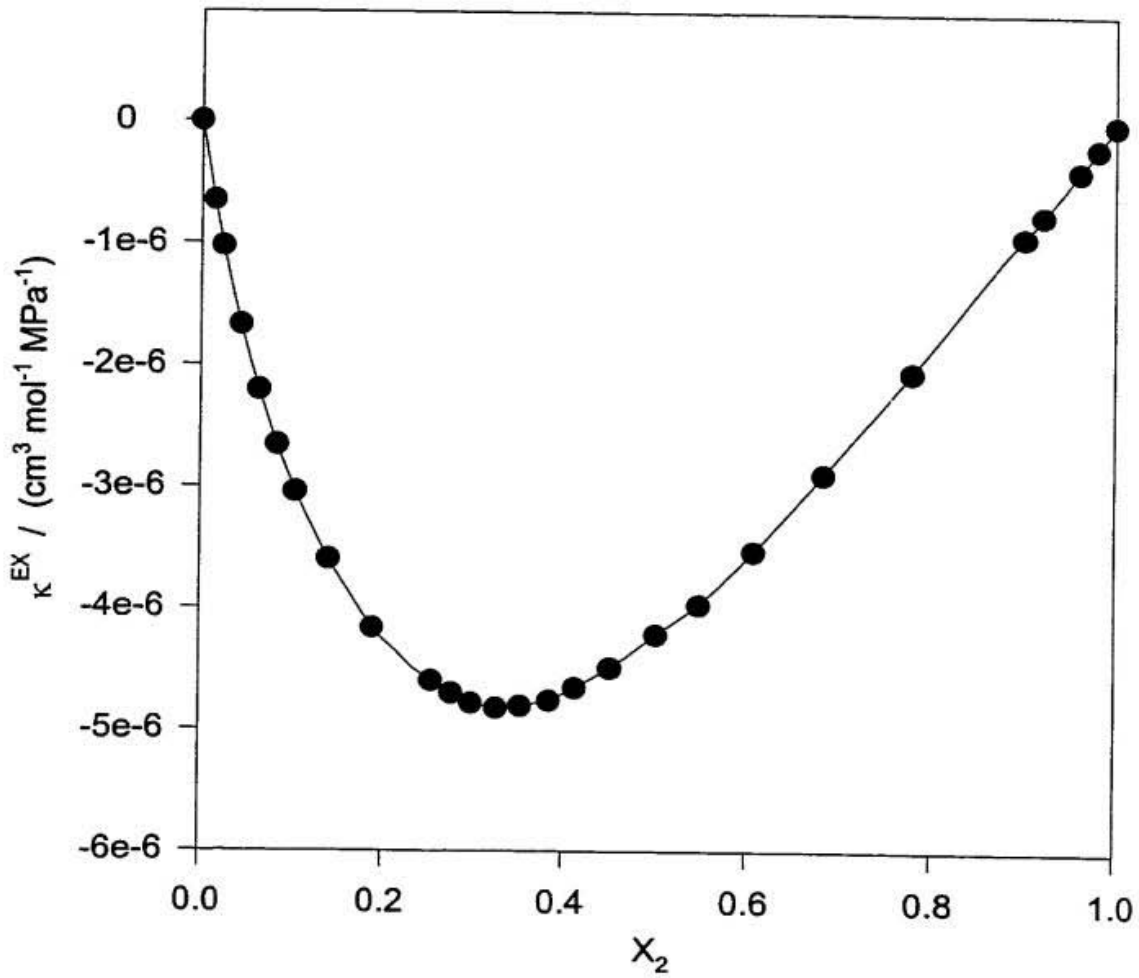

Figure 4.3.2 Excess compressibilities at 298.15 K.

4.3.2 Reduced Excess Heat Capacities

Although the plots of excess heat capacities illustrate the magnitude of the nonideality, the low numerical values in the water-rich region hide strong interactions at low composition and thus fail to reveal all of the important features of the composition dependence, making the interpretation of such curves difficult.

To interpret these results, we have transformed C_p^{EX} to the more composition sensitive property, $C_p^{EX}/(X_1X_2)$, in order to gain a better understanding of the effects of the changes in solution composition. As discussed in Section 1.8, the reduced excess property is calculated from the excess heat capacities using the relation:

$$\frac{C_p^{EX}}{X_2(1-X_2)} = \frac{(C_{p,\phi,2} - C_{p,2}^*)}{X_1} = \frac{(C_{p,\phi,1} - C_{p,1}^*)}{X_2} \qquad (4.3.1)$$

This function is therefore related to the apparent molar quantities over the whole mole fraction range, and its extrapolation to $X_2 = 0$ and $X_2 = 1$ will give the two standard partial molar properties from the intercepts $[C_{p,2}^\circ - C_{p,2}^*]$ and $[C_{p,1}^\circ - C_{p,1}^*]$. Plots of the reduced excess heat capacities, shown in Figures 4.3.3 (using equation 4.2.7) and 4.3.4 (using equation 4.2.8), for temperatures $283.15 \le T \le 328.15$ K provide a clearer vision of the composition dependence than do those of C_p^{EX}. The values of $C_p^{EX}/(X_1X_2)$ at $X_2 = 0$ in the plots were calculated from the standard partial molar heat capacities determined with the Picker calorimeter in Table 3.3.1 From the plots in Figures 4.3.3 and 4.3.4, it

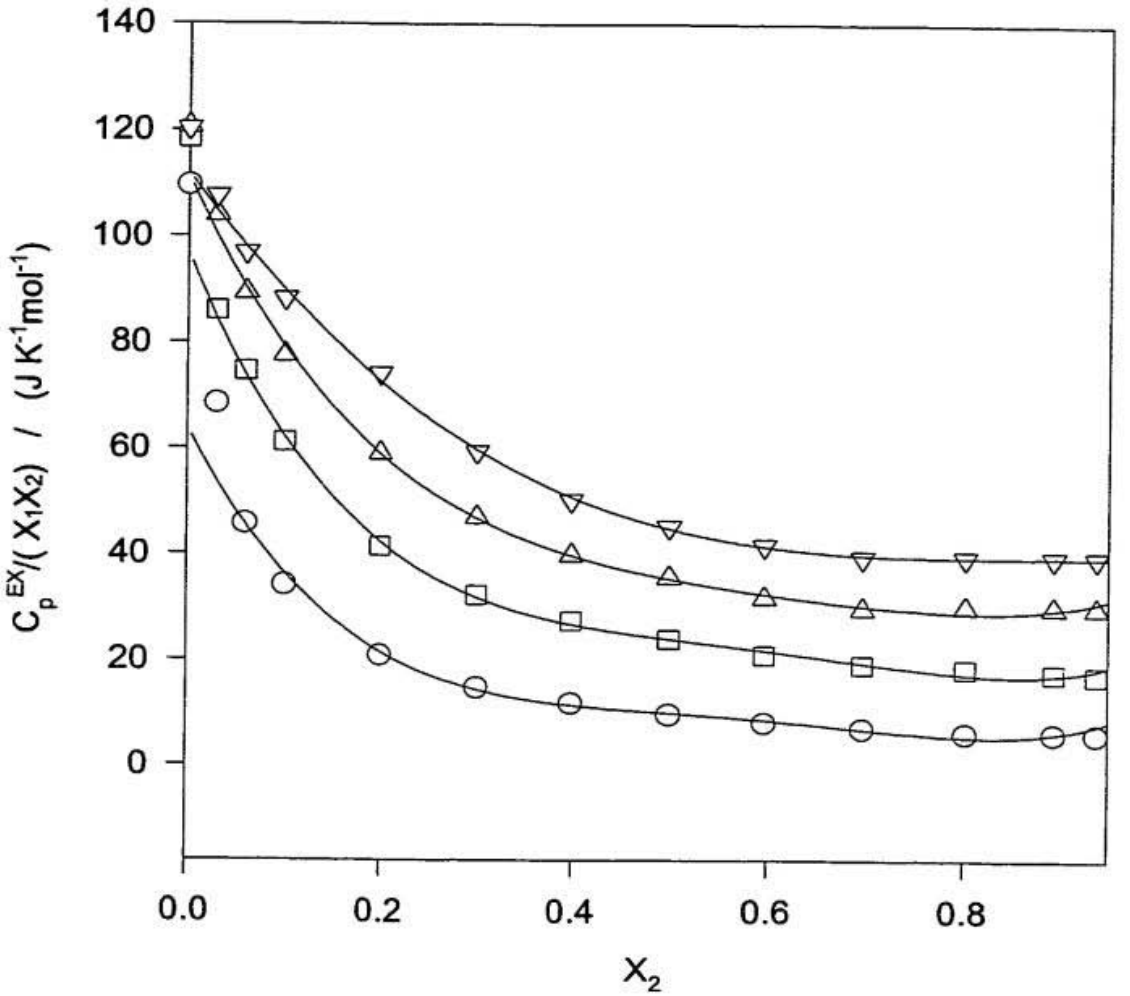

Figure 4.3.3 Reduced excess heat capacities of methyldiethanolamine from 283.15 K to 328.15 K plotted against mole fraction. Symbols are experimental results: ○ 283.15 K; □ 298.15 K; Δ 313.15 K; ∇ 328.15 K. Lines are fitted values of equation 4.2.7

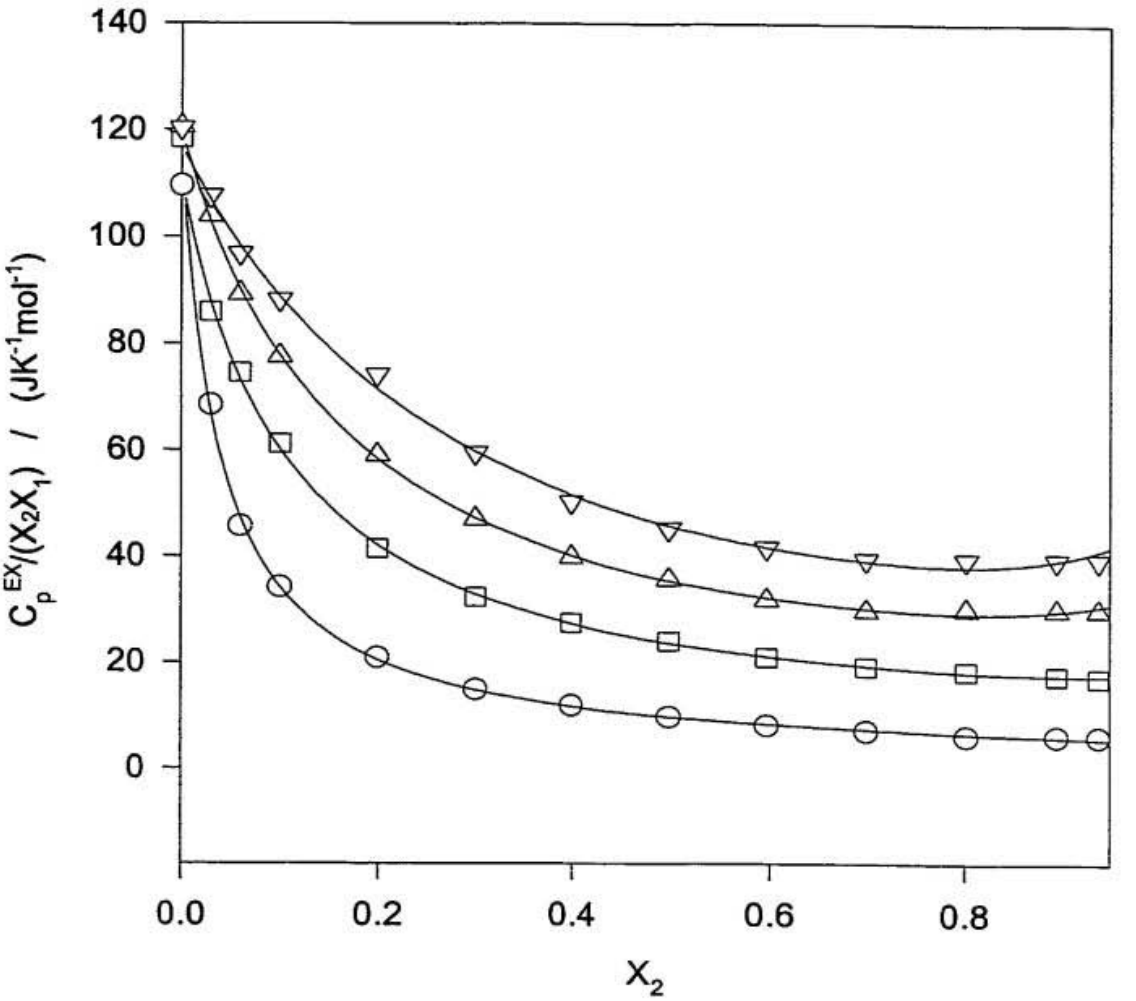

Figure 4.3.4 Reduced excess heat capacities of methyldiethanolamine from 283.15 K to 328.15 K plotted against mole fraction. Symbols are experimental results: ○ 283.15 K; □ 298.15 K; Δ 313.15 K; ▽ 328.15 K. Lines are fitted values of equation 4.2.8.

can be observed that the reduced excess heat capacity decreases sharply from the intercept in the water-rich region and approaches a relatively constant value at higher concentrations. With increasing temperature, the sharpness of the decline is much less and the transition to the plateau is more gradual.

Lumry *et al.* (1982) proposed a qualitative model to interpret the excess thermodynamic functions of ethylene glycol and it has been used by other authors such as Pagé *et al.* (1993) to explain similar miscible hydrogen-bonded solute-water systems. The composition scale is subdivided into three regions in which different effects are predominant: (i) $0 < X_2 \leq 0.1$: the solute occupies "holes" in the open structure of hydrogen-bonded water but disrupts the cooperative fluctuation units of liquid water; (ii) $0.1 \leq X_2 \leq 0.3$: the solute eliminates the extensive hydrogen-bonding connectivity between the water molecules; and (iii) $X_2 \geq 0.3$: water-solute interactions are progressively replaced by solute-solute interactions.

Figure 4.3.5 shows a schematic representation of such a system, with each region characterized by a single Redlich-Kister interaction parameter. Behavior consistent with the Lumry model was observed in the comprehensive thermodynamic study of the water-monoethanolamine system by Pagé *et al.* (1993). The data for MDEA in Figures 4.3.3 and 4.3.4 appears to only display Regions (ii) and (iii).

Monoethanolamine (MEA) is a primary alkanolamine similar to methyldiethanolamine except that a nitrogen center is attached to two hydrogens and only

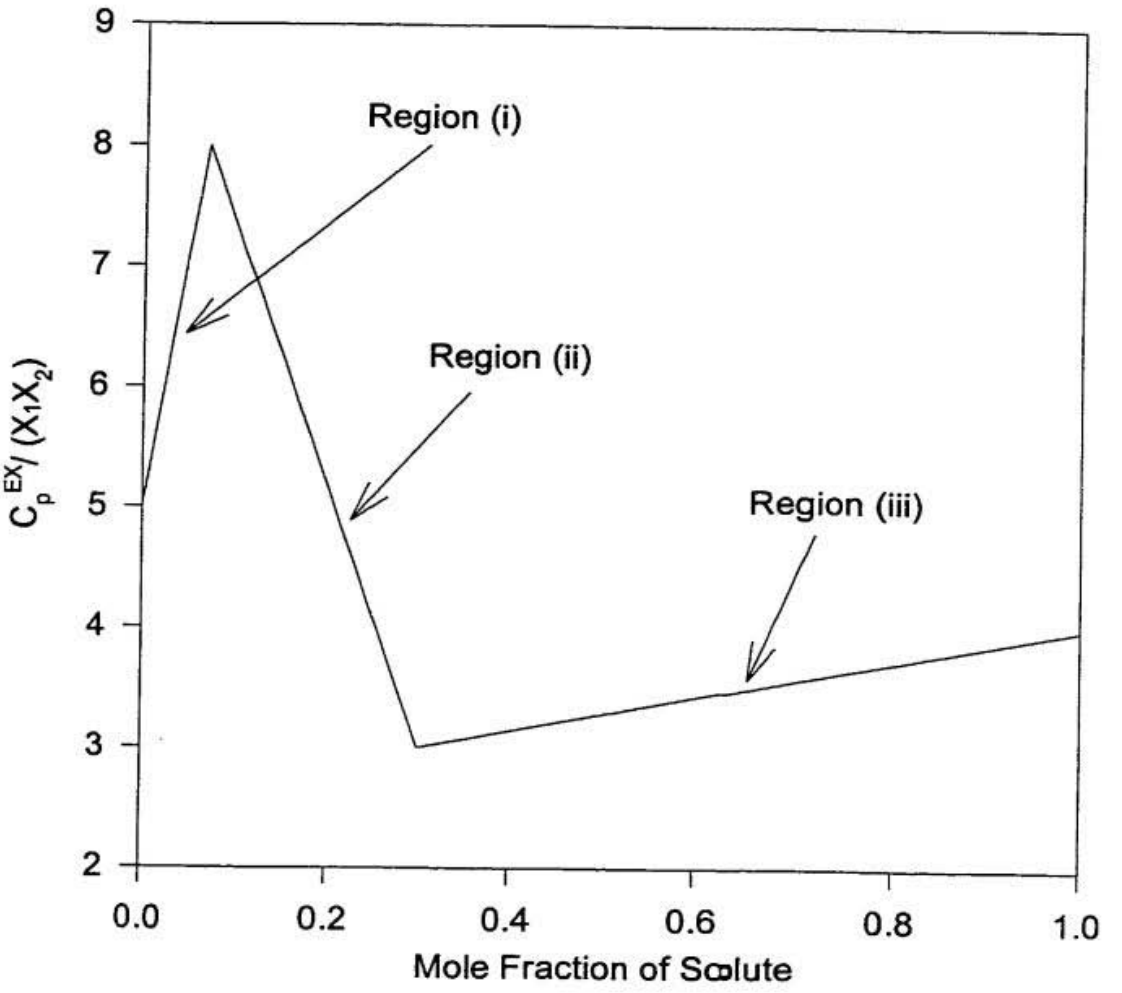

Figure 4.3.5 Schematic of typical reduced excess heat capacity plot: Regions (i), (ii), and (iii) according to Lumry *et al.* (1982)

one ethanol group. Thus, MEA is physically smaller than MDEA and also has less hydrophobic character. The fact that the maximum in $C_p^{EX}/(X_1X_2)$ at low mole fractions was observed for MEA but not for MDEA may be due to two possible reasons: (1) MDEA is too large to be located preferentially in the voids of the water structure at low concentrations and/or (2) the increase in $C_p^{EX}/(X_1X_2)$ for MDEA occurs at concentrations below 0.1 $mol \cdot kg^{-1}$ such that it cannot be detected by our instruments.

Water structure changes are very sensitive to temperature. Because of hydrophobic effects on water structure, nonpolar organic groups can introduce large positive excess heat capacity effects. The behavior of MDEA and MEA in water at finite concentrations illustrates the interplay of opposing effects that can be found in solution thermodynamics. In one molecule, alkanolamines contain two or more functional groups which can hydrogen-bond with the water, and so disrupt the water "structure", and also apolar groups which, by virtue of their large negative entropy of hydration, reinforce hydrogen bonding in the surrounding water. Positive values of $C_p^{EX}/(X_2X_1)$ may be interpreted as being due to "structure making" which decreases the entropy at low temperatures but is broken down as the temperature increases, giving a positive contribution to $(\partial S^{EX}/\partial T)_p$ and consequently to C_p^{EX}.

When comparing the two fitting equations used to model the excess heat capacities, it can be seen from both the excess heat capacity plots and the reduced excess heat capacity plots that equation 4.2.8 is more successful than the Redlich-Kister equation

(equation 4.2.7). Not only does equation 4.2.8 require fewer parameters but it also provides a better fit to the data in the important water-rich region.

4.4 Conclusions

These measurements yield some of the first experimental excess heat capacities for aqueous solutions of MDEA over such a range of temperatures covering the entire composition scale. The CSC 4100 DSC allows for accurate and rapid measurements during the temperature scan and the presence of three sample chambers allows for the measurement of samples in triplicate. The ease of use and sensitivity of the instrument make it desirable for operations above 373 K with the proper care and attention.

The type of nonideality seen in this work is also observed in many mixtures where changes in hydrophobic interactions are best observed in a $C_p^{EX}/(X_2X_1)$ plot. (Tanaka *et al.*, 1986). For our work, this interesting behavior is most dramatic at temperatures below 298 K. In conclude, the C_p^{EX} become progressively more positive as the temperature increases with the maxima shifting to larger mole fractions in the water-rich region.

Chapter 5: Bibliography

Abraham M.H. and Marcus Y. (1986). The Thermodynamics of Solvation of Ions. Part I. The Heat Capacity of Hydration at 298.15 K. *J. Chem. Soc. Faraday Trans. I.* **82**, 3255-3274.

Albert H.J. and Wood R.H. (1984). High-Precision Densimeter for Fluids at Temperatures to 700K and Pressures to 40 MPa. *Rev. Sci. Instrum.* **55**, 589-593.

Allred G.C. and Woolley E.M. (1981). Heat Capacities of Aqueous HCl, NaOH, and NaCl at 283.15 , 298.15, and 313.15 K : ΔC_p° for Ionization of Water. *J. Chem. Thermodyn.* **13**, 147-154.

Anderson G.M., Castet S., Schott J., and Mesmer R.E. (1991). The Density Model for Estimation of Thermodynamic Parameters of Reactions at High Temperatures and Pressures. *Geochim. Cosmochim. Acta.* **55**, 1769-1779.

Anderson G.M. and Crerar D.A. (1993). *Thermodynamics in Geochemistry: The Equilibrium Model.* Oxford University Press, Inc. New York.

Archer D.G. (1992). Thermodynamic Properties of the NaCl + H_2O System II. Thermodynamic Properties of NaCl(aq), NaCl·$2H_2O$(cr), and Phase Equilibria. *J. Phys. Chem. Ref. Data* **21**, 793-823.

Archer D.G. and Wang P. (1990). The Dielectric Constant of Water and Debye-Hückel Limiting Slopes. *J. Phys. Chem. Ref. Data* **19**, 371-411.

Astarita G., Savage D.W., and Bisio A. (1983). *Gas Treating with Chemical Solvents.* John Wiley & Sons, New York

Balakrishnan P.V. (1988). Liquid-Vapor Distribution of Amines and Acid Ionization Constants of Their Ammonium salts in Aqueous Systems at High Temperature. *J. Sol. Chem.* **17**, 825-840.

Biggerstaff J.L. and Wood R.H. (1988). Apparent Molar Volumes of Aqueous Argon, Ethylene, and Xenon from 300 to 716 K. *J. Phys. Chem.* **92**, 1988-1994.

Bernal J.D. and Fowler R.H. (1933). A Theory of Water and Ionic Solution, with Particular Reference to Hydrogen and Hydroxyl Ions. *J. Chem. Phys.* **1**, 515.

Born M. (1920). Volumen und Hydratationswärme der Ionen. *Z. Phys.* **1**, 45-48

Bradley D.J. and Pitzer K.S. (1979). Thermodynamics of Electrolytes. 12. Dielectric Properties of Water and Debye-Hückel Parameters to 350°C. *J. Phys. Chem.* **83**, 1599-1603.

Chalikian T.V., Sarvazyan A.P., Funck T., Cain C.A., and Breslauer K.J. (1994). Partial Molar Characteristics of Glycine and Alanine in Aqueous Solutions at High Pressures Calculated from Ultrasonic Velocity Data. *J. Phys. Chem.* **98**, 321-328

Chiu L.-F., Liu H.-F., and Li M.-H. (1999). Heat Capacity of Alkanolamines by Differential Scanning Calorimetery. *J. Chem. Eng. Data* **44**, 631-636.

Christensen J.J., Christensen S.P., Schofield R.S., Faux P.W., Harding P.R., and Izatt R.M. (1984). The Excess Enthalpies of Carbon Dioxide + Pyridine at 308.15, 358.15, and 413.15 K from 7.50 to 12.50 MPa. *J. Chem. Thermodyn.* **16**, 249-255.

Christensen J.J., Zebolsky D.M., and Izatt R.M. (1985). The Excess Enthalpies of Carbon Dioxide + Toluene at 470.15 and 573.15 K from 7.60 to 12.67 MPa. *J. Chem. Thermodyn.* **17**, 1-10.

Christensen J.J., Cordray D., Zebolsky D.M., and Izatt R.M. (1986). The Excess Enthalpies of Carbon Dioxide + Decane from 293.15 to 573.15 K at 12.50 MPa. *J. Chem. Thermodyn.* **18**, 53-61.

Cobble J.W. and Turner P.J. (1985). *Additives for pH Control in PWR Secondary Water.* Electric Power Research Inst. (EPRI) Report NP-4209.

Corti H.R., Fernandez-Prini R.J., and Svarc F. (1990). Densities and Partial Molar Volumes of Aqueous Solutions of Lithium, Sodium, and Potassium Hydroxides up to 250°C. *J. Solution Chem.* **19**, 793-809.

Davis M. (1993). Thermodynamic and Related Studies of Amphiphile + Water Systems. *Chem. Soc. Rev.* **22**, 127.

Desnoyers J.E. and Perron G.(1997). Treatment of Excess Thermodynamic Quantities for Liquid Mixtures. *J. Sol. Chem.* **26**, 749-755.

Desnoyers J.E., de Visser C., Perron G., and Picker P. (1976). Reexamination of the Heat Capacities Obtained by Flow Microcalorimetry. Recommendation for the Use of a Chemical Standard. *J. Solution Chem.* **5**, 605-616.

Féron D. and Lambert I. (1992). Thermal Stability of Three Amines in Pressurized Water Reactor Secondary Systems. Laboratory and Loop Experiments. *J. Sol. Chem.* **21**, 919-932.

Fernandez-Prini R.J., Corti H.R., and Japas M.L. (1992). *High-Temperature Aqueous Solutions: Thermodynamic Properties*. CRC Press, Boca Raton, FL.

Franck E.U. (1956). Hochverdichteter Wasserdampf II. Ionendissociation von KCl in H_2O bis 750°C. *Z. Phys. Chem.* (NF) **8**, 107-126.

Franck E.U. (1961). Überkritisches Wasser als Electrolytisches Lösungsmittel. *Angew. Chem.* **73**, 309-322.

Frazier H.D. and Kohl A.L. (1950). *Ind. Eng. Chem.* **42**, 2282-2292.

Gianni P. and Lepori L. (1996). Group Contributions to the Partial Molar Volume of Ionic Organic Solutes in Aqueous Solution. *J. Sol. Chem.* **25**, 1- 42.

Goldman S. and Bates R.G. (1972). Calculation of Thermodynamic Functions for Ionic Hydration. *J. Phys. Chem.* **76**, 1476-1484.

Grolier J-P.E. (1994) in Marsh K.N. and O'Hare P.A., ed; *Solution Calorimetry*; Chapter 4: *Heat Capacity of Organic Liquids*. Blachwell Scientific Publications, Cambridge.

Guthrie J.P. (1977). Additivity Schemes Permitting the Estimation of Partial Molar Heat Capacities of Organic Compounds in Aqueous Solution. *Can. J. Chem*, **55**, 3700-3706.

Hawrylak B.E. (1997). Thermodynamic Properties of Alkanolamines in Aqueous Media. B.Sc. Honours Thesis, St. Francis Xavier University, Antigonish, Nova Scotia.

Haar L., Gallagher J.S., and Kell G.S. (1984). Thermodynamic and Transport Properties and Computer Programs for Vapor and Liquid States of Water in SI Units. *NBS/NRC Steam Tables* (Hemisphere, Washington).

Helgeson H.C. and Kirkham D.H. (1974). Theoretical Prediction of the Thermodynamic Behaviour of Aqueous Electrolytes at High Temperatures and Pressure: I Summary of the Thermodynamic/Electrostatic properties of the Solvent. *Amer. J. Sci.* **274**, 1089-1198.

Helgeson H.C. and Kirkham D.H. (1976). Theoretical Prediction of the Thermodynamic Behaviour of Aqueous Electrolytes at High Temperatures and Pressure: III Equation of State for Aqueous Species at Infinite Dilution. *Amer. J. Sci.* **276**, 97-240.

Helgeson H.C., Kirkham D.H., and Flowers G.C. (1981). Theoretical Predictions of the Thermodynamic Behaviour of Aqueous Electrolytes at High Pressures and Temperatures. IV. Calculation of Activity Coefficients, Osmotic Coefficients, and Apparent Molar and Standard and Relative Partial Molar Properties to 600°C and 5kBar. *Amer. J. Sci.* **281**, 1249-1516.

Hershey J.P., Damesceno R., and Millero F.J. (1984). Densities and Compressibilities of Aqueous HCl and NaOH from 0 to 45°C. The Effect of Pressure on the Ionization of Water. *J. Solution Chem.* **13**, 825-849.

Hill P.G. (1990). A Unified Fundamental Equation for the Thermodynamic Properties of H_2O. *J. Phys. Chem. Ref. Data* **19**, 1233-1274

Holmes H.F. and Mesmer R.E (1983). Thermodynamic Properties of Aqueous Solutions of the Alkali Metal Chlorides to 250°C. *J. Phys. Chem.* **87**, 1242-1255.

Hovey J.K., Hepler L.G., and Tremaine P.R. (1988). Apparent Molar Heat Capacities and Volumes of Aqueous $HClO_4$, HNO_3, $(CH_3)NOH$, and K_2SO_4 at 298.15 K. *Thermochim Acta.* **126**, 245-253.

Hsu C-H. and Li M-H. (1997). Densities of Aqueous Blended Amines. *J. Chem. Eng. Data* **42**, 502-507.

Hwang S.H., DesMarteau D.D., Beyerlein A.L., Smith N.D., and Joyner P. (1992). The Heat Capacity of Fluorinated Propane and Butane Derivatives by Differential Scanning Calorimetry. *J. Thermal Anal.* 38, 2515-2528.

Johnson J.W., Oelkers E.H., and Helgeson H.C. (1992). SUPCRT92: A Software Package for Calculating the Standard Molal Thermodynamic properties of Minerals, Gases, Aqueous Species, and Reactions from 1 to 5000 bar and 0 to 1000°C. *Computers and Geosciences* **18**, 899-947.

Jones F.M. and Arnett E.M. (1974). Thermodynamics of Ionization and Solution of Aliphatic Amines in Water. *Prog. Phys. Org. Chem.* **11**, 263-314.

Kharakoz D.P. (1991). Volumetric Properties of Proteins and Their Analogues in Diluted Water Solution. 2. Partial Adiabatic Compressibilities of Amino Acids at 15-70°C. *J. Phys. Chem.* **95**, 5634-5642.

Kim J-H., Dobrogowska C., Hepler L.G. (1987). Thermodynamics of Ionization of Aqueous Alkanolamines. *Can. J. Chem.* **65**, 1726-1728.

Kratky O., Leopold H., and Stabinger H. (1969). Density Determinations of Liquids and Gases to an Accuracy of 10^{-6} g·cm^{-3}, with a Sample Volume of only 0.6 cm^3 (English Title from Chem. Abs.) *Angew. Phys.* **27**, 273-277.

Kohl A.L. and Riesenfeld F.C. (1974).*Gas Purification 2nd Edition*. Gulf Publishing Company: Houston.

Levelt Sengers J.M.H. (1991). in *Supercritical Fluid Technology: Reviews in Modern Theory and Application*; Bruno T.J. and Ely J.F., ed; Chapter 1: Thermodynamics of Solutions Near the Solvents Critical Point. CRC Press, Boca Raton, FL.

Lumry R., Battistel E., and Jolicoeur C. (1982). Geometric Relaxation in Water: Its Role in Hydrophobic Hydration. *Faraday Symp. Chem. Soc.* **17**, 93-108.

Maham Y., Hepler L.G., Mather A.E., Hakin A.W., Marriott R.A. (1997). Molar Heat Capacities of Alkanolamines from 299.1 to 397.8 K: Group Additivity and Molecular Connectivity Analysis. *J. Chem. Soc., Faraday Trans.* **93**,1747-1750.

Maham Y., Teng T.T., Mather A.E., Hepler L.G. (1995). Volumetric Properties of (Water + Diethanolamine) Systems. *Can. J. Chem.* **73**, 1514-1519.

Mains G.J., Larson J.W. and Hepler L.G. (1984). General Thermodynamic Analysis of the Contributions of Temperature-Dependent Chemical Equilibria to Heat Capacities of Ideal Gases and Ideal Associated solutions. *J. Phys. Chem.* **88**, 1257-1261.

Marsh K.N. and O'Hare P.A., ed; (1994). *Solution Calorimetry*; Chapter 4: *Heat Capacity of Organic Liquids*. Blackwell Scientific Publications, Cambridge.

Marshall W.L and Franck E.U. (1981). Ion Product of Water Substance, 0-1000°C, 1-10,000 bars, New International Formulation and its Background. *J. Phys. Chem. Ref. Data* **10**, 295-304.

Mesmer R.E., Marshall W.L., Palmer D.A., Simonson J.M., and Holmes H.F. (1988). Thermodynamics of Aqueous Association and Ionization Reactions at High Temperatures and Pressures. *J. Solution Chem.* **17**, 699.

Mesmer R.E., Palmer D.A., and Simonson J.M. (1991) in Pitzer K.S., ed.; Activity Coefficients in Electrolyte Solution, 2nd Edition. Chapter 8: Ion Association at High Temperatures and Pressures. CRC Press, Boca Raton, FL. 496-498.

Millero F.J. (1970). The Apparent and Partial Molar Volume of Aqueous Sodium Chloride Solutions at Various Temperatures, *J. Phys. Chem.* **74**, 356-362.

Millero F.J. (1979). Activity Coefficients in Electrolyte Solutions: Vol. 2. Pytkowicz, M. ed., CRC Press, Boca Raton, FL.

Millero F.J. and Kubinski T. (1975). Speed of Sound in Seawater as a Function of Temperature and Salinity of Water. *J. Acoust. Soc. Am.* **57**, 312.

Millero F. J., Ward G.K., and Chetirkin P.V. (1977). Relative Sound Velocities of Sea Salts at 25°C. *J. Acoust. Soc. Am.* **61**, 1492.

Mraw S.C. and Nass-O'Rourke D.F. (1980). Accuracy of Differential Scanning Calorimetry for Heat Capacities of Organic Compounds at High Temperature. New Method for Enthalpy of Fusion by DSC. *J. Chem. Thermodyn.* **12**, 691.

Mraw S.C. and Nass-O'Rourke D.F. (1981). Accuracy of Differential Scanning Calorimetry for Heat Capacities of Organic Compounds at High Temperature. New Method for Enthalpy of Fusion by DSC. *J. Chem. Thermodyn.* **13**, 199.

Oscarson J.L., Wu G., Faux P.W., Izatt R.M., and Christensen J.J. (1989). Thermodynamics of Protonation of Alkanolamines in Aqueous Solution to 325°C. *Thermochim. Acta*. **154**, 119-127.

Pagé M., Huot J-Y., and Jolicoeur C. (1993). A Comprehensive Thermodynamic Investigation of Water-Ethanolamine Mixtures at 10, 25, and 40°C. *Can. J. Chem.* **71**, 1064-1072.

Perron G., Couture L. and Desnoyers J.E. (1992). Correlation of the Volumes and Heat Capacities of Solutions with their Solid-Liquid Phase Diagrams. *J. Sol. Chem.* **21**, 433-443.

Perron G. and Desnoyer J.E. (1979). Volumes and Heat Capacities of Benzene Derivatives in Water at 25°C: Group Additivity of the Standard Partial Molar Quantities. *Fluid Phase Equilibria*. **2**, 239-262.

Picker P., Tremblay E., Philip P.R., and Desnoyers J.E. (1971). Heat Capacity of Solutions by Flow Microcalorimetry. *J. Chem. Thermodyn.* **3**, 631-642.

Picker P., Tremblay E., and Jolicoeur C. (1974). A High Precision Digital Readout Flow Densimeter for Liquids. *J. Solution Chem.* **3**, 377-384.

Pitzer K.S., Peiper J.C., and Busey R.H. (1984). Thermodynamic Properties of Aqueous Sodium Chloride Solutions. *J. Phys. Chem. Ref. Data* **13**, 1-102

Pitzer K.S. (1991). Activity Coefficients in Electrolytes Solutions 2nd Edition. CRC Press. Boca Raton, Florida.

Prausnitz J.M., Lichtenthaler R.N., and de Azevedo E.G. (1986). Molecular Thermodynamics of Fluid-Phase Equilibria 2nd Edition. Prentice-Hall Inc. New Jersey. 193-266.

Randall M. and Taylor M.D. (1941). Heat Capacity and Density of aqueous Solutions of Potassium Iodate, Potassium Acid Sulfate, Iodic Acid, and Sulfuric Acid at 25°C. *J. Phys. Chem.* **45**, 959-967.

Redlich O. and Kister A.T. (1948). *Ind. Eng. Chem.* **40**, 345.

Rinker E. B., Oelsehlager D.W., Colussi A.T., Henry K.R., and Sandall O.C. (1994). Viscosity, Density, and Surface Tension of Binary Mixtures of Water and N-Methyldiethanolamine and Water and Diethanolamine and Tertiary Mixtures of These Amines with Water over the Temperature Range 20-100°C. *J. Chem. Eng. Data* **39**, 392-395.

Sandler S.I. (1994). *Models for Thermodynamic and Phase Equilibria Calculations.* Marcel Dekker, Inc. New York.

Shvedov D. and Tremaine P.R. (1997). Thermodynamic Properties of Aqueous Dimethylamine and Dimethylammonium Chloride at Temperatures from 283 K to 523 K: Apparent Molar Volumes, Heat Capacities, and Temperature Dependence of Ionization. *J. Sol. Chem.* **26**, 1113-1143.

Shock E.L. and Helgeson H.C. (1988). Calculation of the Thermodynamic and Transport Properties of Aqueous Species at High Temperatures: Correlation Algorithms for Ionic Species and Equation of State predicyions to 5 kb and 1000°C. *Geochim. Cosmochim. Acta.* **52**, 2009-2036.

Shock E.L. and Helgeson H.C. (1990). Calculation of the Thermodynamic and Transport Properties of Aqueous Species at High Pressures and Temperatures: Standard Partial Molar Properties of Organic Species. *Geochim. Cosmochim. Acta.* **54**, 915-945.

Speight J.G. (1993). *Gas Processing: Environmental Aspects and Methods.* Butterworth-Heinemann Ltd: Oxford.

Tanaka R., Toyama S., and Murakami S. (1986). Heat Capacities of $\{xC_nH_{2n+1}OH + (1-x)C_7H_{16}\}$ for n = 1 to 6 at 298.15 K. *J. Chem. Thermodynamics.* **18**, 63-73.

Tanger J.C. and Helgeson H.C. (1988). Calculation of the Thermodynamic and Transport Properties of Aqueous Species at High Pressures and Temperatures: Revised Equations of State for the Standard Partial Molar Properties of Ions and Electrolytes. *Am. J. Sci.* **288**, 19-98.

Teng T.T., Maham Y., Hepler L.G., and Mather A.E. (1994). Viscosity of Aqueous Solutions of N-Methyldiethanolamine and of Diethanolamine. *J. Chem. Eng. Data* **39**, 290-293.

Tremaine P.R. and Goldman S. (1978). Calculation of Gibbs Free Energies of Aqueous Electrolytes to 350°C from an Electrostatic Model for Ionic Hydration. *J. Phys. Chem.* **82**, 2317-2321.

Tremaine P.R., Sway K., and Barbero J.A., (1986). The Apparent Molar heat Capacity of Aqueous Hydrochloric Acid from 10 to 140°C. *J. Sol. Chem.* **15**, 1-22.

Tremaine P.R., Shvedov D., Xiao C. (1997). Thermodynamic Properties of Aqueous Morpholine and Morpholinium Chloride at Temperatures from 10 to 300°C: Apparent Molar Volumes, Heat Capacities, and Temperature Dependence of Ionization. *J. Phys. Chem. B* **101**, 409-419.

Verrall R.E. and Conway B.E. (1966). Partial Molar Volumes and Adiabatic Compressibilities of Tetraalkylammonium and Aminium Salts in Water. I. Compressibility Behavior. *J. Phys. Chem.* **70**, 3952-3960.

Verrall R.E. and Conway B.E. (1966). Partial Molar Volumes and Adiabatic Compressibilities of Tetraalkylammonium and Aminium Salts in Water. II. Volume and Volume Change Relationships. *J. Phys. Chem.* **70**, 3961-3969.

Van Ness H.C. and Abbott M.M. (1982). *Classical Thermodynamics of Nonelectrolyte Solutions: With Applications to Phase Equilibria*. McGraw-Hill, New York.

White D.E. and Wood R.H. (1982). Absolute Calibration of Flow Calorimeters Used for Measuring Differences in Heat Capacities. A Chemical Standard for Temperatures Between 325 and 600 K. *J. Solution Chem.* **11**, 223-236.

Woolley E.M. and Hepler L.G. (1977). Heat Capacity of Weak Electrolyte and Ion Association Reactions: Method and Application to Aqueous $MgSO_4$ and HIO_3 at 298K. *Can. J. Chem.* **55**, 158-163.

Wood R.H., Buzzard C.W., Majer V., and Inglese A. (1989). A Phase-Locked Loop for Driving Vibrating Tube Densimeters. *Rev. Sci. Instrum.* **60**, 493-494.

Xiao C., Tremaine P.T., and Simonson J.M. (1996). Apparent Molar Volumes of $La(CF_3SO_3)_3$(aq) $Gd(CF_3SO_3)_3$(aq) at 278 K, 298 K, and 318 K at Pressures to 30 MPa. *J. Chem. Eng. Data* **41**, 1075-1078.

Xiao C, Bianchi H., and Tremaine P.R. (1997). Excess Molar Volumes and Densities of (Methanol + Water) at Temperatures Between 323 K and 573 K and Pressures of 7.0 MPa and 13,5 MPa. *J. Chem. Thermodynamics* **29**, 261-286.

Xiao C. and Tremaine P.R. (1997). Apparent Molar Volumes of Aqueous Sodium Trifluoromethanesulfonate and Trifluoromethanesulfonic Acid from 283 K to 600 K and Presures up to 20 MPa. *J. Solution Chem.* **26**, 277-294.

Young T.F. and Smith M.B. (1954). Thermodynamic Properties of Mixtures of Electrolytes in Aqueous Solutions. *J. Phys. Chem.* **58**, 716-724.

Appendix

Appendix 1: Experimental data tables of apparent molar volumes, heat capacities, and compressibilities for methyldiethanolamine and methyldiethanolammonium chloride.

Appendix 2: Experimental data tables of molar heat capacities and excess heat capacities for methyldiethanolamine and methyldiethanolammonium chloride.

Table A.1.1 Relative densities $\rho-\rho_1^*$ and apparent molar volumes V_ϕ for aqueous solutions of methyldiethanolamine; where T denotes temperature, p denotes pressure, ρ_1^* denotes the density of water, and m denotes molality.

T / K	p / MPa	ρ_1^* / g·cm^{-3}	m / mol·kg^{-1}	$\rho-\rho_1^*$ / g·cm^{-3}	V_ϕ / cm^3·mol^{-1}
		$T_{average}$ = 283.15 K; $p_{average}$ = 0.10 MPa			
283.15	0.10	0.999705	0.12065	1.23493e-3	108.86
283.15	0.10	0.999705	0.20426	2.07012e-3	108.86
283.15	0.10	0.999705	0.30671	3.10200e-3	108.76
283.15	0.10	0.999705	0.50172	5.08172e-3	108.52
283.15	0.10	0.999705	0.70352	7.05586e-3	108.41
283.15	0.10	0.999705	0.89819	9.03520e-3	108.17
283.15	0.10	0.999705	1.0879	0.01077	108.13
283.15	0.10	0.999705	1.3574	0.01329	107.97
283.15	0.10	0.999705	1.6524	0.01616	107.68
283.15	0.10	0.999705	2.1607	0.02029	107.62
		$T_{average}$ = 298.15 K; $p_{average}$ = 0.10 MPa			
298.15	0.10	0.997041	0.12065	1.15132e-3	109.83
298.15	0.10	0.997041	0.20426	1.92410e-3	109.86
298.15	0.10	0.997041	0.30671	2.85718e-3	109.86
298.15	0.10	0.997041	0.50172	4.61326e-3	109.78
298.15	0.10	0.997041	0.70352	6.43282e-3	109.63
298.15	0.10	0.997041	0.89819	8.17572e-3	109.48
298.15	0.10	0.997041	1.0879	9.70556e-3	109.49
298.15	0.10	0.997041	1.3574	0.01191	109.39
298.15	0.10	0.997041	1.6524	0.01445	109.15
298.15	0.10	0.997041	2.1607	0.01801	109.17
		$T_{average}$ = 313.15 K; $p_{average}$ = 0.10 MPa			
313.15	0.10	0.992206	0.12065	1.07405e-3	110.94
313.15	0.10	0.992206	0.20426	1.80280e-3	110.97
313.15	0.10	0.992206	0.30671	2.67527e-3	110.97
313.15	0.10	0.992206	0.50172	4.31675e-3	110.90
313.15	0.10	0.992206	0.70352	5.96988e-3	110.83
313.15	0.10	0.992206	0.89819	7.57459e-3	110.70
313.15	0.10	0.992206	1.0879	8.96251e-3	110.74
313.15	0.10	0.992206	1.3574	0.01093	110.71
313.15	0.10	0.992206	1.6524	0.01320	110.52
313.15	0.10	0.992206	2.1607	0.01640	110.57

T K	p MPa	ρ_1^* g·cm^{-3}	m mol·kg^{-1}	$\rho-\rho_1^*$ g·cm^{-3}	V_ϕ cm^3·mol^{-1}
		$T_{average}$ = 328.15 K; $p_{average}$ = 0.10 MPa			
328.15	0.10	0.985686	0.12065	4.97033e-4	111.93
328.15	0.10	0.985686	0.20426	1.05510e-3	112.01
328.15	0.10	0.985686	0.30671	1.74682e-3	112.09
328.15	0.10	0.985686	0.50172	2.56886e-3	112.09
328.15	0.10	0.985686	0.70352	4.07596e-3	112.02
328.15	0.10	0.985686	0.89819	5.59571e-3	112.04
328.15	0.10	0.985686	1.0879	7.06078e-3	111.88
328.15	0.10	0.985686	1.3574	8.36845e-3	111.98
328.15	0.10	0.985686	1.6524	0.01226	112.02
328.15	0.10	0.985686	2.1607	0.01512	111.99
		$T_{average}$ = 337.47 K; $p_{average}$ = 10.186 MPa			
337.42	10.173	0.985315	0.20426	1.654e-3	112.41
337.43	10.182	0.985320	0.30671	2.367e-3	112.72
337.52	10.184	0.985264	0.50172	3.993e-3	112.29
337.45	10.187	0.985291	1.0879	8.018e-3	112.43
337.46	10.195	0.985315	2.1607	0.01462	112.30
337.50	10.189	0.985282	3.5723	0.02132	112.36
337.52	10.191	0.985277	4.9938	0.02646	112.46
		$T_{average}$ = 425.94 K; $p_{average}$ = 10.322 MPa			
425.94	10.318	0.919916	0.20426	1.179e-3	122.56
425.94	10.321	0.919924	0.30671	1.676e-3	122.85
425.93	10.321	0.919932	0.50172	2.827e-3	122.50
425.93	10.320	0.919957	1.0879	5.556e-3	122.75
425.95	10.323	0.919969	2.1607	9.868e-3	122.81
425.95	10.322	0.919981	3.5723	0.01399	123.02
425.94	10.332	0.919952	4.9938	0.01704	123.21
		$T_{average}$ = 523.34 K; $p_{average}$ = 10.400 MPa			
523.38	10.392	0.805930	0.20426	9.365e-4	140.63
523.30	10.397	0.805961	0.30671	1.315e-3	141.02
523.30	10.399	0.806000	0.50172	2.014e-3	141.31
523.32	10.406	0.806044	1.0879	4.120e-3	141.28
523.30	10.405	0.806040	2.1607	7.527e-3	141.15
523.31	10.400	0.806062	3.5723	0.01115	141.07
523.44	10.399	0.805981	4.9938	0.01460	140.79

T K	p MPa	ρ_1^* g·cm^{-3}	m mol·kg^{-1}	$\rho-\rho_1^*$ g·cm^{-3}	V_ϕ cm^3·mol^{-1}
	$T_{average}$ = 335.21 K; $p_{average}$ = 20.190 MPa				
335.21	20.184	0.990724	0.20426	2.114e-3	109.50
335.20	20.189	0.990728	0.30671	2.668e-3	111.11
335.24	20.189	0.990718	0.50172	3.813e-3	112.10
335.17	20.184	0.990739	1.0879	7.675e-3	112.22
335.16	20.198	0.990752	2.1607	0.01348	112.39
335.24	20.194	0.990718	3.5723	0.01972	112.42
335.28	20.195	0.990695	4.9938	0.02427	112.57
	$T_{average}$ = 384.00 K; $p_{average}$ = 20.216 MPa				
384.00	20.200	0.959763	0.20426	1.3120e-3	116.98
383.98	20.208	0.959782	0.30671	2.023e-3	116.75
383.99	20.214	0.959782	0.50172	3.282e-3	116.65
384.01	20.224	0.959772	1.0879	6.456e-3	116.92
384.02	20.216	0.959756	2.1607	0.01116	117.19
384.01	20.221	0.959761	3.5723	0.01617	117.27
383.97	20.229	0.959789	4.9938	0.01982	117.42
	$T_{average}$ = 424.37 K; $p_{average}$ = 20.182 MPa				
424.34	20.163	0.926740	0.20426	1.067e-3	122.35
424.34	20.173	0.926744	0.30671	1.623e-3	122.20
424.35	20.185	0.926744	0.50172	2.821e-3	121.66
424.36	20.187	0.926736	1.0879	5.7058e-3	121.72
424.39	20.186	0.926712	2.1607	0.01003	121.86
424.40	20.189	0.926700	3.5723	0.01446	121.97
424.43	20.191	0.926673	4.9938	0.01756	122.18

T K	p MPa	ρ_1^* g·cm^{-3}	m mol·kg^{-1}	$\rho-\rho_1^*$ g·cm^{-3}	V_ϕ cm^3·mol^{-1}
	$T_{average}$ = 475.67 K; $p_{average}$ = 20.088 MPa				
475.67	20.083	0.875297	0.20426	1.130e-3	128.75
475.67	20.078	0.875293	0.30671	1.515e-3	129.46
475.66	20.082	0.875306	0.50172	2.367e-3	129.63
475.67	20.085	0.875292	1.0879	4.738e-3	129.75
475.68	20.098	0.875294	2.1607	8.262e-3	129.92
475.67	20.094	0.875302	3.5723	0.01181	130.07
475.68	20.094	0.875293	4.9938	0.01465	130.13
	$T_{average}$ = 524.57 K; $p_{average}$ = 20.083 MPa				
524.57	20.048	0.814276	0.20426	9.151e-4	139.42
524.57	20.075	0.814311	0.30671	1.339e-3	139.52
524.56	20.078	0.814316	0.50172	2.004e-3	139.96
524.55	20.090	0.814346	1.0879	4.118e-3	139.91
524.57	20.100	0.814333	2.1607	7.624e-3	139.70
524.57	20.097	0.814332	3.5723	0.01136	139.58
524.58	20.095	0.814304	4.9938	0.01465	139.40

Table A.1.2 Relative densities (ρ-ρ_1^*) and apparent molar volumes V_ϕ for aqueous solutions of methyldiethanolammonium chloride; where m_2 denotes the molality of the amine and m_3 denotes the molality of HCl, T denotes temperature, p denotes pressure, ρ_1^* denotes density of water, and $F_3 = m_3/(m_2 + m_3)$

T K	p MPa	ρ_1^* g·cm^3	m_2 mol·kg^{-1}	m_3 mol·kg^{-1}	ρ-ρ_1^* g·cm^{-3}	V_ϕ cm^3·mol^{-1}	F_3*$V_{\phi,3}$ cm^3·mol^{-1}	$V_{\phi,\lambda}$ cm^3·mol^{-1}
			$T_{average}$ = 283.15 K, $p_{average}$ = 0.10 MPa					
283.15	0.10	0.999705	0.10782	0.00120	3.62216e-3	120.73	0.1800	121.81
283.15	0.10	0.999705	0.22970	0.00239	7.54221e-3	121.01	0.1816	122.09
283.15	0.10	0.999705	0.29132	0.00303	9.46068e-3	121.13	0.1822	122.21
283.15	0.10	0.999705	0.38192	0.00397	0.01222	121.27	0.1829	122.34
283.15	0.10	0.999705	0.59184	0.00615	0.01840	121.42	0.1841	122.50
283.15	0.10	0.999705	0.77081	0.00801	0.02341	121.52	0.1848	122.60
283.15	0.10	0.999705	0.98979	0.01028	0.02925	121.62	0.1854	122.69
283.15	0.10	0.999705	1.2252	0.01273	0.03513	121.77	0.1858	122.85
			$T_{average}$ = 298.15 K, $p_{average}$ = 0.10 MPa					
298.15	0.10	0.997041	0.10782	0.00120	3.42074e-3	122.84	0.1887	123.93
298.15	0.10	0.997041	0.22970	0.00239	7.16856e-3	122.90	0.1905	123.98
298.15	0.10	0.997041	0.29132	0.00303	9.02127e-3	122.91	0.1911	123.99
298.15	0.10	0.997041	0.38192	0.00397	0.01167	123.00	0.1920	124.09
298.15	0.10	0.997041	0.59184	0.00615	0.01757	123.14	0.1934	124.22
298.15	0.10	0.997041	0.77081	0.00801	0.02231	123.28	0.1943	124.40
298.15	0.10	0.997041	0.98979	0.01028	0.02785	123.40	0.1951	124.48
298.15	0.10	0.997041	1.2252	0.01273	0.03347	123.51	0.1958	124.60

T K	p MPa	ρ_1^* g·cm^3	m_2 mol·kg^{-1}	m_3 mol·kg^{-1}	$\rho-\rho_1^*$ g·cm^{-3}	V_ϕ cm^3·mol^{-1}	$F_3*V_{\phi,3}$ cm^3·mol^{-1}	$V_{\phi,2}$ cm^3·mol^{-1}
			$T_{average}$ = 313.15 K, $p_{average}$ = 0.10 MPa					
313.15	0.10	0.992206	0.10782	0.00120	3.35976e-3	123.86	0.1916	124.95
313.15	0.10	0.992206	0.22970	0.00239	6.99840e-3	124.10	0.1939	125.20
313.15	0.10	0.992206	0.29132	0.00303	8.77482e-3	124.23	0.1948	125.32
313.15	0.10	0.992206	0.38192	0.00397	0.01137	124.25	0.1958	125.34
313.15	0.10	0.992206	0.59184	0.00615	0.01708	124.46	0.1977	125.55
313.15	0.10	0.992206	0.77081	0.00801	0.02172	124.56	0.1989	125.65
313.15	0.10	0.992206	0.98979	0.01028	0.02710	124.68	0.2000	125.77
313.15	0.10	0.992206	1.2252	0.01273	0.03261	124.75	0.2010	125.84
			$T_{average}$ = 328.15 K, $p_{average}$ = 0.10 MPa					
328.15	0.10	0.985686	0.10782	0.00120	3.31713e-3	124.88	0.1871	125.99
328.15	0.10	0.985686	0.22970	0.00239	6.86993e-3	125.30	0.1900	126.41
328.15	0.10	0.985686	0.29132	0.00303	8.62454e-3	125.38	0.1911	126.49
328.15	0.10	0.985686	0.38192	0.00397	0.01123	125.27	0.1925	126.38
328.15	0.10	0.985686	0.59184	0.00615	0.01693	125.35	0.1950	126.46
328.15	0.10	0.985686	0.77081	0.00801	0.02154	125.43	0.1966	126.53
328.15	0.10	0.985686	0.98979	0.01028	0.02685	125.59	0.1983	126.69
328.15	0.10	0.985686	1.2252	0.01273	0.03228	125.69	0.1997	126.79

T K	p MPa	ρ_1^* g·cm^3	m_2 mol·kg^{-1}	m_3 mol·kg^{-1}	ρ-ρ_1^* g·cm^{-3}	V_ϕ cm^3·mol^{-1}	F_3*$V_{\phi,3}$ cm^3·mol^{-1}	$V_{\phi,2}$ cm^3·mol^{-1}
			$T_{average}$ = 422.91 K, $p_{average}$ = 10.253 MPa					
422.98	10.245	0.922615	0.10782	1.12e-3	3.70007e-3	127.84	-0.14	129.31
422.91	10.247	0.922713	0.22970	2.39e-3	7.79381e-3	127.72	-0.12	129.17
422.91	10.258	0.922679	0.38192	3.97e-3	0.012529	128.38	-0.11	129.83
422.88	10.260	0.922747	0.59184	6.15e-3	0.018898	128.51	-0.10	129.95
422.88	10.247	0.922751	0.77081	8.01e-3	0.023990	128.75	-0.10	130.18
422.93	10.253	0.922726	0.98979	0.0103	0.030806	127.83	-0.09	129.24
422.91	10.259	0.922772	1.2252	0.0127	0.036772	128.28	-0.08	129.70
			$T_{average}$ = 522.98 K, $p_{average}$ = 10.377 MPa					
522.91	10.363	0.806607	0.10782	1.12e-3	5.60953e-3	112.18	-1.41	114.77
522.97	10.373	0.806529	0.22970	2.39e-3	0.011596	113.71	-1.38	116.28
523.06	10.375	0.806396	0.38192	3.97e-3	0.018335	116.50	-1.35	119.08
523.06	10.381	0.806401	0.59184	6.15e-3	0.027179	118.37	-1.33	120.94
522.98	10.387	0.806527	0.77081	8.01e-3	0.034059	119.96	-1.31	122.52
522.94	10.381	0.806572	0.98979	0.0103	0.041102	122.85	-1.28	125.42
522.95	10.381	0.806554	1.2252	0.0127	0.049854	122.80	-1.26	125.35

T K	p MPa	ρ_1^* g·cm^3	m_2 mol·kg^{-1}	m_3 mol·kg^{-1}	ρ-ρ_1^* g·cm^{-3}	V_ϕ cm^3·mol^{-1}	F_3*$V_{\phi,3}$ cm^3·mol^{-1}	$V_{\phi,2}$ cm^3·mol^{-1}
			$T_{average}$ = 334.22 K, $p_{average}$ = 20.049 MPa					
334.27	20.009	0.991146	0.10782	1.12e-3	3.38369e-3	124.64	0.18	125.75
334.22	20.019	0.991153	0.22970	2.39e-3	6.65021e-3	126.69	0.19	127.81
334.19	20.032	0.991182	0.38192	3.97e-3	0.010964	126.38	0.19	127.51
334.19	20.038	0.991192	0.59184	6.15e-3	0.016291	126.90	0.19	128.02
334.22	20.058	0.991183	0.77081	8.01e-3	0.020776	126.91	0.19	128.03
334.22	20.083	0.991196	0.98979	0.0103	0.026014	126.92	0.20	128.04
334.20	20.106	0.991212	1.2252	0.0127	0.031132	127.14	0.20	128.26
			$T_{average}$ = 377.10 K, $p_{average}$ = 20.204 MPa					
377.06	20.175	0.964779	0.10782	1.12e-3	3.36544e-3	127.32	0.10	128.54
377.06	20.186	0.964788	0.22970	2.39e-3	6.98935e-3	127.68	0.10	128.90
377.06	20.213	0.964800	0.29132	3.03e-3	8.63532e-3	128.30	0.11	129.53
377.07	20.194	0.964791	0.38192	3.97e-3	0.011333	127.91	0.11	129.13
377.11	20.208	0.964777	0.59184	6.15e-3	0.017007	128.17	0.12	129.38
377.17	20.218	0.964741	0.77081	8.01e-3	0.021517	128.45	0.12	129.66
377.14	20.220	0.964737	0.98979	0.0103	0.026748	128.70	0.12	129.92
377.10	20.218	0.964772	1.2252	0.0127	0.032222	128.74	0.13	129.95

T K	p MPa	ρ_1^* g·cm^3	m_2 mol·kg^{-1}	m_3 mol·kg^{-1}	$\rho-\rho_1^*$ g·cm^{-3}	V_ϕ cm^3·mol^{-1}	$F_3*V_{\phi,3}$ cm^3·mol^{-1}	$V_{\phi,2}$ cm^3·mol^{-1}
			$T_{average}$ = 426.76 K, $p_{average}$ = 20.220 MPa					
426.77	20.205	0.924617	0.04960	5.15e-4	1.74479e-3	126.92	-0.17	128.41
426.78	20.215	0.924553	0.22970	2.39e-3	7.77385e-3	127.65	-0.15	129.13
426.77	20.212	0.924566	0.29132	3.03e-3	9.66251e-3	128.17	-0.15	129.65
426.80	*20.233*	*0.924565*	*0.38192*	*3.97e-3*	*0.012785*	*127.39*	*-0.14*	*128.86*
426.78	20.216	0.924517	0.59184	6.15e-3	0.019128	127.87	-0.13	129.32
426.80	20.223	0.924593	0.77081	8.01e-3	0.024404	127.90	-0.12	129.35
426.66	20.230	0.924674	0.98979	0.0103	0.030201	128.41	-0.11	129.86
426.72	20.230	0.924623	1.2252	0.0127	0.036615	128.27	-0.10	129.70
			$T_{average}$ = 475.06 K, $p_{average}$ = 20.179 MPa					
475.03	20.141	0.876070	0.10782	1.12e-3	4.55147e-3	122.00	-0.64	123.91
475.04	20.157	0.876053	0.22970	2.39e-3	8.82369e-3	126.31	-0.62	128.25
475.04	20.168	0.876061	0.29132	3.03e-3	0.011131	126.25	-0.61	128.18
475.07	20.189	0.876056	0.38192	3.97e-3	0.014123	127.40	-0.60	129.33
475.07	20.176	0.876056	0.59184	6.15e-3	0.021050	128.21	-0.58	130.13
475.08	20.197	0.876041	0.77081	8.01e-3	0.026685	128.61	-0.57	130.52
475.09	20.202	0.876036	0.98979	0.0103	0.033209	129.03	-0.56	130.93
475.10	20.203	0.876039	1.2252	0.0127	0.039678	129.57	-0.54	131.47

T K	p MPa	ρ_1^* g·cm^3	m_2 mol·kg^{-1}	m_3 mol·kg^{-1}	$\rho-\rho_1^*$ g·cm^{-3}	V_ϕ cm^3·mol^{-1}	$F_3*V_{\phi,3}$ cm^3·mol^{-1}	$V_{\phi,2}$ cm^3·mol^{-1}
			$T_{average}$ = 523.78 K, $p_{average}$ = 20.161 MPa					
523.78	20.147	0.815393	0.04960	5.15e-4	2.60545e-3	111.49	-1.43	114.10
523.75	20.146	0.815527	0.10782	1.12e-3	5.45396e-3	114.00	-1.41	116.61
523.83	20.144	0.815426	0.22970	2.39e-3	0.011095	116.61	-1.38	119.22
523.83	20.158	0.815509	0.29132	3.03e-3	0.013857	117.31	-1.37	119.91
523.85	20.169	0.815509	0.38192	3.97e-3	0.017762	118.32	-1.36	120.91
523.80	20.163	0.815437	0.59184	6.15e-3	0.026184	120.44	-1.33	123.03
523.74	20.167	0.815565	0.77081	8.01e-3	0.032958	121.61	-1.31	124.20
523.71	20.176	0.815599	0.98979	0.0103	0.040754	122.77	-1.29	125.34
523.72	20.175	0.815636	1.2252	0.0127	0.048709	123.65	-1.26	126.21
			$T_{average}$ = 576.35 K, $p_{average}$ = 20.201 MPa					
576.34	20.162	0.728874	0.10782	1.12e-3	7.40084e-3	83.45	-2.64	86.99
576.31	20.163	0.728855	0.22970	2.39e-3	0.015182	87.28	-2.60	90.81
576.31	20.193	0.729037	0.38192	3.97e-3	0.024099	91.70	-2.56	95.24
576.32	20.212	0.729030	0.59184	6.15e-3	0.035322	96.49	-2.52	100.04
576.37	20.226	0.729013	0.77081	8.01e-3	0.044044	99.91	-2.49	103.47
576.38	20.221	0.728914	0.98979	0.0103	0.053814	103.52	-2.46	107.08
576.42	20.228	0.728927	1.2252	0.0127	0.063737	106.29	-2.43	109.85

Table A.1.3 Apparent molar heat capacities $C_{p,\phi,2}$ for aqueous methyldiethanolamine solutions where m denotes molality; ρ_1^* and $c_{p,1}^*$ denote density and heat capacity of water; $C_{p,\phi}^{rel}$ is the relaxation contribution; α is the degree of dissociation; $\Delta W/W_o = c_p\rho/(c_{p,1}^*\rho_1^*)-1$

m mol·kg^{-1}	α	$c_p\rho/(c_{p,1}^*\rho_1^*)-1$	$C_{p,\phi}^{exptl}$ J·K^{-1}·mol^{-1}	$C_{p,\phi}^{rel}$ J·K^{-1}·mol^{-1}	$C_{p,\phi,2}$ J·K^{-1}·mol^{-1}
		$T = 283.15$ K			
0.20426	3.22416e-3	-3.80034e-3	376.53	1.36	375.98
0.30671	2.63193e-3	-6.01237e-3	370.96	1.11	370.50
0.50172	2.05841e-3	-0.01049	362.49	0.87	362.11
0.70352	1.73858e-3	-0.01527	356.47	0.73	356.14
0.89819	1.53883e-3	-0.02003	350.86	0.65	350.56
1.0879	1.39836e-3	-0.02439	348.22	0.59	347.94
1.3574	1.25194e-3	-0.03087	343.31	0.53	343.06
1.6524	1.13477e-3	-0.03844	336.49	0.47	336.25
2.1607	9.92428e-4	-0.04987	331.89	0.42	331.68
		$T = 298.15$ K			
0.12066	5.43422e-3	-2.06786e-3	384.97	1.40	384.67
0.20426	4.17926e-3	-3.57642e-3	382.89	1.08	382.65
0.30671	3.41188e-3	-5.38552e-3	381.86	0.88	381.66
0.50172	2.66863e-3	-8.90593e-3	379.15	0.69	378.99
0.70352	2.25400e-3	-0.01245	377.17	0.58	377.03
0.89819	1.99518e-3	-0.01602	374.32	0.52	374.19
1.0879	1.81309e-3	-0.01955	372.23	0.47	372.10
1.3574	1.62327e-3	-0.03015	370.32	0.42	370.21
1.6524	1.47137e-3	-0.03863	364.86	0.38	364.75
2.1607	1.28684e-3	-0.06297	362.62	0.33	362.52

m mol·kg^{-1}	α	$c_p\rho/(c_{p,1}^{*}\rho_1^{*})-1$	$C_{p,\phi}^{expt}$ J·K^{-1}·mol^{-1}	$C_{p,\phi}^{rel}$ J·K^{-1}·mol^{-1}	$C_{p,\phi,2}$ J·K^{-1}·mol^{-1}
		T = 313.15 K			
0.12066	6.58065e-3	-1.89758e-3	392.65	0.96	392.88
0.20426	5.04750e-3	-3.04912e-3	396.02	0.73	396.21
0.30671	4.12109e-3	-4.59643e-3	395.09	0.60	395.24
0.50172	3.22361e-3	-7.16688e-3	393.94	0.47	394.06
0.70352	2.72286e-3	-0.01035	393.10	0.40	393.20
0.89819	2.41027e-3	-0.01339	390.33	0.35	390.40
1.0879	2.19033e-3	-0.01607	389.85	0.32	389.92
1.3574	1.96106e-3	-0.02007	387.87	0.29	387.92
1.6524	1.77758e-3	-0.02476	384.11	0.26	384.15
2.1607	1.55468e-3	-0.03183	382.12	0.23	382.15
		T = 328.15 K			
0.30671	4.71887e-3	-4.04551e-3	404.45	0.33	404.91
0.50172	3.69144e-3	-6.28540e-3	406.55	0.26	406.91
0.70352	3.11814e-3	-8.60727e-3	406.72	0.22	407.03
0.89819	2.76023e-3	-0.01102	405.18	0.20	405.45
1.0879	2.50840e-3	-0.01334	404.22	0.18	404.46
1.3574	2.25014e-3	-0.01752	399.32	0.14	399.50
1.6524	2.03577e-3	-0.02062	396.95	0.13	397.11
2.1607	1.78052e-3	-0.02691	390.98	0.10	391.10

Table A.1.4 Apparent molar heat capacities $C_{p,\phi,2}$ for aqueous methyldiethanolammonium chloride solutions where m_2 denotes the molality of the amine and m_3 denotes the molality of HCl; ρ_1^* and $c_{p,1}^*$ denote density and heat capacity of water; $C_{p,\phi,3}$ is the apparent molar heat capacity of HCl.; $\Delta W/W_o = c_p\rho/(c_{p,1}^*\rho_1^*)-1$; and $F_3 = m_3/(m_2 + m_3)$

m_2 mol·kg^{-1}	m_3 mol·kg^{-1}	$c_p\rho/(c_{p,1}^*\rho_1^*)-1$ J·K^{-1}·mol^{-1}	$C_{p,\phi}^{expt}$ J·K^{-1}·mol^{-1}	$F_3 \cdot C_{p,\phi,3}$ J·K^{-1}·mol^{-1}	$C_{p,\phi,2}$ J·K^{-1}·mol^{-1}
		$T = 283.15$ K			
0.10782	0.00120	-8.58266e-3	171.44	-1.443	174.68
0.22970	0.00239	-0.01835	166.51	-1.403	169.66
0.29132	0.00303	-0.02308	167.34	-1.387	170.48
0.38192	0.00397	-0.03004	166.71	-1.364	169.83
0.59184	0.00615	-0.04517	169.31	-1.319	172.40
0.77081	0.00801	-0.05736	171.40	-1.284	174.48
0.98979	0.01028	-0.07122	174.94	-1.245	178.02
1.2252	0.01273	-0.08510	178.79	-1.205	181.87
		$T = 298.15$ K			
0.10782	0.00120	-7.98174e-3	201.62	-1.208	204.94
0.22970	0.00239	-0.01666	203.53	-1.172	206.83
0.29132	0.00303	-0.02090	204.77	-1.158	208.07
0.38192	0.00397	-0.02704	205.88	-1.141	209.17
0.59184	0.00615	-0.04040	210.02	-1.109	213.32
0.77081	0.00801	-0.05115	213.00	-1.088	216.31
0.98979	0.01028	-0.06364	215.54	-1.065	218.86
1.2252	0.01273	-0.07621	218.18	-1.044	221.50
		$T = 313.15$ K			
0.10782	0.00120	-7.46430e-3	223.32	-1.082	226.73
0.22970	0.00239	-0.01544	228.58	-1.043	232.01
0.29132	0.00303	-0.01938	229.93	-1.029	233.36
0.38192	0.00397	-0.02510	230.35	-1.011	233.77
0.59184	0.00615	-0.03746	234.84	-0.979	238.27
0.77081	0.00801	-0.04750	236.96	-0.959	240.39
0.98979	0.01028	-0.05908	239.44	-0.938	242.88
1.2252	0.01273	-0.07104	240.62	-0.919	244.05

m_2 mol·kg^{-1}	m_3 mol·kg^{-1}	$c_p\rho/(c_{p,1}^{*}\rho_1^{*})-1$ J·K^{-1}·mol^{-1}	$C_{p,\phi}^{expt}$ J·K^{-1}·mol^{-1}	$F_3 \cdot C_{p,\phi,3}$ J·K^{-1}·mol^{-1}	$C_{p,\phi,2}$ J·K^{-1}·mol^{-1}
		$T = 328.15$ K			
0.29132	0.00303	-0.01873	240.98	-0.970	244.47
0.38192	0.00397	-0.02384	245.68	-0.950	249.19
0.59184	0.00615	-0.03563	249.08	-0.916	252.60
0.77081	0.00801	-0.04526	250.51	-0.893	254.01
0.98979	0.01028	-0.05649	252.17	-0.870	255.67
1.2252	0.01273	-0.06728	255.89	-0.849	259.41

Table A.1.5 Sound velocities U, apparent molar expansivities E_ϕ, relative molar increments of sound velocity [U], apparent molar adiabatic compressibilities $\kappa_{S,\phi}$, and isothermal compressibilities $\kappa_{T,\phi}$ of methyldiethanolamine where m denotes molality.

m mol·kg^{-1}	U m·s^{-1}	E_ϕ cm^3·mol^{-1}·K^{-1}	[U]	$\kappa_{S,\phi}$ cm^3·MPa^{-1}·mol^{-1}	$\kappa_{T,\phi}$ cm^3·MPa^{-1}·mol^{-1}
		T = 283.15 K			
0.30671	1474.25	0.088395	66.55	-0.01666	-0.01566
0.50172	1489.68	0.090813	63.95	-0.01439	-0.01336
0.70352	1505.07	0.093315	62.84	-0.01344	-0.01237
0.89819	1519.35	0.095729	62.25	-0.01311	-0.01201
1.0879	1532.75	0.098081	61.87	-0.01278	-0.01166
1.3574	1550.89	0.101423	61.47	-0.01255	-0.01138
1.6524	1569.54	0.105080	61.08	-0.01245	-0.01125
2.1607	1598.73	0.111382	60.39	-0.01185	-0.01057
		T = 298.15 K			
0.30671	1520.04	0.074364	55.00	-4.3947e-3	-2.0865e-3
0.50172	1532.93	0.076782	52.49	-2.2168e-3	1.8377e-4
0.70352	1545.75	0.079284	51.37	-1.3487e-3	1.1464e-3
0.89819	1557.62	0.081697	50.75	-9.2939e-4	1.6580e-3
1.0879	1568.70	0.084049	50.34	-5.4588e-4	2.1307e-3
1.3574	1583.64	0.087391	49.88	-2.1597e-4	2.5861e-3
1.6524	1598.91	0.091049	49.42	-2.1000e-5	2.9223e-3
2.1607	1622.56	0.097351	48.63	6.9945e-4	3.8778e-3

m mol·kg^{-1}	U m·s^{-1}	E_ϕ cm^3·mol^{-1}·K^{-1}	[U]	$\kappa_{S,\phi}$ cm^3·MPa^{-1}·mol^{-1}	$\kappa_{T,\phi}$ cm^3·MPa^{-1}·mol^{-1}
			T = 313.15 K		
0.30671	1547.67	0.073106	45.08	5.0501e-3	8.23791e-3
0.50172	1557.71	0.075524	42.06	7.5979e-3	0.01093
0.70352	1567.67	0.078026	40.69	8.7177e-3	0.01220
0.89819	1576.88	0.080440	39.94	9.2618e-3	0.01289
1.0879	1585.47	0.082792	39.43	9.7331e-3	0.01350
1.3574	1597.02	0.086134	38.89	0.01018	0.01414
1.6524	1608.79	0.089791	38.39	0.01044	0.01463
2.1607	1626.92	0.096093	37.60	0.01117	0.01573

Table A.1.6 Sound velocities U, apparent molar expansivities E_ϕ, relative molar increments of sound velocity [U], apparent molar adiabatic compressibilities $\kappa_{S,\phi}$, and isothermal compressibilities $\kappa_{T,\phi}$ of methyldiethanolammonium chloride where I denotes ionic strength.

m mol·kg^{-1}	U m·s^{-1}	E_ϕ cm^3·mol^{-1}·K^{-1}	[U]	$\kappa_{S,\phi}$ cm^3·MPa^{-1}·mol^{-1}	$\kappa_{T,\phi}$ cm^3·MPa^{-1}·mol^{-1}
		T = 283.15 K			
0.29435	1475.42	0.141929	72.85	-0.02725	-0.02559
0.38588	1484.32	0.140456	73.03	-0.02730	-0.02565
0.59799	1504.93	0.137703	74.12	-0.02820	-0.02658
0.77882	1522.50	0.135976	75.34	-0.02926	-0.02767
1.00007	1544.00	0.134528	76.96	-0.03072	-0.02914
1.23791	1567.11	0.133698	78.79	-0.03233	-0.03076
		T = 298.15 K			
0.29435	1521.86	0.094508	62.39	-0.01474	-0.01149
0.38588	1529.66	0.093035	62.45	-0.01471	-0.01151
0.59799	1547.74	0.090282	63.27	-0.01533	-0.01224
0.77882	1563.15	0.088555	64.27	-0.01609	-0.01307
1.00007	1582.00	0.087107	65.64	-0.01721	-0.01425
1.23791	1602.26	0.086277	67.19	-0.01850	-0.01557
		T = 313.15 K			
0.29435	1551.70	0.066721	57.52	-9.1758e-3	-5.9214e-3
0.38588	1558.68	0.065248	56.97	-8.6903e-3	-5.5227e-3
0.59799	1574.84	0.062495	57.03	-8.5540e-3	-5.5590e-3
0.77882	1588.62	0.060767	57.63	-8.9845e-3	-6.0959e-3
1.00007	1605.47	0.059320	58.62	-9.7432e-3	-6.9457e-3
1.23791	1623.59	0.058490	59.85	-0.01074	-7.9980e-3

Table A.2.1 Molar heat capacities C_p and excess molar heat capacities C_p^{EX} of aqueous solutions of methyldiethanolamine where X_2 denotes the mole fraction of methyldiethanolamine.

X_2	C_p $J \cdot K^{-1} \cdot mol^{-1}$	C_p^{EX} $J \cdot K^{-1} \cdot mol^{-1}$	C_p $J \cdot K^{-1} \cdot mol^{-1}$	C_p^{EX} $J \cdot K^{-1} \cdot mol^{-1}$	C_p $J \cdot K^{-1} \cdot mol^{-1}$	C_p^{EX} $J \cdot K^{-1} \cdot mol^{-1}$
	T = 278.15 K		**T = 283.15 K**		**T = 288.15 K**	
0.03001	83.08	1.898	83.17	1.995	83.24	2.160
0.05999	88.38	1.790	89.28	2.577	89.95	3.233
0.10010	95.80	1.980	97.18	3.079	98.28	4.023
0.19967	113.92	2.147	115.80	3.342	117.47	4.484
0.29985	131.57	1.734	134.04	3.109	136.23	4.405
0.39915	149.13	1.387	152.09	2.842	154.68	4.186
0.49941	166.89	1.070	170.16	2.426	173.05	3.696
0.59669	184.21	0.844	187.63	1.955	190.82	3.168
0.69783	202.16	0.562	205.80	1.477	209.22	2.552
0.80156	220.64	0.342	224.43	0.974	227.80	1.619
0.89402	237.09	0.120	241.08	0.575	244.52	0.957
0.93813	245.00	0.071	248.99	0.348	252.44	0.580
	T = 293.15 K		**T = 298.15 K**		**T = 303.15 K**	
0.03001	83.45	2.325	83.70	2.505	83.92	2.643
0.05999	90.63	3.772	91.23	4.207	91.73	4.555
0.10010	99.36	4.829	100.32	5.513	101.17	6.091
0.19967	119.15	5.574	120.76	6.613	122.30	7.604
0.29985	138.36	5.628	140.38	6.781	142.29	7.868
0.39915	157.15	5.427	159.45	6.575	161.62	7.639
0.49941	175.78	4.883	178.34	5.993	180.76	7.029
0.59669	193.69	4.196	196.27	5.038	198.85	5.950
0.69783	212.13	3.292	214.91	4.040	217.61	4.790
0.80156	230.95	2.270	233.93	2.918	236.81	3.556
0.89402	247.68	1.322	250.63	1.659	253.56	2.094
0.93813	255.58	0.785	258.53	0.994	261.42	1.272

X_2	C_p $J \cdot K^{-1} \cdot mol^{-1}$	C_p^{EX} $J \cdot K^{-1} \cdot mol^{-1}$	C_p $J \cdot K^{-1} \cdot mol^{-1}$	C_p^{EX} $J \cdot K^{-1} \cdot mol^{-1}$	C_p $J \cdot K^{-1} \cdot mol^{-1}$	C_p^{EX} $J \cdot K^{-1} \cdot mol^{-1}$
	T = 308.15 K		**T = 313.15 K**		**T = 318.15 K**	
0.03001	84.19	2.839	84.45	3.027	84.54	3.043
0.05999	92.16	4.827	92.53	5.040	92.86	5.207
0.10010	101.92	6.578	102.60	6.991	103.22	7.346
0.19967	123.77	8.545	125.20	9.440	126.58	10.287
0.29985	144.13	8.895	145.90	9.863	147.61	10.779
0.39915	163.69	8.629	165.68	9.553	167.62	10.422
0.49941	183.08	7.997	185.32	8.901	187.50	9.746
0.59669	201.35	6.836	203.77	7.659	206.22	8.517
0.69783	220.25	5.534	222.84	6.266	225.42	6.978
0.80156	239.60	4.176	242.34	4.771	245.04	5.332
0.89402	256.37	2.483	259.11	2.830	261.81	3.146
0.93813	264.22	1.520	266.94	1.733	269.63	1.921
	T = 323.15 K		**T = 328.15 K**		**T = 333.15 K**	
0.03001	84.70	3.111	84.81	3.132	84.97	3.188
0.05999	93.16	5.342	93.45	5.460	93.75	5.574
0.10010	103.80	7.658	104.37	7.944	104.94	8.218
0.19967	127.92	11.090	129.23	11.848	130.51	12.563
0.29985	149.29	11.646	150.93	12.468	152.55	13.249
0.39915	169.51	11.244	171.38	12.028	173.25	12.784
0.49941	189.63	10.537	191.73	11.278	193.82	11.975
0.59669	208.57	9.267	210.94	10.016	213.33	10.754
0.69783	227.97	7.664	230.52	8.315	233.07	8.926
0.80156	247.63	5.778	250.30	6.270	252.99	6.738
0.89402	264.50	3.439	267.22	3.728	269.98	4.013
0.93813	272.33	2.106	275.05	2.282	277.82	2.457

X_2	C_p $J \cdot K^{-1} \cdot mol^{-1}$	C_p^{EX} $J \cdot K^{-1} \cdot mol^{-1}$	C_p $J \cdot K^{-1} \cdot mol^{-1}$	C_p^{EX} $J \cdot K^{-1} \cdot mol^{-1}$	C_p $J \cdot K^{-1} \cdot mol^{-1}$	C_p^{EX} $J \cdot K^{-1} \cdot mol^{-1}$
	T = 338.15 K		**T = 343.15 K**		**T = 348.15 K**	
0.03001	85.09	3.203	85.22	3.209	85.43	3.290
0.05999	94.07	5.700	94.42	5.851	94.83	6.041
0.10010	105.53	8.499	106.15	8.800	106.83	9.138
0.19967	131.77	13.236	133.01	13.868	134.23	14.460
0.29985	154.16	13.993	155.77	14.705	157.38	15.388
0.39915	175.14	13.522	177.04	14.250	178.99	14.977
0.49941	195.90	12.631	197.99	13.251	200.09	13.841
0.59669	215.35	11.068	218.07	12.048	220.31	12.477
0.69783	235.61	9.489	238.15	9.997	240.70	10.443
0.80156	255.61	7.088	258.22	7.366	260.83	7.564
0.89402	272.67	4.181	275.47	4.379	278.25	4.474
0.93813	280.57	2.555	283.43	2.682	286.30	2.740
	T = 353.15 K		**T = 358.15 K**		**T = 363.15 K**	
0.03001	85.69	3.398	85.97	3.531	86.46	3.849
0.05999	95.31	6.286	95.88	6.598	96.54	6.993
0.10010	107.58	9.530	108.41	9.990	109.35	10.535
0.19967	135.45	15.013	136.65	15.527	137.85	16.005
0.29985	159.00	16.047	160.65	16.686	162.32	17.309
0.39915	181.00	15.714	183.07	16.468	185.23	17.251
0.49941	202.23	14.405	204.41	14.946	206.64	15.472
0.59669	222.98	13.287	225.12	13.476	227.81	14.151
0.69783	243.26	10.819	245.82	11.120	248.39	11.337
0.80156	263.43	7.674	266.13	7.778	268.84	7.797
0.89402	281.12	4.570	284.05	4.625	287.07	4.643
0.93813	289.27	2.799	292.31	2.830	295.47	2.844

X_2	C_p $J \cdot K^{-1} \cdot mol^{-1}$	C_p^{EX} $J \cdot K^{-1} \cdot mol^{-1}$
	T = 368.15 K	
0.03001	87.26	4.464
0.05999	97.31	7.485
0.10010	110.42	11.181
0.19967	139.05	16.447
0.29985	164.03	17.920
0.39915	187.49	18.069
0.49941	208.93	15.984
0.59669	229.97	14.200
0.69783	250.97	11.463
0.80156	271.80	7.955
0.89402	290.28	4.736
0.93813	298.79	2.898